Proefschrift ter verkrijging van het doctoraat in de medische wetenschappen

Early Therapy Predicition

in Breast Cancer

by means of Receptor Imaging

Bieke Van Den Bossche

Promotor: Prof. C. Van de Wiele

Co-promotor: Prof. R.A. Dierckx

Academiejaar 2004-2005.

Universiteit Gent, Faculteit Geneeskunde en Gezondheidswetenschappen

Vakgroep Experimentele Cancerologie, Radiotherapie en Kerngeneeskunde

TABLE OF CONTENTS

CHAPTER ONE

INTRODUCTION

Over the past decade, impressive antineoplastic activity of somatostatin analogues has been demonstrated in many in vitro and in vivo tumour models, including breast cancer [1,2]. Somatostatin analogues, e.g. octreotide, exert their antiproliferative effects directly through upregulation of intracellular tyrosine phosphatase activity as a consequence of ligand binding to somatostatin receptors (SSTRs) leading to deactivation of growth-factor receptors as well as indirectly by suppressing levels of tumour growth factors such as insulin-like growth factor 1 (IGF-1) and growth hormone (figure B) [3]. Together with oestradiol, insulin-like growth factors (IGF-1 and IGF-2)) are the most potent mitogens for breast cancer cells and their growth effect is mediated predominantly via IGF-1 receptors (IGF-1Rs) [4,5]. Somatostatin, suppresses IGF-1 secretion both through reduction of growth-hormone (GH)-dependent hepatic IGF-1 expression as through direct inhibition of IGF-1 gene transcription [3].

The excellent preclinical results obtained with somatostatin analogues in experimental tumour models led to clinical trials in patients suffering from metastasised breast cancer. Unfortunately, enrolment of heavily pretreated metastasised patients in early clinical trials did not allow for definitive conclusions as to the antitumour activity of these agents [6,7,8,9]. More recent clinical trials assessed the efficacy of somatostatin analogues in combination treatment in untreated metastasised breast cancer patients. Bontenbal et al randomized 22 postmenopausal metastasised breast cancer patients to receive either 40mg of the antioestrogen tamoxifen per day or the combination 40mg tamoxifen plus 75µg of the antiprolactin CV 205-502 orally and thrice a day 0.2mg of octreotide subcutaneously as first line endocrine therapy [10]. An objective response was found in 36 % of patients treated with tamoxifen in monotherapy and in 55% of patients treated with combination therapy. Median time to progression was 33 weeks for patients treated with tamoxifen and 84 weeks for patients treated with combination therapy. Unfortunately, the numbers were too small to draw definite conclusions and the addition of CV 205-502 did not permit direct assessment of the contribution of the octreotide to overall gain when compared to tamoxifen in monotherapy. Ingle et al included 135 eligible postmenopausal metastasised breast carcinoma patients which were randomized to tamoxifen 10mg twice daily alone or tamoxifen plus octreotide at a dose of 150µg thrice daily [11]. The two groups were well balanced, except the tamoxifen group had higher proportions of patients with visceral disease (50% versus 37%) and of patients with a disease free interval longer than 5 years (47% versus 34%). The median time to progression was estimated to be 14.2 months with tamoxifen and 10.3 months with tamoxifen plus

octreotide. No significant difference in progression free survival time (P=0.26) and distribution of survival times (P=0.92) was found between both groups. When considering the 106 patients with measurable disease, the objective response rate was 49% with tamoxifen alone and 43% with tamoxifen plus somatostatin analogue (P=0.70). Of interest, the percentage of decline in serum IGF-1, from pretreatment levels to those following 3-6 weeks of treatment, was significantly greater (P<0.01) with tamoxifen plus octreotide than with tamoxifen alone.

So far, no convincing clinical benefit of adding somatostatin analogues to tamoxifen has been demonstrated in metastasised breast cancer patients. The question is, can we really expect benefit of adding somatostatin analogues to tamoxifen in patients with metastasised breast cancer?

Firstly, although the combination of tamoxifen and somatostatin results in a more pronounced reduction of tumour growth factor IGF-1 levels, the level of circulating IGF-1 may be less relevant. In this regard, Guvakova and Surmacz demonstrated that in ER-positive MCF-7 tamoxifen-responsive breast cancer cells and in derived clones overexpressing either IGF-1R or its major substrate IRS-1, a 4-day treatment with 10nM tamoxifen produced a similar cytostatic effect, regardless of the amplification of IGF signalling (figure C) [(12)]. It was shown that tamoxifen resulted in functional uncoupling of ligand-receptor signalling by downregulation of IGF-1 induced tyrosine phosphorylation of IGF-1R and inhibition of IRS-1/phosphatidylinositol 3' (IP3)-kinase signalling. Thus, tamoxifen treatment when effective may result in functional uncoupling of IGF-1/IGF-1R signalling in patients suffering from breast carcinoma. This could explain why the higher reduction in IGF-1 levels obtained by combining tamoxifen and somatostatin does not result in a higher response rate when compared to tamoxifen in monotherapy.

Secondly, cell line experiments suggest that in breast carcinoma the SSTR, predominantly subtype 2, is an oestrogen response element that is upregulated in the presence of oestradiol and downregulated in the presence of antiestrogens such as tamoxifen (figure A), similar to the progesterone receptor. Oestradiol was shown to time- and dose-dependently upregulate transcription of the SSTR2 gene in both oestrogen receptor (ER)-positive, endocrine-responsive breast tumour cell lines, T47D and ZR75-1, but not in the ER-negative MDA MB231 cell line (figure C) [(13)]. Conversely, in both T47D and ZR75-1 cells the pure antioestrogen ICI 182 780 inhibited oestradiol-induced SSTR2 mRNA expression. Thus, in breast carcinoma patients, effective antioestrogen treatment may result in downregulation of

SSTR thereby preventing somatostatin analogues from exerting their direct tumour growth inhibitory activity.

Hence, as tamoxifen administration in oestrogen-dependent tumours may result in downregulation of the somatostatin receptor and inhibition of phosphorylation of IGF-1R, somatostatin could neither directly or indirectly exert its inhibitory activity.

If cell line data prove correct in humans, response to tamoxifen treatment could be monitored noninvasively by means of sequential somatostatin receptor scintigraphy respectively prior to and rapidly, within 3 weeks, following tamoxifen treatment initiation. Uptake of radiolabelled somatostatin derivatives through SSTR2 binding in human breast carcinoma has been previously described [(14)]. In tamoxifen-responsive tumours, and not -unresponsive tumours, a decrease in tumour uptake of radiolabelled octreotide is to be expected.

FIGURES

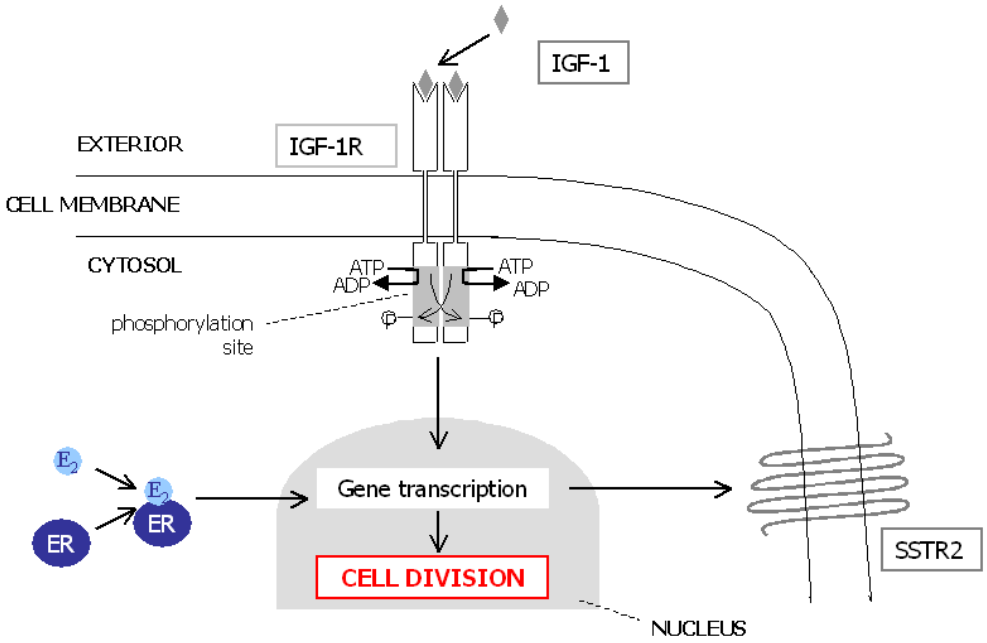

Figure A . Binding of oestradiol (E_2) to a functional oestrogen receptor (ER) in oestrogen-dependent tumour cells results in upregulation of the somatostatin receptor (subtype 2, SSTR2). Insulin like growth factor-1 (IGF-1) binding to the IGF-1 receptor (IGF-1R) results in autophosphorylation, triggering a cascade of events, ultimately leading to cell division.

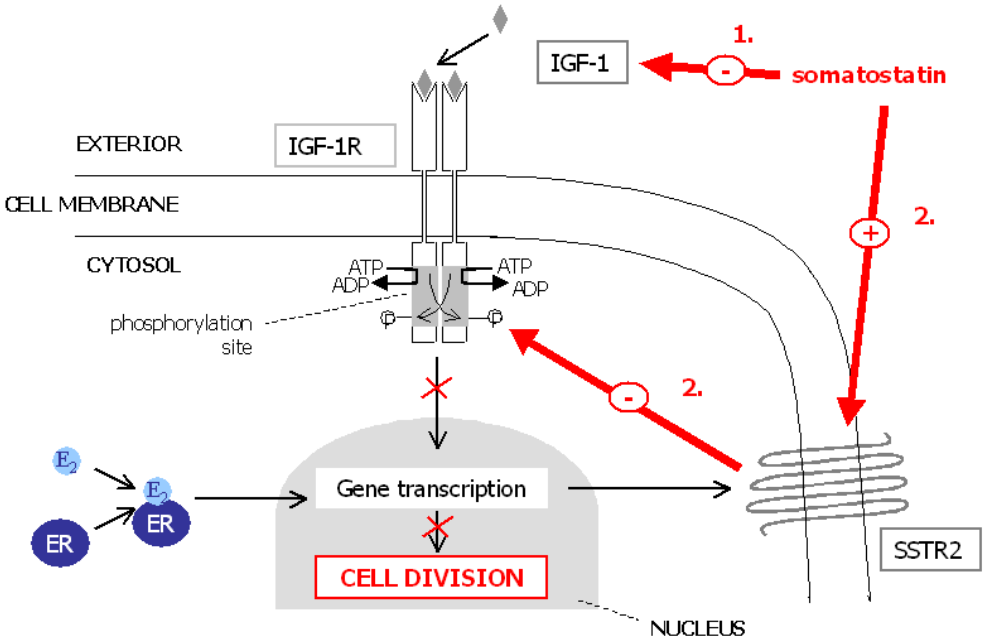

Figure B. Somatostatin decreases cell proliferation indirectly (1.) by reducing the circulating levels of the tumour growth factor IGF-1 and directly (2.) through binding to its receptor thereby activating a phosphatase which can dephosphorylate IGF-1R thereby also inhibiting signalling to the nucleus and thus cell proliferation.

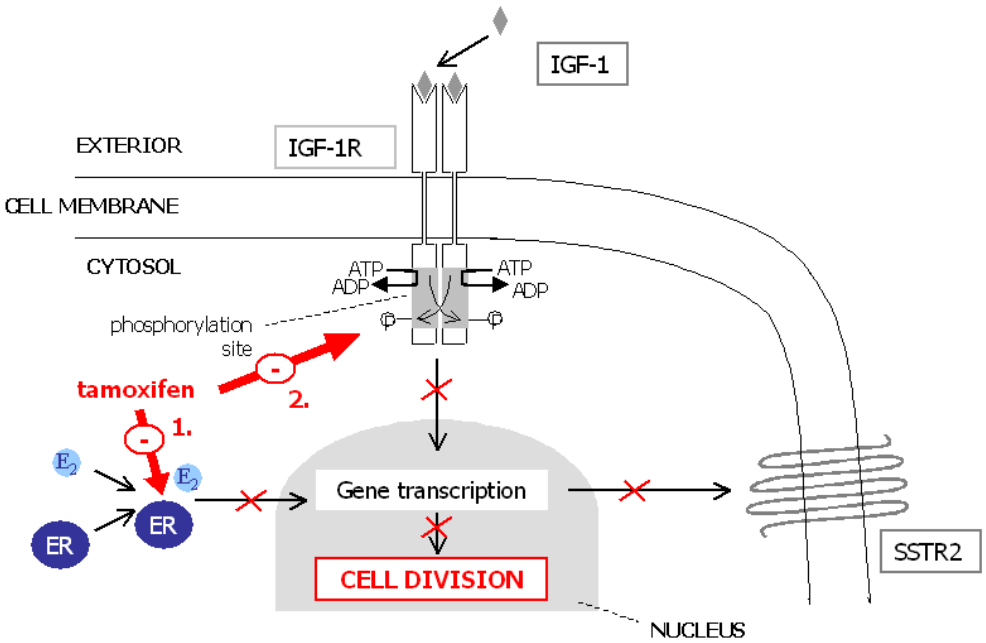

Figure C. Tamoxifen prohibits E_2 from binding to ER, in oestrogen-dependent tumour cells resulting in downregulation of SSTR2 (1.). Additionally tamoxifen inhibits phosphorylation of IGF-1R (2.). In this setting, somatostatin can neither directly or indirectly exert its inhibitory activity.

REFERENCES

1. Setyono-Han B, Henkelman MS, Foekens JA, et al: Direct inhibitory effects of somatostatin (analogues) on the growth of human breast cancer cells. Cancer Res 47: 1566-1570, 1987

2. Scambia G, Panici PB, Baiocchi G, et al: Antiproliferative effects of somatostatin and the somatostatin analog SMS 201-995 on three human breast cancer cell lines. J Cancer Res Clin Oncol 114: 306-308, 1988

3. Pollak MN and Schally AV: Mechanisms of antineoplastic action of somatostatin analogs. Proc Soc Exp Biol Med 217: 143-152, 1998

4. Osborne CK, Clemmons DR, and Arteaga CL: Regulation of breast cancer growth by insulin-like growth factors. J Steroid Biochem Mol Biol 37: 805-809, 1990

5. Surmacz E: Function of the IGF-I receptor in breast cancer. J Mammary Gland Biol Neoplasia 5: 95-105, 2000

6. Vennin P, Peyrat JP, Bonneterre J, et al: Effect of the long-acting somatostatin analogue SMS 201-995 (Sandostatin) in advanced breast cancer. Anticancer Res 9: 153-155, 1989

7. Stolfi R, Parisi AM, Natoli C, et al: Advanced breast cancer: response to somatostatin. Anticancer Res 10: 203-204, 1990

8. Di Leo A, Ferrari L, Bajetta E, et al: Biological and clinical evaluation of lanreotide (BIM 23014), a somatostatin analogue, in the treatment of advanced breast cancer. A pilot study by the I.T.M.O. Group. Italian Trials in Medical Oncology. Breast Cancer Res Treat 34: 237-244, 1995

9. Ingle JN, Kardinal CG, Suman VJ, et al: Octreotide as first-line treatment for women with metastatic breast cancer. Invest New Drugs 14: 235-237, 1996

10. Bontenbal M, Foekens JA, Lamberts SW, et al: Feasibility, endocrine and anti-tumour effects of a triple endocrine therapy with tamoxifen, a somatostatin analogue and an antiprolactin in post-menopausal metastatic breast cancer: a randomized study with long-term follow-up. Br J Cancer 77: 115-122, 1998

11. Ingle JN, Suman VJ, Kardinal CG, et al: A randomized trial of tamoxifen alone or combined with octreotide in the treatment of women with metastatic breast carcinoma. Cancer 85: 1284-1292, 1999

12. Guvakova MA and Surmacz E: Tamoxifen interferes with the insulin-like growth factor I receptor (IGF-IR) signaling pathway in breast cancer cells. Cancer Res 57: 2606-2610, 1997

13. Xu Y, Song J, Berelowitz M, et al: Estrogen regulates somatostatin receptor subtype 2 messenger ribonucleic acid expression in human breast cancer cells. Endocrinology 137: 5634-5640, 1996

14. van Eijck CH, Krenning EP, Bootsma A, et al: Somatostatin-receptor scintigraphy in primary breast cancer. Lancet 343: 640-643, 1994

OUTLINE OF THE THESIS

This thesis **aim**s to elucidate the role of oestrogen in SSTR expression and to explore the potential of the visualization of this molecular event by means of nuclear medicine techniques for selection of breast cancer patients likely to respond to endocrine treatment.

In **chapter 2** receptor imaging in oncology by means of nuclear medicine is reviewed extensively.

In **chapter 3** oestrogen-mediated regulation of SSTR expression is demonstrated on a protein level in 3 human breast cancer cell lines.

In **chapter 4** the biodistribution and dosimetry of ^{99m}Tc-depreotide (P829) is validated in patients suffering from breast carcinoma.

In **chapter 5** ^{99m}Tc-depreotide scintigraphy is compared with ^{99m}Tc-MDP bone scan for the detection of bone metastases in patients with breast cancer.

In **chapter 6** the potential of sequential 99mTc-depreotide scintigraphy for early endocrine therapy prediction is investigated in advanced breast cancer patients.

In **chapter 7** the general discussion and future perspectives are given.
In **chapter 8** the thesis is briefly summarized in English, French and Dutch.

CHAPTER TWO

Receptor Imaging in Oncology by means of Nuclear Medicine: Current Status

Bieke Van Den Bossche[1] and Christophe Van de Wiele[1].

[1]Division of Nuclear Medicine, Ghent University Hospital, Ghent, Belgium

Journal of Clinical Oncology 2004; 22(17):3593-3607.

---

1. Abstract

To date, our understanding of the role of receptors and their cognate ligands in cancer is being successfully translated into the design and development of an arsenal of new, less toxic and more specific anticancer drugs. As most of these novel drugs are cytostatic, objective response as measured by morphological imaging modalities (eg, computed tomography or magnetic resonance imaging) cannot be used as a surrogate marker for drug development or for clinical decision making. Positron emission tomography (PET) can be used to image and quantify the in vivo distribution of positron-emitting radioisotopes such as oxygen-15, carbon-11 and fluorine-18 that can be substituted or added into biologically relevant and specific receptor radioligands. Similarly, single-photon emission computed tomography (SPECT) can be used to image and quantify the in vivo distribution of receptor-targeting compounds labeled with indium-111, technetium-99m and iodine-123. By virtue of their whole-body imaging capacity and the absence of errors of sampling and tissue manipulation as well as preparation, both techniques have the potential to address locoregional receptor status noninvasively and repetitively. This article reviews available data on the in vivo evaluation of receptor systems by means of PET or SPECT for identifying and monitoring patients with sufficient receptor overexpression for tailored therapeutic interventions, and also for depicting tumor tissue and determining the currently largely unknown heterogeneity in receptor expression among different tumor lesions within and between patients.

2. Introduction

Key to the coordination of the functions of individual cells within the intact organism is intercellular communication, a means by which the individual cell is regulated in its specialized functions in a manner that serves the integrated needs of the organism as a whole. The process of intercellular signaling is achieved through myriad molecules that interact

specifically with their respective docking sites or receptor proteins. Subsequent to binding of ligand, either in endocrine, paracrine or autocrine function, the receptor proteins serve a transducing function and signal to intracellular portions of themselves or other associated proteins that ligand has been bound. This in turn activates specific effector pathways, resulting in metabolic and structural changes in the cell that constitute the signature effect of the agonist. Many receptor systems are widely expressed, suggesting a core of regulatory interactions that are common to all cell types. Under normal physiological conditions, receptors and their cognate ligands collaborate and succeed in selecting one of a few mutually exclusive programs: temporary quiescence, cell division, terminal differentiation or activation of differential activities, senescence, or apoptosis (programmed cell death). However, in cancer, several receptor systems are subverted, most commonly by mutations, ranging from upregulation, downregulation and deregulation to deactivation, deletion or constitutive activation.

To date, our understanding of the role of receptors and their cognate ligands in cancer is being successfully translated into the design and development of an arsenal of new, less toxic and more specific anticancer drugs (eg, growth-factor– and receptor-specific inhibitors). These drugs are designed specifically to correct the precise molecular abnormalities that are responsible for the causation and progression of human tumors. Because most of these novel drugs are cytostatic, objective response as measured by morphological imaging modalities eg, computed tomography [CT] or magnetic resonance imaging) cannot be used as a surrogate marker for drug development or for clinical decision making.

Although survival is the gold standard end point for registration of an experimental anticancer drug, its use for guiding early clinical development decisions is not practical. One alternative would be an end point of time to progression (TTP), suggesting that stable disease will result from cytostatic therapy. However, in the past, criteria for determining progressive disease and their diagnostic correlates have not been standardized, which is one of the principal reasons that TTP usually is not an acceptable registration end point for the Food and Drug Administration. In addition, accurate information related to prior treatment, extent of disease, comorbidity, and performance status at regular intervals in control patients is not only difficult to collect in a systematic fashion but is also difficult to analyze appropriately. Thus, the opportunity presented is to replace morphological imaging criteria and clinical criteria such as TTP by more specific end points that are made for specific molecular receptor targeting pathways. Although the use of nucleic acid microarrays is a potential alternative, the

need for repetitive invasive biopsies does not allow the assessment of heterogeneity between tumor lesions or of sequential changes within one lesion in routine clinical practice. In addition, levels of nucleic acids are not necessarily related to protein levels.

Positron emission tomography (PET) can be used to image and quantify the in vivo distribution of positron-emitting radioisotopes such as oxygen-15, carbon-11 and fluorine-18 (^{18}F) that can be substituted or added into biologically relevant and specific receptor radioligands. Similarly, single-photon emission computed tomography (SPECT) can be used to image and quantify the in vivo distribution of receptor-targeting compounds labeled with indium-111 (^{111}In), technetium-99m (^{99m}Tc) and iodine-123 (^{123}I). By virtue of their whole-body imaging capacity and the absence of errors of sampling and tissue manipulation as well as preparation, both techniques have the potential to address locoregional receptor status noninvasively and repetitively. Thus, in vivo evaluation of receptor systems by means of PET or SPECT might prove useful not only to identify and monitor patients with sufficient receptor overexpression for tailored therapeutic interventions, but also to depict tumor tissue and determine the currently largely unknown heterogeneity in receptor expression among different tumor lesions within and between patients.

3. SPECT versus PET

The gamma camera or SPECT camera is able to detect scintillations (flashes of light) produced when gamma rays resulting from radioactive decay of single-photon–emitting radioisotopes interact with a sodium iodide crystal at the front of the camera (1).The scintillations are detected by photomultiplier tubes, and although the areas of crystal seen by tubes overlap, the location of each scintillation can be computed from the relative response in each tube (Fig 1). The energy of each scintillation is also measured from the response of the tubes, and the electrical signal to the imaging computer consists of the location and photon energy. In front of the crystal resides a collimator that is made of lead and usually manufactured with multiple elongated holes (parallel-hole collimator). The holes allow only gamma rays that are traveling perpendicular to the crystal face to enter. The gamma photons absorbed by the crystal therefore form an image of the radiopharmaceutical distribution in front of the camera. By rotating the camera around the patient and acquiring images at different angles, tomographic images or SPECT images can be generated through the use of specific reconstruction algorithms (2).

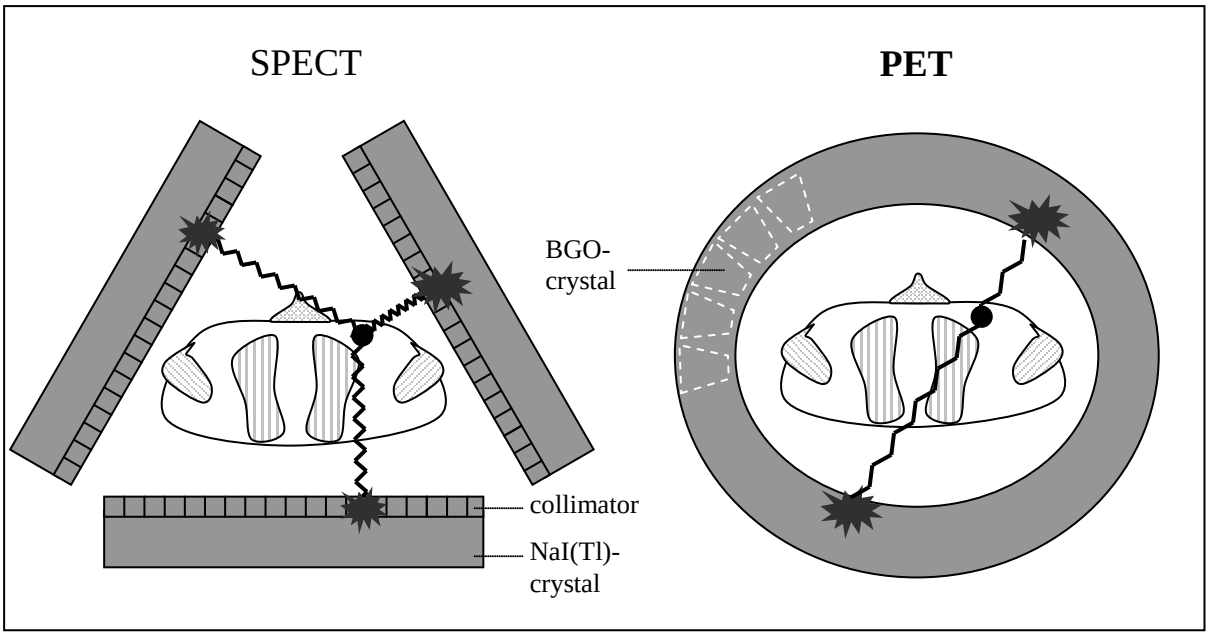

BGO, bismuth germanate; NaI, sodium iodide; Tl, thallium.

Figure 1. Single-photon emission computed tomography (SPECT) versus positron emission tomography (PET). Triple headed gamma-camera (left). Through rotation of the camera around the patient, tomographic SPECT images are acquired. Dedicated PET camera (right). Through simultaneous detection of two annihilation photons, the localization of the positron emitter is measured (coincidence detection).

As with SPECT, PET relies on computerized reconstruction procedures to produce tomographic images; PET, however, indirectly detects positron emission (3). Positrons, when emitted by radioactive nuclei, combine with an electron from the surroundings and are annihilated. On annihilation, both the positron and the electron are then converted to electromagnetic radiation in the form of two high-energy photons, which are emitted 180 degrees away from each other. It is this annihilation radiation that can be detected externally and is used to measure both the quantity and the location of the positron emitter. Simultaneous detection of two of these photons by detectors on opposite sides of an object places the site of the annihilation on or about a line connecting the centers of the two opposing detectors. At this point, the distribution of annihilations is mapped by computer. If the annihilation originates outside the volume between the two detectors, only one of the photons can be detected, and because the detection of a single photon does not satisfy the coincidence condition, the event is rejected.

Given that radioisotopes suitable for PET have a short half-life (eg, 110 min for ^{18}F), an on-site cyclotron is needed for production of such isotopes (4). In addition, special radiosynthesis

facilities are required, restricting the availability of noncommercially available PET radiopharmaceuticals to specialized centers. In contrast, the synthesis of SPECT radiopharmaceuticals is relatively less expensive. Because the half-lives of the isotopes used in SPECT are longer than those of isotopes used in PET (hours versus minutes), longer acquisition times are possible in SPECT. This allows receptor imaging at equilibrium, a prerequisite in order to obtain reliable information with respect to relative receptor density measurements. Conversely, the resolution of a conventional PET camera is twice as good as that of a conventional gamma camera, and PET allows for more accurate quantitation when compared with SPECT.

4. Receptor radiopharmaceutical prerequisites

The general structure of a radiophamaceutical targeting a receptor is shown in Figure 2 (5). A ligand such as a peptide, protein, hormone or organic molecule for the target has to be defined. The second important component of the molecule is the radioactive part. This consists of an organic molecule (chelator or tyrosine) to which the radionuclide can be attached. The two parts can be connected with a linker (organic molecule). In some special cases, the radionuclide can be attached directly to the ligand.

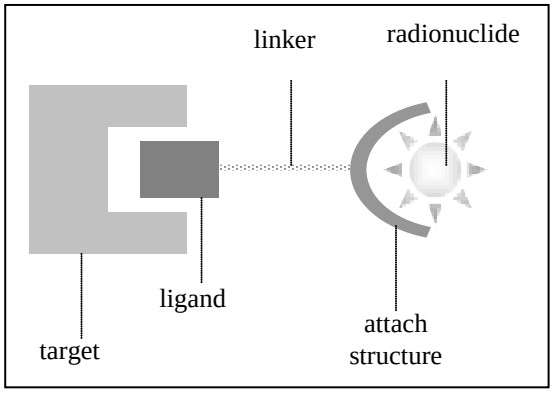

Figure 2. Body of a radiopharmaceutical.

For imaging purposes, receptor radiopharmaceuticals need to fulfill the following three requirements: high specific activity (radioactivity per unit mass of the radiopharmaceutical, > 1Ci/mmol) because receptors are satiable systems with limited uptake capacity in vivo, high receptor affinity with low nonspecific binding, and appropriate metabolic and clearance characteristics (6;7). Because of the high specific activity available with receptor radiopharmaceuticals and the concern of excessive dosimetry to humans, the dissociation constant (K_d) as a measure of affinity of the ligand to the receptor, should be in the range of 0.1-50 nmol/L. If affinity is too high (K_d < 0.1 nmol/L), the rate-limiting step becomes a

measure of flow rate or membrane transport, rather than the ligand-receptor binding process. If affinity is too low (K_d > 50 nmol/L), the signal-to-noise ratio may be significantly decreased because of the large amount of unbound free tracer in circulation, and tumor visualization may merely reflect vasculature or blood volume in the tissue of interest. Low nonspecific binding and appropriate metabolic and clearance characteristics are required to obtain optimal tumor-to-background ratios that allow depiction of tumor lesions.

Finally, to reduce adverse pharmacological effects and decrease receptor occupancy or saturation of receptor sites, usually, only a minimized amount of radiopharmaceutical is administered. Nevertheless, occasionally, some radiopharmaceuticals may have significant pharmacological effects, even at sub-nanogram quantities.

5. Imaging intracellular receptors

I. ESTROGEN RECEPTOR IMAGING

Radiolabeled estradiol derivatives: *Pretreatment imaging.* Several halogenated derivatives of estradiol, such as vynilestradiol (steroidal) and hexestrol (nonsteroidal) have been synthesized, a number of which have reached the clinical stage. These include substituents of estradiol halogenated at the 16α-position and vynilestradiol derivatives halogenated at the 17α-position, either in cis (Z) or trans (E) position (Table 1).

In a feasibility study using a bromoestradiol tracer on four primary and four metastatic breast carcinoma patients, McElvany et al. found three abnormal scintigrams in patients with primary breast carcinoma, two of whom underwent a biopsy and found to be estrogen receptor (ER) -positive (8). Two patients with advanced tumors who were receiving antiestrogen therapy showed negative results and one abnormal scan was obtained in an ER-positive patient with chest wall metastases. No uptake of tracer was seen in the single ER-negative primary tumor.

In a series of 28 breast carcinoma patients, SPECT imaging performed using 16α-123-iodoestradiol-17β demonstrated eight of nine patients with histologically proven breast cancers, four of which were ER-positive, three were ER-negative and two were of undetermined ER status (9). There was one false-negative of unknown ER status. Four of four metastases and six of six known axillary nodes were visualized. Initially there were 12 false-positive axillary nodes and two false-positive scans showing mediastinal involvement. However, with clinical follow-up, two of 12 axillae and one of 12 mediastinums were found

to contain cancer of adequate volume to be detected by common radiographic techniques. In a series of 21 women, 14 with breast carcinoma and seven with benign breast tumors, seven of nine ER-positive (> 10 fmol/mg tissue) tumors were visualized using 16α-123-iodoestradiol-17β, whereas all 12 ER-negative tumors (seven of which had benign disease) were not (10). In 42 patients of 62 patients with known ER status, an overall sensitivity of 66% (20 of 30) and specificity of 92% (11 of 12) was found by Scheidhauer et al. in a multicenter study using 16α-123 iodoestradiol-17β. In a series of 29 women undergoing diagnosis for primary or recurrent breast carcinoma, using 16α-123 iodoestradiol-17β, Kenady et al. found that scintigraphic detection was most noteworthy in patients with chest wall tumors and inflammatory breast cancer (12). Data on the sensitivity and specificity when compared with ER status in this series, however, are lacking.

Mintun et al. found a correlation of 0.96 (P <.001) between 18-fluorine-fluoroestradiol (^{18}F-FES) uptake values, expressed as percentage of injected dose (ID)/ ml x 10^{-4}, and ER concentration (in femtomoles per milligram protein) of breast tumor specimen obtained from nine patients with primary breast carcinoma (13). This high correlation, however, is likely an overestimation because the linear regression line in this series is fully determined by the two patients with the highest ER concentration. In a subsequent study by the same group on 16 patients with clinical or radiographic evidence of metastatic disease, metastatic lesions within the regions imaged on PET studies were identified by other imaging studies in 14 of 16 patients (14). The pretherapy PET images with FES demonstrated accumulation of the radiopharmaceutical in the lesion or lesions of 11 of these 14 patients (79%) and in 53 of 57 lesions (93%). In vivo regional uptake values expressed as percentage ID per milliliter, however, were not systematically available. On the basis of the available data in a small subgroup of seven patients, the correlation between pretherapy percentage ID per milliliter uptake versus ER status (r=0.36; P=.43) was much poorer when compared with the initial results presented by Mintun et al in primary tumors. Dehdashti et al in a series of 53 patients (32 patients with primary breast tumors and 21 with clinical or radiologic evidence of distant metastases or disease recurrence) found a good overall agreement 88% (35 of 40) between in vitro ER assays and FES-PET percentage ID per milliliter (15). Of interest, all five patients for whom results did not agree were positive on in vitro ER status but negative on FES-PET (standardized uptake value [SUV] < 1.0). Only one of these patients was treated with hormonal therapy and she did not respond.

Mortimer et al. assessed the value of FES in women with breast cancer for predicting response to systemic therapy (16). Results of FES-PET were related to ER status. Cancers were considered functionally hormone sensitive if the SUV of the lesion on FES-PET was $\geq$ 1.0 and were considered hormone resistant if FES SUV was less than 1.0. In this series, all 20 ER-negative tumors were also FES-negative. However, of the 21 ER-positive tumors, 16 were FES-positive and five were FES-negative. Thirteen patients were treated with hormone therapy, and eight (61%) responded to that therapy. Only one of five patients whose tumors were ER-positive but FES-negative received hormone therapy, and this treatment resulted in disease stabilization only. When compared with the in vitro assays of ER status, FES-PET had a sensitivity of 76 % and specificity of 100 %. More recently, the same group investigated the ability of FES-PET to detect hormone-induced changes in tumor metabolism (metabolic flare) and changes in available levels of ER, and the potential of FES-PET to predict hormonal responsiveness of breast cancer. Forty women with biopsy-proved advanced ER-positive breast cancer underwent FES-PET before and 7 to 10 days after initiation of tamoxifen therapy and results were correlated with response to hormonal treatment. Lesions of responders had higher baseline FES uptake (SUV, 4.4 $\pm$ 2.4) than those of nonresponders (SUV, 1.8 $\pm$ 1.3; P = .0007), and the degree of ER blockade was greater in the responders (mean percentage decrease, 54.8% $\pm$ 14.2%) than in the nonresponders (mean percentage decrease, 19.4% $\pm$ 17.3%; P = .0003) (17). Mankoff et al. examined the heterogeneity of ER expression in 27 patients with metastatic breast cancer from ER-positive primary tumors using dynamic FES-PET. One of 18 patients without prior hormonal therapy and two of nine patients with prior therapy had one or more ER-negative sites of disease (18).

^{123}I-labeled *cis*-methoxy-iodovinylestradiol (^{123}I-*cis*-MIVE) was injected into 19 women, eight of whom were referred for initial evaluation of breast cancer and 11 of whom were referred for postoperative follow-up (19). Nine of the latter patients had bone metastases. The primary tumor (size, 8 to 10 mm) was visualized in two of four patients with high ER concentration (162 to 455 fmol/mg) and was not detectable in four patients with low ER concentration (6 to 32 fmol/mg). Axillary lymph node metastases were detected in two patients and bone metastases were detected in four of 10 patients with metastasized disease.

Rijks et al. reported on their results obtained using ^{123}I-*cis*-MIVE in 25 patients, 12 with primary breast cancer and 13 with metastasis evident from other imaging modalities (20). Planar imaging showed uptake in 11 of 12 primary carcinomas and in nine of 13 patients with metastasized disease. ER immunohistochemistry data available in 10 of 12 primary and 11 of

13 patients with metastasized disease were concordant with ^{123}I-*cis*-MIVE imaging in all 10 primary and in 10 of 11 patients with metastasized disease.

Authors	Tracer	Nb patients	M0/M+	ER status assessment	cut-off for ER-positivity
McElvany et al., 1982	BES	8	4/4	LBA	$\geq$ 10
Preston et al., 1990	IES	28	NA	NA	NA
Schober et al., 1990	IES	14	NA	LBA	$\geq$ 10
Scheidhauer et al., 1991	IES	30	19/11	LBA	$\geq$ 10
Kenady et al., 1993	IES	29	NA	LBA	$\geq$ 3
Mintun et al., 1988	FES	13	13/0	LBA	$\geq$ 3
McGuire et al., 1991	FES	16	3/13	LBA	$\geq$ 3
Dehdashti et al., 1995	FES	53	32/21	LBA	$\geq$ 3
Mortimer et al., 1996	FES	43	26/17	LBA	$\geq$ 3
Mankoff et al., 2000	FES	27	0/27	IHC	-/+
Mortimer et al., 2001	FES	40	19/21	IHC	-/+
Ribeiro-Barras et al., 1992	cis-MIVE	19	10/9	LBA	$\geq$ 6
Rijks et al., 1997	cis-MIVE	25	12/13	IHC	-/+
Nachar et al., 1999	cis-MIVE	10	10/0	LBA	$\geq$ 9
Bennink et al., 2001	cis-MIVE	22	22/0	IHC	-/+
Bennink et al., 2004	cis-MIVE	23	0/23	IHC	-/+

Abbreviations: ER, estrogen receptor; BES, 16$\tilde{7}$7 -bromoestradiol; LBA, ligand binding assay (units are in femtomoles per milligram cytosol protein); IES, 16α-123-iodoestradiol-17β; NA, not available; IHC, immunohistochemistry; FES, 16α-18-fluoroestradiol; MIVE, methoxy-123-iodovynilestradiol; M0, nonmetastasised; M+, metastasized; -, negative staining; +, positive staining.

Table 1. Methodologic and population characteristics of available data on radiolabeled estradiol derivative imaging in patients with breast carcinoma.

In a series of 13 patients studied by Nachar et al and referred for ^{123}I-*cis*-MIVE scintigraphy because of abnormal mammography or a suspected mass at physical examination, five of 10 histologically proven breast carcinoma showed specific tracer uptake. In eight breast carcinoma patients a good agreement with in vitro ER determination was found whereas in two patients scan results were false-positive (21). Bennink et al compared ^{123}I-*cis*-MIVE scintigraphy with immunohistologic staining for determination of ER status in 22 patients with primary palpable breast cancer. Staining was positive in 18 patients and ^{123}I-*cis*-MIVE scintigraphy was concordantly positive in 17 patients with planar imaging and in 18 patients

with SPECT imaging, resulting in sensitivities of 94% and 100%, respectively. The correlation between immunohistologic and planar scintigraphic scores of ER status was 0.72 (P<.01) (22). The same group studied the ability of ^{123}I-*cis*-MIVE scintigraphy to predict response or resistance to antiestrogen therapy in patients with metastatic ER-positive breast carcinoma. They included 23 patients with a positive ^{123}I-*cis*-MIVE scan and repeated scintigraphy 4 weeks after initiation of tamoxifen therapy. Seventeen of 21 patients with clear uptake on baseline scintigraphy showed complete blockade of ER activity on ^{123}I-*cis*-MIVE scintigraphy and four showed mixed or no blockade. All patients with clear baseline uptake and complete ER blockade after tamoxifen had a significantly longer progression-free survival (14.4 months *v* 1.8 months; P<.01) (23).

Radiolabeled estradiol derivatives*: Pre- and post-treatment imaging.* Tamoxifen treatment results in a decrease of absolute and free or bioavailable plasma estradiol as well as in an increase in blood protein-bound estradiol, resulting in a reduction of cellular uptake and membrane sequestration (24-26). In addition, tamoxifen decreases intra-tumoral estradiol synthesis resulting in a higher occupation of ERs by tamoxifen and consequently a reduced bioavailability to the free fraction of estradiol (27-29). This should result in a decrease of radiolabeled estradiol uptake after effective tamoxifen treatment that can be visualized by sequential imaging, before and as early as 3 to 4 weeks after treatment initiation. In turn, sequential imaging could thus allow prediction of response to antiestrogen treatment with a higher accuracy than that of single radiolabeled estradiol derivative imaging or ER measurements, as recently suggested using sequential ^{18}F-

FES and 11β-methoxy-^{123}I-vinylestradiol (^{123}I-z-MIVE) imaging in a small series of 11 and 23 patients, respectively, in whom tamoxifen treatment was initiated. In the latter series the accuracy for prediction of response to tamoxifen treatment was 100% (30;31).

Radiolabeled tamoxifen derivatives. To avoid the need for two scanning episodes to rapidly monitor or predict response to tamoxifen treatment, as is the case with ^{18}F-FES and ^{123}I-z-MIVE, a number of authors have focused on the development of radiolabeled tamoxifen derivatives. Because tamoxifen has several other cellular antiproliferative effects including inhibiting the intracellular signal transducer protein kinase C, binding to membranous calmodulin, and inducing functional uncoupling of breast tumor cell insulin-like growth factor-1 (IGF-1) receptors, measuring tumor uptake of radiolabeled tamoxifen could provide more accurate information about the effect of antiestrogen therapy when compared with radiolabeled estradiol derivatives (32-34). In addition, in vivo imaging of radiolabeled

tamoxifen tumor uptake, retention, and eventually efflux not only could help to increase our understanding of the action of tamoxifen, it also could help to increase our knowledge of the mechanisms involved in resistance to the drug. This in turn could provide new targets for the design of therapeutic agents that can both effectively antagonize ER-dependent pathways and circumvent or prevent the emergence of inevitable resistance to the drug in vivo. To date, tamoxifen has been labeled with ^{18}F, ^{123}I and, after borohydride coupling with diethylenetriamine pentaacetic acid (DTPA), also with ^{111}In (35;36). Human breast carcinoma xenografts were imaged successfully in rats with the latter agent. However, proof of specific receptor interaction of this tamoxifen analog by saturation studies has yet to be established.

In contrast both ^{18}F and ^{123}I tamoxifen derivatives were shown to specifically interact with the ER. In addition, PET using ^{18}F-tamoxifen recently was shown to provide useful information in predicting the effect of tamoxifen therapy in patients with recurrent or metastatic ER-positive breast cancers (37). Those tumors that showed good uptake of radiolabeled tamoxifen showed a positive response to tamoxifen therapy. Conversely, the SPECT ligand ^{123}I-dimethyl-*N*,*N*-tamoxifen (ITX) has shown favorable biodistribution and dosimetry characteristics in humans and preferential uptake in ER and progesterone receptor (PR) -positive tumors, which are more likely to respond to antiestrogen treatment (Fig 3) (38;39). Additional studies assessing the predictive value of ITX imaging for therapy response prediction to tamoxifen are mandatory.

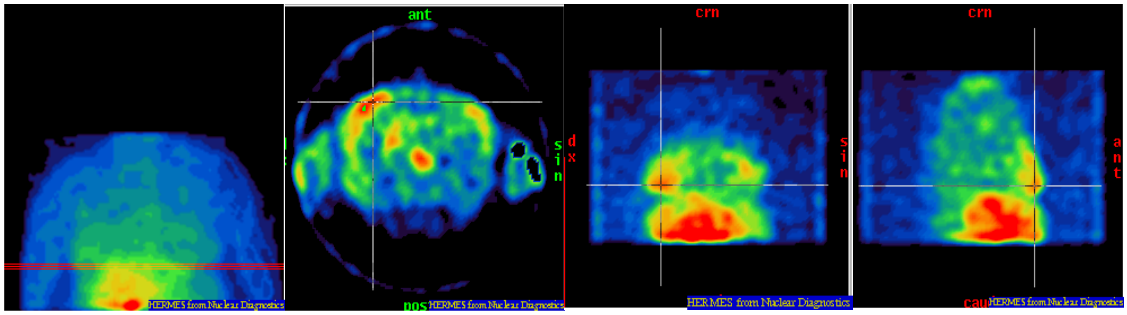

Figure 3. Imaging of breast cancer with *trans*-(iodine-123) iodomethyl-*N*,*N*-diethyltamoxifen (ITX). ITX uptake in the primary breast tumor of a 66-year-old patient with $T_3N_1M_o$ breast carcinoma as visualized by single-photon emission tomography (transaxial,sagittal and coronal slice) performed 30 minutes after injection of ITX. Physiological uptake in homolateral and contralateral noninvolved breast tissue, as well as persisting (intracardiac) blood pool activity, are also visualized.

II. PR IMAGING

Since the PR is an estrogen response element that is transcribed after effective binding of the estradiol-ER complex to DNA in ER-positive, estradiol-responsive breast tumor cells, visualization of PR-positive breast tumors by means of PR-specific radioligands may also prove valuable for therapy response prediction to antiestrogen treatment. Several PR-specific radioligands have been synthesized and validated in animal models. Their potential for PR imaging human breast tumors, however, needs to be assessed (40-42).

III. ANDROGEN RECEPTOR IMAGING

Although androgen receptor (AR) concentrations are not very reliable predictors of prostate carcinoma patient response to hormonal therapy, an AR-based radiotracer might be useful for imaging the disease to assist in its staging but especially to monitor treatment response through sequential imaging. Hormonal therapy of prostate cancer consists of treatment with inhibitors of androgen production aiming at a reduction of endogenous androgen levels and thus an increase of the number of unoccupied ARs that could be assessed noninvasively by means of receptor radiopharmaceutical imaging, thus providing information on treatment response.

Several ^{18}F-labeled androgens have been synthesized and evaluated in estrogen-treated rats, which lack the glycoprotein sex hormone-binding globulin (SHBG) that binds androgen with high affinity, with promising results (43-45). These include derivatives of testosterone, dihydrotestosterone (an in vivo reduction product of testosterone) and miboreline (a synthetic androgen). Given that SHBG in prostate model systems significantly affects the metabolism, clearance, and distribution of radiolabeled androgens in several tissues, the biodistribution and prostate imaging potential of ^{18}F-labeled dihydrotestosterone and miboreline were also studied in baboons, which are known to display high levels of circulating SHBG, similar to men (46). Prostate uptake was observed with all ^{18}F-androgens studied. The highest levels of unmetabolized radioligand in blood up to 45 minutes postinjection and prostate-to-bone ratios 37-fold greater when compared with those in rats, however, were obtained using a ^{18}F-miboreline derivative that was selected for additional evaluation in men with prostate cancer. To the best of our knowledge no studies were reported with this agent in humans.

6. Imaging cell surface receptors

Cell surface receptor-targeting radiopharmaceuticals developed for imaging human malignancies target either proteins formed of a core structure of seven transmembrane α-helical sequences with intracellular coupling to trimeric G-proteins or G-protein coupled receptors (GPCR's) (Fig 4); or target large glycoproteins that generally possess a single transmembrane sequence and tyrosine kinase activity grouped into four families (Fig 5). The families are grouped on the basis of sequence homology of their kinase domains, their structure, and the structural similarity of their ligands, the tyrosine kinase receptors (TKRs).

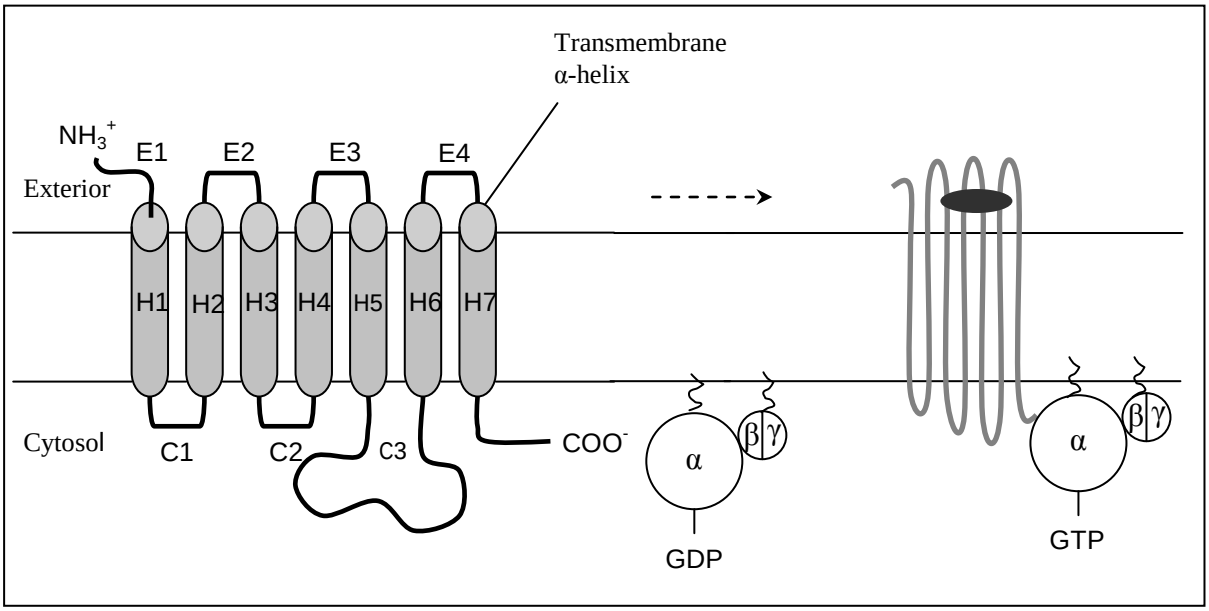

E1-E4, extracellular loops; H1-H7, transmembrane domains; C1-C3, cytosolic loops GDP, guanosine diphosphate; GTP, guanosine triphosphate.

Figure 4. Schematic diagram of the general structure of G-protein–coupled receptors. All receptors of this type contain seven transmembrane α-helical regions. Loop C3 and in some cases C2 are important for interactions with the coupled G-protein. Agonist binding results in a conformational change of the cytosolic portion of the molecule, permitting binding of G-protein complex consisting of 3 subunits termed alpha, beta and gamma.

The final common pathway for most of these receptor systems is activation of a kinase cascade culminating in activation of extracellular signal-regulated kinase (ERK). This serine plus threonine kinase translocates into the cell nucleus where it propagates the mitogenic signal by phosphorylating and activating appropriate transcription factors to induce the expression of genes necessary for initiating the cell division cycle. Cell surface growth factor receptor-targeting radiopharmaceuticals developed to date are predominantly radiolabeled

peptides and to a lesser degree radiolabeled monoclonal antibodies or fragments of monoclonal antibodies. This is not surprising because the slow blood clearance and low tumor targeting of the latter, related to their high molecular weight, often results in suboptimal tumor-to-background ratios (47). Conversely, peptides bearing specific receptor recognition units exhibit more favorable pharmacokinetic characteristics, such as rapid uptake by target tissue and rapid blood clearance (48). However, their short biological plasma half-life, caused by rapid proteolytic cleavage, may prove to be a major obstacle because peptides may not live long enough to reach their intended target. Thus, peptides may need to be metabolically stabilized for imaging purposes. This can be achieved by introducing molecular modifications such as substitution of D-amino acids for L-amino acids, incorporation of amino-alcohols, or insertion of unusual amino acids or side chains (49). After binding to their receptor, radiolabeled agonist peptides are rapidly internalized and digested by intralysosomal proteolytic enzymes. In the case of ^{123}I-labeled peptides, the radioactive iodine label usually is rapidly released from the tumor cell, compromising sensitivity. In contrast, the use of radiometal chelators (eg, DTPA or tetraazacyclododecanetetraacetic acid [DOTA]) or conjugated amino acids allowing complexation of ^{111}In or ^{99m}Tc as well as the use of prosthetic groups such as *N*- succinimidyl-4-(^{18}F)-fluorobenzoate for incorporation of ^{18}F in peptides, results in intralysosomal entrapment of the label and/or transchelation to intracellular proteins, enhancing residence time at the target site (50). Accordingly, these residual zing labels are preferable to radioiodinated labels (51).

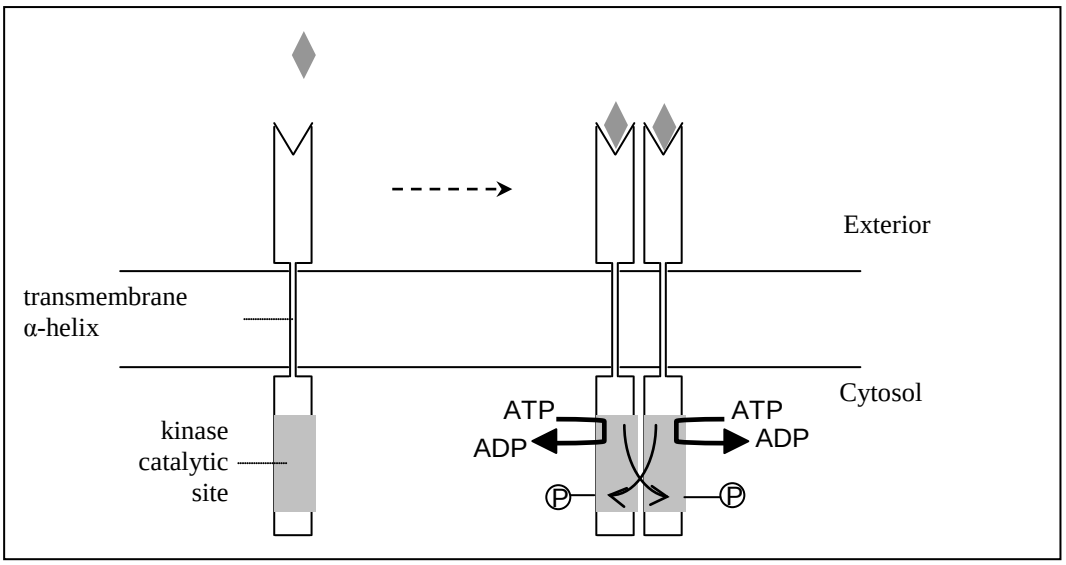

ATP, adenosine triphosphate; ADP, adenosine diphosphate.

Figure 5. General structure and activation of receptor tyrosine kinases (RTKs). Ligand binding causes autophosphorylation of a distinct set of tyrosine residues in the cytosolic domain of the dimer partner.

I. IMAGING OF G-PROTEIN–COUPLED RECEPTORS

Somatostatin receptor(s). Both in vitro and in vivo studies suggest that a wide variety of tumors express somatostatin receptors (SSTRs). Of the five different subtypes of SSTRs known to date, subtypes 1 and 2 appear to be most prominent in most SSTR-overexpressing tumors (52). The latter can be visualized using both ^{111}In- and ^{99m}Tc-radiolabeled octreotide analogs.

In neuroendocrine tumors, despite a high expression of SSTRs on growth hormone producing pituitary adenomas, the diagnostic value of ^{111}In-DTPA-octreotide (Octreoscan; Mallinckrodt Medical, Petten, the Netherlands) SSTR imaging (SSTRI) is limited because other pituitary tumors, pituitary metastases from other malignancies, and granulomatous diseases of the pituitary may also be positive (53). For the purpose of visualizing gastrinomas, ^{111}In-DTPA-octreotide scintigraphy is as sensitive as other imaging techniques combined, including angiography and ultrasonography; however, it is simpler to perform and more cost effective (54). Results of SSTRI in large cohorts of gastrinoma patients caused physicians to alter patient management in up to 25% to 50% of patients. In insulinoma patients, on the other hand, results obtained by SSTRI are poor (55-57). In carcinoid tumors, ^{111}In-DTPA-octreotide scintigraphy identifies 80% to 100% of known localizations as well as unexpected tumor sites, not suspected with conventional imaging (Fig 6) (58). In these patients, SSTRI could be used to select patients who are more likely to respond to octreotide treatment (SSTR-positive patients) or more likely to benefit from chemotherapy (SSTR-negative patients) (59).

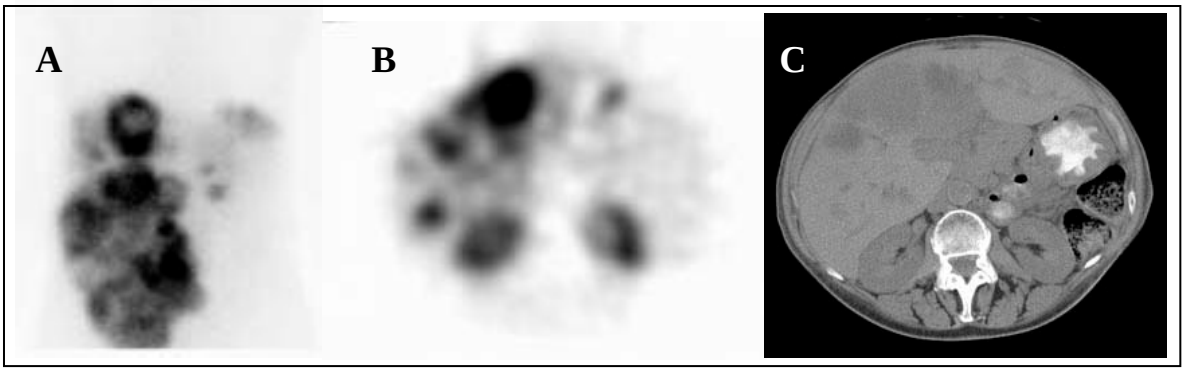

Figure 6. ^{111}In-DTPA-octreotide scan (planar and SPECT) in carcinoid tumor. The planar octreotide image (A) demonstrates multiple areas of abnormal tracer uptake within the liver which is massively enlarged in a patient with metastatic carcinoid to the liver. Transaxial SPECT (B) and CT (C) slices show multiple liver lesions on corresponding sites.

In paraganglioma, the documented potential of ^{111}In-DTPA-octreotide scintigraphy to visualize multicentricity and distant metastases, occurring in up to 10% of patients, suggests SSTRI could be used as a screening test, to be followed by morphological imaging (60;61). Early studies in small-cell lung cancer (SCLC), performed using ^{111}In-DTPA-octreotide, were encouraging, and SCLC tumors and metastases were detected in 86% to 100% of patients (62). However, more recent studies were disappointing, suggesting that ^{111}In-DTPA-octreotide scintigraphy misses a large number of metastases and primary tumors (63;64). Nevertheless, it seems that ^{111}In-DTPA-octreotide scintigraphy might have some specific value in the detection of brain involvement in patients with limited disease (65;66).

Finally, results obtained with the PET tracer gallium-86-DOTA-Tyr-octreotide (^{68}Ga-DOTA-TOC) in patients with neuroendocrine tumors proved promising, with high tumor-to-nontumor contrast and higher detection rates when compared with ^{111}In-DTPA-octreotide (67;68)

The ^{99m}Tc-labeled octreotide analog depreotide (NeoTect; Diatide Inc, Londonderry, NH), a 10–amino acid peptide with affinity for $SSTR_2$, $SSTR_3$ and $SSTR_5$ was successfully used to characterize malignancy in solitary pulmonary nodules, including SCLC (Fig 7) (69). Conversely, the detection rate of ^{99m}Tc-depreotide scintigraphy was lower than that of ^{111}In-DTPA-octreotide scintigraphy in patients with endocrine tumors (70). Another ^{99m}Tc-labeled octreotide derivative, ethylenediamine N,N-diacetic acid/hydrazinonicotinic acid–Tyr-octreotide (^{99m}Tc-EDDA/HYNIC-TOC), exhibited similar capacity for differentiation between benign and malignant solitary pulmonary nodules as ^{99m}Tc-depreotide, and overall had a higher sensitivity for the localization of SSTR-expressing tumors compared with ^{111}In-DTPA-octreotide (71;72).

In other tumors, such as in non-Hodgkin's lymphoma, a substantial number of lesions are not visualized and uptake is low when compared with neuroendocrine tumors; the role of ^{111}In-DTPA-octreotide scintigraphy in this patient population is limited (73;74). In contrast, the sensitivity of SSTRI for detection of Hodgkin's lymphoma lesions is higher than that of conventional imaging, resulting in a clinical stage upgrading in up to 30% of patients. Therefore, ^{111}In-DTPA-octreotide scintigraphy may be useful in the clinical staging and management of patients with Hodgkin's disease (75;76). Although the majority of well-differentiated astrocytomas are SSTR-positive as compared with undifferentiated glioblastomas, the prerequisite of a locally open blood-brain barrier, often unperturbed in low-grade astrocytomas, limits the role of SSTRI for the grading of glia-derived tumors (77;78).

Finally, data on SSTRI in patients suffering from breast carcinoma are limited and additional studies are needed to define its potential in this patient population (79).

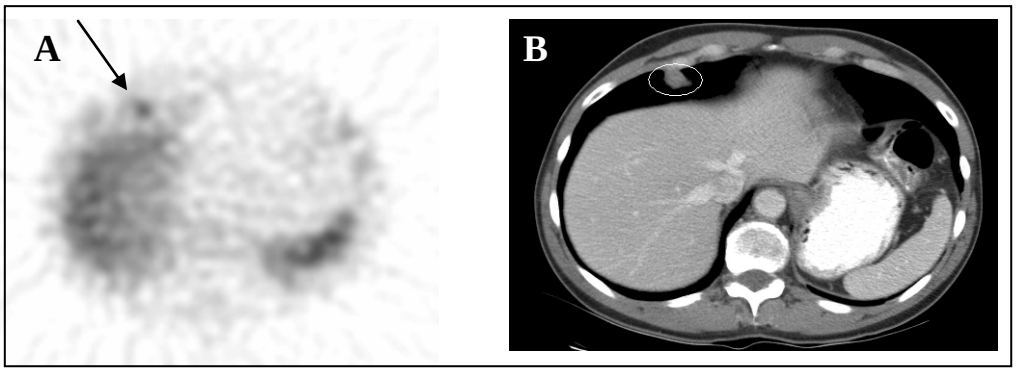

Figure 7. Technetium-99m (^{99m}Tc)-depreotide single-photon emission tomography (SPECT) in non-small-cell lung cancer (NSCLC) in a 45-year-old male, former smoker (39 pack years). Computed tomography for coronary calcium evaluation shows solitary pulmonary nodule in right lower lobe (B). ^{99m}Tc-depreotide SPECT shows a hot spot at the corresponding site (A, arrow). The patient was diagnosed with stage I squamous cell cancer after biopsy and resection.

Bombesin, gastrin releasing peptide receptor. The main mammalian member of the bombesin family of peptides is gastrin-releasing peptide (GRP), a 27–amino acid peptide isolated first from porcine antral mucosa (80). Existing experimental evidence supports an important role for this peptide in the growth of a variety of cancer tumor cell lines, either in vitro or grown in nude mice, through direct interaction with GRP receptors (GRP-Rs) (81-84). In human tumors, the role of GRP/GRP-R is less clear. Overexpression of GRP-R when compared with normal surrounding noncancerous tissue has been described in SCLC, prostate, breast, colorectal and gastric cancer (85-89). In these tumors, stimulation of GRP-R may occur through paracrine-produced GRP released by neuroendocrine cells (present in, eg, human prostate and lung), particularly because GRP may diffuse several micrometers through tissue to exert its effect on nearby cells. Conversely, stimulation of GRP-R may occur through tumor-produced and -released GRP. Interestingly, therapeutic interventions targeting the GRP/GRP-R system have proven successful in animal models as well as in humans (90-94).

During the past few years, several radiolabeled GRP analogs with delayed proteolysis have been developed for the purpose of GRP-R imaging in vivo (see Table 1). Although of potential interest, with the exception of ^{99m}Tc-RP527 (an N_3S core containing peptide), none of these ligands has been studied in humans (95-98). ^{99m}Tc-RP527 showed specific tumor uptake in four of six breast cancer and one of four prostate carcinoma patients (99).

Cholecystokinin B receptor. Gastrin and cholecystokinin, both found in the brain and the intestines, exert their functions through interaction with cholecystokinin B (CCK-B) and CCK-A receptors. Autoradiography studies demonstrate that CCK-B/gastrin receptors are overexpressed in up to 90% of medullary thyroid cancers (MTC), in approximately 60% of SCLC, and to a lesser extent in stromal ovarian tumors, gastrointestinal adenocarcinomas, neuroendocrine tumors, and malignant gliomas, which is not so for the CCK-A receptor (100;101).

Several groups have synthesized CCK peptide analogs that can be labeled with radionuclides. ^{111}In-DOTA-CCK was internalized by CCK-B–receptor-positive CA20948 cells and specifically taken up in xenografted CA20948 tumors as well as in stomach tissue (fundic mucosa) in Lewis rats (102;103). Behr et al studied 45 metastatic MTC patients, 23 of whom had known disease and 22 of whom had occult disease, with ^{111}In-DTPA-D-glutamic acid(1)-minigastrin (104). Normal uptake was confined essentially to the stomach as a result of CCK-B–receptor-specific binding and to the kidneys as excretory organs. All tumor manifestations known from conventional imaging were visualized as early as 1 hour postinjection, with increasing tumor-to-background ratios over time. In 20 of 22 patients with occult disease, at least one lesion was identified (patient-based sensitivity, 91%). Among them were local recurrences and lymph node, pulmonary, hepatic, splenic and bone marrow metastases. Kwekkeboom et al studied the efficacy of an octapeptide ^{111}In-DTPA-CCK analog in seven patients with biochemical or radiological evidence of MTC (105). In four of five patients in whom serum calcitonin levels were monitored, a significant rise was found after the injection, indicating retained biological activity of the radiopeptide. In all patients there was visualization of the CCK-B–receptor-positive stomach. In one of two patients with known MTC lesions, some of the lesions were visualized. In addition, some lesions were visualized in one of five other patients who had elevated serum tumor markers but negative localizing studies. The uptake in the presumed tumor sites was low— four-fold lower than after injection of ^{111}In-DTPA-D-Phe1-octreotide.

Vasoactive Intestinal Peptide receptor. Vasoactif intestinal peptide (VIP), a 28–amino acid peptide, has been shown to stimulate growth and proliferation of a wide variety of cancer cell lines and human cancers, including tumors of the gastrointestinal tract and lung (amongst others) (106-109). Two different types of receptors for VIP have been identified: Vpac1 and Vpac2 receptors. Although the majority of tumors express Vpac2 receptors (eg, up to 60% of

human non-small-cell lung cancer [NSCLC]), few cancers (mainly tumors of the central nervous system) express Vpac1 receptors, which have low affinity for VIP (110;111).

^{123}I-VIP scintigraphy has been used successfully to image endocrine tumors of the gastrointestinal tract, pancreatic cancer, colorectal cancer and liver cancer (112-116). In a cohort of carcinoid patients undergoing ^{123}I-VIP imaging, 82% of scans (32 of 38) were positive in primary or recurrent tumors, 82% (53 of 65) in patients with metastatic sites, and 25% (four of 16) were positive in patients with symptoms but otherwise negative work-ups. Overall, additional lesions not seen on conventional imaging were noticed in 25% (25 of 103) of scans as verified by surgical intervention or long-term follow-up (114). In a group of 60 pancreatic cancer patients, primary pancreatic tumors were visualized by ^{123}I-VIP in 90% (19 of 21) patients with disease confined to the pancreas and in 32% (eight of 25) patients with both locoregional and disease metastatic to the liver. The overall sensitivity for primary pancreatic adenocarcinoma was 58% (27 of 46 scans). Liver metastases were imaged in 29 of 32 patients (scan sensitivity, 90%) and abdominal lymph node metastases were imaged in four of five patients. In five patients, ^{123}I-VIP scintigraphy indicated the malignant lesion before CT (115). Of 80 consecutive patients with histologically verified colorectal cancer, seven of eight primary (87%) and 21 of 24 (82%) locally relapsing cancers were imaged with ^{123}I-VIP. Negative scans were obtained in all 13 patients in whom the cancer had been curatively resected. All patients with lymph node metastases showed positive ^{123}I-VIP scans (four of four), and positive scans were obtained in 25 of 28 patients (89%) with liver metastases and in two of three patients with lung metastases. In four patients with relapsing cancer, the ^{123}I-VIP scan indicated the presence of disease before CT, and in two patients the diagnosis of scar tissue instead of a local recurrence of rectal cancer as suggested by CT could be established. The authors concluded that ^{123}I-VIP receptor scanning is a sensitive method for radioimaging of colorectal cancer with the potential to provide valuable additional information to conventional radiological methods (116).

To date, there are no reports of the potential of ^{123}I-VIP to visualize NSCLC. Because of the high levels of pulmonary VIP receptor expression and related prominent physiologic lung uptake of ^{123}I-VIP, a low sensitivity for the detection of primary and secondary lung lesions is to be anticipated. However, a more favorable distribution pattern with low lung uptake in humans was recently reported for ^{99m}Tc-TP 3654, a VIP modified at the C-terminus (117). Initial results of the imaging potential of this radiopharmaceutical are promising and warrant additional study.

Sigma receptors. To date, two sigma receptor subtypes, type 1 and 2, have been identified. Overexpression of both receptor subtypes as compared with normal tissue has been reported to occur in a wide variety of neural and non-neural human cancer cell lines as well as human tumor biopsy tissue samples (118;119). Although the exact role of both receptors in tumor growth needs to be elucidated further, available data suggest that sigma-2 receptors may serve as biomarkers of tumor proliferation (120).

High-affinity sigma receptor radiopharmaceuticals developed for imaging include *N*-[2-(1'piperidinyl)ethyl]-3-[123I]iodo-4-methoxybenzamide (P-^{123}IMBA), halogenated arylsulfonamides, [18F]*N*-4'-fluoronezyl-4-(3-bromophenyl)acetamide, and a number of ^{99m}Tc-ethylenediamines (121-127). P-^{125}IMBA demonstrated saturable binding to T47D human ductal cells line and in vivo uptake in a rat mammary tumor model (121). Caveliers et al. injected 10 patients who had a newly diagnosed breast mass and two control patients with 148 to 185 MBq P-^{123}IMBA and found uptake in eight of 10 masses (122). Control patients with benign breast conditions presented a normal scan. The relationship between in vivo uptake and sigma receptor status was not established.

Neurotensin receptor. Several neurotensin analogs, among others with the dimethyl Gly-Ser-Cys-(Acm)-Gly (RP414) chelating sequence, allowing complexation of ^{99m}Tc, have been shown to bind to neurotensin receptors with high affinity (128;129). With the exception of the RP414-NT(B8-13) analog, which had biologic half-life in human plasma of up to 30 minutes, all of these are rapidly degraded in human plasma, limiting their clinical usefulness. Studies assessing the imaging potential of RP414-NT(B8-13) are underway.

Other receptors. Radiolabeled peptides targeting the melanocortin receptor-1 include the melanocyte stimulating hormone analogs ^{99m}Tc-labeled Ac-Nle-Ala-His-D-Phe-Arg-Cys-Trp-NH_2 and the metal-cyclized ^{99m}Tc-Cys-3,4,10,D-Phe-7)-a-melanocyte stimulating hormone (130). These radiopharmaceuticals may prove to be attractive vehicles for the diagnosis and treatment monitoring of human malignant melanoma.

The calcitonin receptor has been targeted using the calcitonin receptor binding peptide P1410, which has a four–amino acid chelating sequence that can bind ^{99m}Tc. This radiopharmaceutical was shown to bind to calcitonin receptor expressing T47D and MCF-7 breast tumor cells, both in vitro and in nude mice xenografts. Tumor-to-muscle and tumor-to-blood ratios were 4.5 and 5.7 (90 min postinjection), respectively. Additional studies with this radiopharmaceutical are awaited (131).

II. IMAGING OF TYROSINE-KINASE RECEPTORS

Epidermal growth factor/epidermal growth factor receptor. The epidermal growth factor receptor (EGFR) is frequently overexpressed in NCSLC, bladder, cervical, ovarian, kidney, and pancreatic cancers, and occurs with high incidence in squamous cell carcinomas of the head and neck (132-137). The predominant mechanism leading to EGFR overexpression is *EGFR* gene amplification, with more than 15 copies per cell reported in certain tumors (138). In general, elevated levels of EGFR expression are associated with late stage of disease progression and often correlate with high metastatic rate and increased tumor proliferation (139;140). Accordingly, an association between the expressions of these molecules and shortened survival has been reported in a variety of human malignancies (141-143). Several cytostatic molecules, which either target the EGFR or interfere with its signal transduction pathway, are currently being studied for their antineoplastic potential (eg, monoclonal antibody C225) (144;145).

Intracutaneous injection of ^{123}I-EGF allowed the visualization of pathologic, but also nonpathologic, lymph nodes in patients with cervix carcinoma (146). Direct intravenous injection of recombinant ^{131}I-EGF localized to squamous lung cancer efficiently; six of nine patients imaged showing positive tumor scans. The best tumor-to-background ratio was obtained at 50 to 74 hours (147). ^{111}In-DTPA-EGF was significantly internalized by EGFR expressing MDA-MB-468 breast cancer cell lines ($1.3x10^6$ EGFRs/cell) but not by MCF-7 cells ($1.5x10^4$ EGFRs/cell) (148).

Of the radiolabeled antibodies, ^{99m}Tc-labeled anti-EGF monoclonal antibody was shown to visualize NSCLC, breast tumors, and a number of other tumor types with fairly high sensitivity (149). Other radiolabeled antibodies that have been validated in vitro and in vivo in tumor-xenografted nude mice, include ^{123}I- or ^{111}In-labeled monoclonal antibody 425 and ^{111}In-DTPA-poly(ethylene glycol) monoclonal antibody 225 (150-152).

HER2/Neu receptor. The orphan Her2/Neu receptor (HER2/NeuR) is significantly enhanced in several types of human cancers, including breast, ovarian, gastric, lung, bladder, and kidney carcinomas (153-158). A number of studies suggest a pivotal role for HER2/NeuR in determining the prognosis for individual breast and lung cancer patients (159-162). In addition, HER2/NeuR is also a predictive marker for response to hormonal treatment as well as to chemotherapy in cancer patients (163). Despite the absence of ligands for HER2/Neu, HER2/Neu can be activated in response to EGF and transforming growth factor alpha by forming heterodimers with EGFR, resulting in the most potent activation of downstream

pathways and cell proliferation (164). Several approaches towards the selective prevention and interception of HER2/Neu relevant signaling are being investigated. The most effective approach so far reported is the development of the recombinant humanized version of murine monoclonal antibody 4D5, better known as trastuzumab (Herceptin; Genentech, San Francisco, CA), which is approved by the US Food and Drug Administration. In single-agent therapy, up to 15% responses have been reported in HER2/Neu–overexpressing breast cancers. In combination with paclitaxel or doxorubicin plus cyclophosphamide, trastuzumab was shown to significantly increase response duration, time to progression, and survival in first-line metastatic breast cancer patients (165).

As shown by Behr et al in breast carcinoma patients, pretherapeutic immunoscintigraphy by means of ^{111}In-DTPA-trastuzumab holds potential to more accurately predict therapeutic efficacy and cardiotoxicity compared with immunohistochemistry (the current basis for patient selection). Cardiotoxicity is a well-known adverse effect from trastuzumab therapy (166).

IGF-1 receptors. IGF-1 receptors (IGF-1R) are involved in the pathogenesis of a variety of human tumors but especially in breast and prostate carcinoma (167;168). IGF-1Rs upregulated on epithelial breast tumor cells are stimulated in a paracrine manner IGF release from stromal fibroblasts surrounding the normal and malignant epithelium (169). Several approaches have been initiated to develop small molecule inhibitors or other strategies to interfere with the pathogenic IGF-1R signaling (170;171).

In circulation, IGFs are complexed to a number of different IGF-binding proteins (IGFBPs), explaining the high blood pool activity and low tumor-to-background ratios obtained after injection of ^{123}I-IGF-1 (172). In contrast, ^{123}I-des(1-3)IGF-1, which lacks the N-terminal tripeptide Gly-Pro-Glu, does not bind significantly to one of the six known circulating binding proteins targeting the IGF-1, and yields more favorable tumor-to-background ratios in tumor mice models (unpublished data).

Vascular endothelial growth factor and fibroblast growth factor receptors. Vascular endothelial growth factor (VEGF) is one of the main inducers of endothelial cell proliferation and permeability of blood vessels through direct binding with VEGF receptor 1 (VEGFR-1) and VEGFR-2 (173). Similarly, fibroblast growth factors (FGFs) have been implicated in background angiogenesis, although their exact role is less well known. With the aim of visualizing ongoing background angiogenesis, VEGF and FGF-1 have both been radiolabeled for SPECT imaging. VEGF (165) and VEGF(121) were radiolabeled with ^{123}I (174). Both

bound more specifically to a variety of human tumor cells and tissues as compared with normal peripheral-blood cells and adjacent non-neoplastic tissue. In comparison with ^{123}I-VEGF(121), ^{123}I-VEGF(165) not only bound to a higher number of different tumors but also with higher capacity, suggesting ^{123}I-VEGF(165) may be a useful tracer for in vivo imaging, as recently confirmed in a small series of 18 patients (175).

Recombinant human FGF-1 was radiolabeled with ^{99m}Tc by the HYNIC method (176). The radiopharmaceutical retained its representative molecular mass, heparin affinity, cellular binding to both low- and high-affinity sites, and mitogenic activity. Gamma camera imaging in rats confirmed high liver uptake that was significantly decreased by heparin. Finally, FGF-2 has been directly targeted using ^{111}In-3H3, a murine monoclonal antibody that recognizes FGF-2 (177). This molecule was retained at high levels in tumor tissue expressing FGF-2 but not in non-FGF-2– producing tumors. Whether in the long run VEGF or FGF receptor targeting radioligands will be successful to monitor antiangiogenic treatment is uncertain because the detailed angiogenic profile of most human tumors still needs to be established, and it is possible that signaling through VEGFRs and FGFRs may be subject to acquired resistance mechanisms over time.

7. General discussion

Intracellular Receptors

The tumor's need of estradiol to bring about a biologic effect is highly variable among tumoral and can vary over time within tumors, depending on local environmental conditions (178). The local estradiol needs are provided through both uptake and local biosynthesis, which in ER-positive tumors are inversely related (179). Thus, a lack of concordance between radiolabeled estradiol uptake and ER status, as well as of predictive value of radiolabeled estradiol uptake for tamoxifen therapy response, may be anticipated. Currently, available data on imaging of radiolabeled estradiol derivative uptake in human breast carcinoma for measuring ER status in vivo are limited to halogenated estradiol-17β and vynilestradiol derivatives (8-23). Because of the use of different methodologies and cutoff values for measuring ER positivity, the use of both quantitative PET and semiquantitative SPECT, and the difference in patient populations studied, direct comparison of these data is not possible. Individual data, however, fail to substantiate a direct relationship between estradiol receptor radioligand uptake and ER status, in keeping with pathophysiologic findings.

Most of the hormonal treatment strategies targeting the ER pathway result in a decrease of absolute and free or bioavailable plasma estradiol as well as in an increase in steroid-binding-protein–bound estradiol, resulting in a reduction of cellular uptake and membrane sequestration (24-26;180).

In addition, blocking agents such as antiestrogens decrease intratumoral estradiol synthesis, resulting in a higher occupation of ERs by the antiestrogen itself, and consequently, a reduced availability to the already reduced available free fraction of estradiol (27-29). Theoretically, this should also result in a decreased uptake of radiolabeled estradiol derivatives after tamoxifen treatment initiation when compared with baseline uptake. Available data, although limited, support the usefulness of sequential radiolabeled estradiol derivative imaging for the purpose of predicting response to treatment as early as 1 week after treatment initiation, in keeping with pathophysiologic data (30;31).

Reported intratumoral levels of tamoxifen and its metabolites after steady-state are five- to seven-fold greater when compared with serum or plasma levels, suggesting accumulation against a concentration gradient (181;182). In patients treated for less than 2 weeks with tamoxifen 30 mg/d, a significant difference in the intratumoral tamoxifen concentration between ER-positive and ER-negative tumors was observed (450.1 ± 75.3 and 120.9 ± 49.9 ng/g, respectively; $P = .04$) (183). However, after at least 2 weeks of therapy, approaching steady-state conditions, no significant difference was found, with both ER-positive and ER-negative tumors accumulating high intratumoral concentrations. Thus, both ER-positive and ER-negative breast tumors progressively accumulate tamoxifen but ER-positive tumors do so much more rapidly. The use of a bolus injection of ITX and consecutive imaging should allow for this difference in ER-related uptake kinetics to emerge visually, with higher expected uptake values for ER -positive tumors. However, given that the apparent distribution volume for tamoxifen is 50 to 60 L/kg, suggesting extensive tissue binding related to its lipophilic characteristics, a high background activity may be anticipated (184). In this regard, in a study from patients receiving 40 mg/d for at least 30 days (ie, steady-state), tamoxifen and its metabolites were found to accumulate in nonmalignant human tissues 10- to 60-fold above serum levels expressed as nanograms per gram wet weight tissue to nanograms per milliliter serum (185). Despite this drawback, depiction of uptake of ^{123}I- and ^{18}F-labeled tamoxifen derivatives in human breast carcinoma has proven feasible, albeit with fairly low tumor-to-background ratios (37;39). Although uptake of ^{18}F-tamoxifen has been shown to provide useful information in predicting the effect of tamoxifen therapy, this was only true in a limited

number of patients (37). Larger studies assessing the potential of radiolabeled tamoxifen derivatives for predicting response to tamoxifen therapy are mandatory.

Although more significant correlations with the response to hormonal treatment in clinical studies have been observed with PR positivity than with ER positivity, to date, a clinically useful PR-targeting radiopharmaceutical is lacking (40;186). Similarly, attempts to delineate the AR in humans also have been less successful than for the ER. A number of derivatives have been suggested, but have had only limited evaluation in humans (40;43;46).

Cell Surface Receptors

The concept that targeting cell surface receptor–expressing tumor cells in vivo by means of a radiolabeled ligand is feasible and clinical relevant is now well substantiated. Multiple studies have shown that ^{111}In-DTPA-octreotide is an effective imaging agent that can be useful in the management of patients with neuroendocrine tumors not only for the detection of occult metastases and monitoring therapy, but also for predicting response to therapy with octreotide or beta-emitting analogs (eg, yttrium-90-DOTA-Tyr(3)-octreotide) (54, 58-62,65,66,187). As compared with ^{111}In-labeled octreotide, the recently developed ^{99m}Tc-labeled octreotide analogs have several advantages, such as reduced radiation burden, improved availability, and improved image quality. Nevertheless, only one analog, ^{99m}Tc-depreotide, has become commercially available and introduced in clinical practice (67). In the future, both ^{111}In-DTPA and ^{99m}Tc-labeled octreotide analogs are likely to be replaced by PET analogs such as ^{68}Ga-labeled octreotide analog. The higher sensitivity and better resolution of PET allows a more straightforward detection of small tumors or tumors bearing only a low density of SSTRs, such as breast carcinoma (67;68).

Aside from SSTRs, a large variety of other cell surface receptors appear to be (over)expressed on a multitude of tumor types, and few radiopharmaceuticals targeting these receptors have reached the clinical stage and have been tested in phase I or II studies. In a number of clinical studies, radiolabeled VIP has shown promising results in imaging a broad variety of cancer types (112-117). Behr et al and others have introduced CCK-B receptor–binding peptides for imaging of CCK-B receptor–expressing tumors (104,105). Although these radiopharmaceuticals may in the future prove relevant in the clinical oncologic practice, at this point it is too early to appreciate their clinical potential.

In summary, radiolabeled receptor-binding pharmaceuticals allow for noninvasive assessment of regional receptor proteomics in vivo by means of nuclear medicine. Information obtained by means of these radiopharmaceuticals in oncology patients may prove useful for diagnostic purposes and for predicting and monitoring response to anticancer treatment options in the future.

8. References

1. Eberl S, Zimmerman RE: Nuclear medicine imaging instrumentation, in Muray IPC, Ell PJ (eds): Nuclear Medicine in Clinical Diagnosis and Treatment. Edinburgh, Churchill Livingstone, 1998, pp 1559-1569.
2. Bailey DL, Parker JA: Single photon emission computed tomography, in Muray IPC, Ell PJ (eds): Nuclear Medicine in Clinical Diagnosis and Treatment. Edinburgh, Churchill Livingstone, 1998, pp 1589-1601.
3. Meikle SR, Dahlbom M: Positron emission tomography, in Muray IPC, Ell PJ (eds): Nuclear Medicine in Clinical Diagnosis and Treatment. Edinburgh, Churchill Livingstone, 1998, pp 1603-1616.
4. Boyd RE, Silvester DJ: Radioisotope production, in Muray IPC, Ell PJ (eds): Nuclear Medicine in Clinical Diagnosis and Treatment. Edinburgh, Churchill Livingstone, 1998, pp 1617-1624.
5. Okarvi SM. Recent developments in 99Tcm-labelled peptide-based radiopharmaceuticals: an overview. Nucl Med Commun 20:1093-112, 1999.
6. Eckelman WC. The testing of putative receptor binding radiotracers in vivo. In : Diksic M, Reba RC, Eds. Radiopharmaceuticals and brain pathology studies with PET and SPECT. CRC Press, Boca Raton , 1982, pp 42-62
7. Vera DR, Krohn KA, Scheibe PO, Stadolnil RC: Identifiability analysis of an in vivo receptor-binding radiopharmacokinetic system. IEEE Trans Biomed Eng 32:312-322, 1985
8. McElvany KD, Katzenellebogen JA, Shafer KE, et al: 16α-(^{77}Br)Bromoestradiol-17β: dosimetry and preliminary clinical studies. J Nucl Med 23:425-430, 1982
9. Preston DF, Spicer JA, Baranvzuk C, Fabian KG, et al: Clinical results of breast cancer detection by imageable estradiol (I-123 E2). Eur J Nucl Med A159:430, 1990 (abstr)

10. Schober O, Schicha H, Reiners C, et al: Breast cancer imaging with radioiodinated oestradiol. The Lancet 1522, 1990
11. Scheidhauer K, Müller S, Smolarz K, et al: Tumor-szintigraphie mit ^{123}J-markiertem östradiol beim mammakarzinom-rezeptorszintigraphie. Nucl Med 30:84-99, 1991
12. Kenady DE, Pavlik EJ, Nelson K, et al: Images of estrogen-receptor-positive breast tumors produced by estradiol labeled with iodine I 123 at 16α. Arch Surg 128:1373-1381, 1993
13. Mintun MA, Welch MJ, Siegel BA, et al: Breast cancer : PET imaging of estrogen receptors. Radiology 169:45-48, 1988
14. McGuire AH, Dehdashti F, Siegel BA et al: Positron tomographic assessment of α-(^{18}F)Fluoro 17β-estradiol uptake in metastatic breast carcinoma. J Nucl Med 32:1526-1531, 1991
15. Dehdashti F, Mortimer JE, Siegele BA et al: Positron tomographic assessment of estrogen receptors in breast cancer : comparison with FDG-PET and in vitro receptor assays. J Nucl Med 36:1766-1774, 1995
16. Mortimer JE, Dehdashti F, Siegel BA et al: Clinical correlation of FDG and FES-PET imaging with estrogen receptors in breast cancer and response to systemic therapy. Clin Cancer Res 2:933-939, 1996
17. Mortimer JE, Dehdashti F, Siegel BA, et al. Metabolic flair: indicator of hormone responsiveness in advanced breast cancer. J Clin Oncol 19:2797-2803, 2001
18. Mankoff DA, Tewson TJ, Peterson LM, et al. The heterogeneity of estrogen receptor expression in metastatic breast cancer as measured by [^{18}F]-fluoroestradiol PET. J Nucl Med 41: 28P, 2000 (suppl)
19. Foulon C, Guilloteau D, Baulieu JL, et al: Estrogen receptor imaging with 17α-(^{123}I)-iodovynil-11β-methoxyestradiol ($MIVE_2$)-Part I. Radiotracer preparation and characterization. Nucl Med Biol 19:257-261, 1992
20. Rijks LJM, Bakker PJM, van Tienhoven G et al: Imaging of estrogen receptors in primary and metastatic breast cancer patients with iodine-123-labeled Z-MIVE. J Clin Oncol 15:2536-2545, 1997
21. Nachar O, Rousseau JA, Lefebvre B, et al : Biodistribution, dosimetry and metabolism of 11β-methoxy-(17α,20 E/Z)-(^{123}I)iodovynilestradiol in healthy women and breast cancer patients. J Nucl Med 40:1728-1736, 1999

22. Bennink RJ, Rijks LJ, van Tienhoven G, et al. Estrogen receptor status in primary breast cancer: iodine 123-labeled cis-11β-methoxy-17α-iodovinyl estradiol scintigraphy. Radiology 220:774-779, 2001
23. Bennink RJ, van Tienhoven G, Rijks LJ, et al. In vivo prediction of response to antiestrogen treatment in estrogen receptor-positive breast cancer. J Nucl Med 45:1-7, 2004
24. Bertolessi A, Cartei G, Turin D, et al: Behaviour of vaginal epithelial maturation and sex homone binding globulin in post-menopausal breast cancer patients during the first year of tamoxifen therapy. Cytopathology 9:263-270, 1998
25. Rose DP, Chleboswki RT, Connolly JM, et al: Effects of tamoxifen adjuvant therapy and a low-fat diet on serum binding proteins and estradiol bioavailability in postmenopausal breast cancer patients. Cancer Res 52:5386-5390, 1992
26. Lonning PE, Johanessen DC, Lien EA, et al: Influence of tamoxifen on sex hormones, gonadotrophins and sex hormone binding globulin in postmenopausal breast cancer patients. J sterodi Biochem Mol Biol 52:491-496, 1995
27. Pasqualini JR, Schatz B, Varin C, et al: Recent data on estrogen sulfatases and sulfotransferases activities in human breast cancer. J Sterodi Biochem Mol Biol 41:323-339, 1992
28. Pasqualini JR, Chetrite GS: Estrone sulfatase versus estrone sulfotransferase in human breast cancer : potential clinical applications. J Steroid Biochem Mol Biol 69:287-292, 1999
29. Chetrite GS, Kloosterboer HJ, Philippe JC, et al: Effect of Org OD14 (LIVIAL) and its metabolites on human estrogen sulphotransferase activity in the hormone-dependent MCF-7 and T-47D, and the hormone-independent MDA-MB-231, breast cancer cell lines. Anticancer Res 19:269-275, 1999
30. Dehdashti F, Flanagan FL, Mortimer JE, et al: Positron emission tomographic assessment of “metabolic flare” to predict response of metastatic breast cancer to antiestrogen therapy. Eur J Nucl Med 26:51-56, 1999
31. Bennink R, Rijks L, van Tienhoven G et al: Can Z-MIVE scintigraphy predict response to antiestrogen treatment in metastasized ER-positive breast cancer? Eur J Nucl Med 976, 1999 (abstr)
32. O’Brain CA, Liskamp RM, Solomon DH, et al: Inhibition of protein kinase C by tamoxifen. Cancer Res 45:2462-2465, 1985

33. Castoria G, Migliaccio A, Nola E, Auricchio F. In vitro interaction of estradiol receptor with Ca2+-calmodulin. Mol Endocrinol 2:167-174, 1988
34. Guvakova MA and Surmacz E: Tamoxifen interferes with the insulin-like growth factor I receptor (IGF-IR) signalling pathway in breast cancer cells. Cancer Res 57:2606-2610, 1997
35. Delpassand ES, Yang DJ, Wallace S, et al: Synthesis, biodistribution, and estrogen receptor scintigraphy of indium-111-diethylenetriaminepentaacetic acid-tamoxifen analogue. J Pharm Sci 85:553-559, 1996
36. Yang DJ, Li C, Kuang LR, Price JE, et al: Imaging, biodistribution and therapy potential of halogenated tamoxifen analogues. Life Sci 55:53-67, 1994
37. Inoue T, Kim EE, Wallace S, et al: Positron emission tomography using [18F]fluorotamoxifen to evaluate therapeutic responses in patients with breast cancer: preliminary study. Cancer Biother Radiopharm 11:235-45, 1996
38. Van de Wiele C, De Vos F, De Sutter J, et al: Biodistribution and dosimetry of (123-iodine)-iodomethyl-N,Ndiethyl-tamoxifen: an (anti)oestrogen receptor radioligand for therapy efficacy prediction. Eur J Nucl Med 26:1259-1264, 1999
39. Van de Wiele C, Cocquyt V, VandenBroecke R, et al: Iodine-labeled tamoxifen uptake in primary human breast carcinoma. J Nucl Med 42:1818-1820, 2001
40. Katzenellenbogen JA: Designing steroid receptor-based radiotracers to image breast and prostate tumors. J Nucl Med 36: S8-S13, 1995 (suppl 6)
41. Van den Bos JC, Rijks LJM, van Doremalen PAPM, et al: New iodinated progestins as potential ligands for progesterone receptor imaging in breast cancer. Part1: Synthesis and in vitro pharmacological chracterization. Nucl Med Biol 25:781-789, 1998
42. Rijks LJM, van den Bos JC, van Doremalen PAPM, et al: New iodinated progestins as potential ligands for progesterone receptor imaging in breast cancer. Part2: in vivo pharmacological characterization. Nucl Med Biol 25:791-798, 1998
43. Liu AJ, Carlson KE, Katzenelenbogen JA: Synthesis of high-affinity fluorine-substituted ligands for the androgen receptor-potential agents for imaging prostatic-cancer by positron emission tomography. Journal of Medicinal Chemistry 35:2113-2129, 1992
44. Choe YS, Lidstrom PJ, Chi DY, et al: Synthesis of 11-beta-[F-18]fluoro-5-alpha-dihydrotestosterone and 11β-[F-18]fluoro-19-nor-5α-dihydrotestosterone-preparation via halofluorination-reduction, receptor-binding, and tissue distribution. Journal of Medicinal Chemsitry 38:816-825, 1995

45. Choe YS, Katenellenbogen JA: Synthesis of C-6 Fluoroandrogens-evaluation of ligands for tumor receptor imaging. Steroids 60:414-422, 1995
46. Bonasera T, Oneil JP, Xu M, et al: Preclinical evaluation of fluorine-18-labeled androgen receptor ligands in baboons. J Nucl Med 37:1009-1015, 1996
47. Serafini AN: From monoclonal antibodies to peptides and molecular recognition units: an overview. J Nucl Med 34:533-536, 1993
48. Reubi JC: Peptide receptors as molecular targets for cancer diagnosis and therapy. Endocrine Reviews 24:389-427, 2003
49. Signore A, Annovazi A, Chianelli M, et al: Peptide radiopharmaceuticals for diagnosis and therapy. Eur J Nucl Med 28:1555-1565, 2001
50. Heppeler A, Froidevaux S, Eberle AN, et al: Receptor targeting for tumor localisation and therapy with radiopeptides. Curr Med Chem 7:971-994, 2000
51. Duncan JR, Stephenson MT, Wu HP, et al: Indium-111-Diethyletriaminepentaacetic acid-octreotide is delivered in vivo to pancreatic, tumor cell, renal and hepatocyte lysosomes. Cancer Res 57:659-671, 1997
52. Reubi JC, Waser B, Schaer JC, et al: Somatostatin receptor sst1-sst5 expression in normal and neoplastic human tissues using receptor autoradiography with subtype-selective ligands. Eur J Nucl Med 28:836-846, 2001
53. Kwekkeboom DJ, de Herder WW, Krenning EP: Receptor imaging in the diagnosis and treatment of pituitary tumours. J Endocrinol Invest 22:80-88, 1999
54. Gibril F, Reynolds JC, Doppman JL et al: Somatostatin receptor scintigraphy: its sensitivity compared with that of other imaging methods in detecting primary and metastatic gastrinomas. A prospective study. Ann Intern Med 125:26-34, 1996
55. Lebtahi R, Cadiot G, Sarda L et al: Clinical impact of somatostatin receptor scintigraphy in the managment of patients with neuroendocrine gastroenteropancreatic tumors. J Nucl Med 38:853-858, 1997
56. Termanini B, Gibril F, Reynolds JC et al: Value of somatostatin receptor scintigraphy: a prospective study of its effect on clinical managment. Gastroenterology 112:335-347, 1997
57. Jensen RT, Gibril F: Somatostatin receptor scintigraphy in gastrinomas. Ital J Gastroenterol Hepatol 31:S179-S185, 1999 (suppl 2)
58. Kwekkeboom DJ, Krenning EP, Bakker WH et al: Somatostatin analogue scintigraphy in carcinoid tumours. Eur J Nucl Med 20:283-292, 1993

59. Nilsson O, Kolby L, Wangberg B, et al: Comparative studies on the expression of somatostatin receptor subtypes, outcome of octreotide scintigraphy and response to octreotide treatment in patients with carcinoid tumours. Br J Cancer 77:632-637, 1998
60. Grufferman S, Gillman MW, Pasternak LR, et al: Familial carotid body tumours: case reports and epidemiologic review. Cancer 46:2116-2122, 1980
61. Kwekkeboom DJ, Krenning EP: Somatostatin receptor imaging. Sem Nucl Med 32:84-91, 2002
62. EP Krenning, DJ Kwekkeboom, WH Bakker, et al: Somatostatin receptor scintigraphy with [^{111}In-DTPA-D-Phe^{1}]-octreotide: the Rotterdam experience with more than 1000 patients. Eur J Nucl Med 20:716-731, 1993
63. Berenger N, Moretti JL, Boaziz C, et al: Somatostatin receptor imaging in small cell lung cancer. Eur J Cancer 32A:1429-1431, 1996
64. Bohuslavizki KH, Brenner W, Gunther M, et al: Somatostatin receptor scintigraphy in the staging of small cell lung cancer. Nucl Med Commun 17:191-196, 1996
65. Kwekkeboom DJ, Kho GS, Lamberts SWJ, et al: The value of octrotide scintigraphy in patients with lung cancer. Eur J Nucl Med 21:1106–1113, 1994
66. E Bombardieri, F Crippa, Cataldo I, et al: Somatostatin receptor imaging of small cell lung cancer (SCLC) by means of 111In-DTPA-octreotide scintigraphy. Eur J Cancer 31A :184-188, 1995
67. Hoffman M, Maecke H, Borner R, et al: Biokinetics and imaging with the somatostatin receptor PET radioligand (68)Ga-DOTATOC: preliminary data. Eur J Nucl Med 28(12):1751-1757, 2001
68. Kowalski J, Henze M, Schuhmacher J, et al: Evaluation of positron emission tomography imaging using [68Ga]-DOTA-D Phe(1)-Tyr(3)-octreotide in comparison to [111In]-DTPAOC SPECT. First results in patients with neuroendocrine tumors. Mol Imaging Biol 5(1):42-48, 2003
69. Blum J, Handmaker H, Lister-James J, et al: A multicenter trial with a somatostatin analog^{99m}Tc depreotide in the evaluation of solitary pulmonary nodules. Chest 117:1232–1238, 2000
70. Lebtahi R, Le Cloirec J, Houzard C, et al. Detection of neuroendocrine tumors: ^{99m}Tc-P829 scintigraphy compared with ^{111}In-pentreotide scintigraphy. J Nucl Med 43:889-895, 2002

71. Plachcinska A, Mikolajczak R, Maecke HR, et al: 99mTc-EDDA/HYNIC-TOC scintigraphy in the differential diagnosis of solitary pulmonary nodules. Eur J Nucl Med Mol Imaging DOI:10.1007/s00259-004-1511-3
72. Gabriel M, Decristoforo C, Donnemiller E, et al: An intrapatient comparison of ^{99m}Tc-EDDA/HYNIC-TOC with ^{111}In-DTPA-octreotide for diagnosis of somatostatin receptor-expressing tumors. J Nucl Med 44(5):708-716, 2003
73. Van Hagen PM, Krenning EP, Reubi JC, et al: Somatostatin analogue scintigraphy of malignant lymphoma. Br J Haematol 83:75-79, 1993
74. Leners N, Jamar F, Fiasse R, et al : Indium-111 pentreotide uptake in endocrine tumors and lymphoma. J Nucl Med 37:916-922, 1996
75. van den Anker-Lugtenburg PJ, Lowenberg B, Lamberts SW, et al: The relevance of somatostatin receptor expression in malignant lymphomas. Metabolism 45:96-97, 1996 (suppl 1)
76. Lugtenburg PJ, Krenning EP, Valkema R, et al: Somatostatin receptor scintigraphy useful in stage I-II Hodgkin's disease: more extended disease identified. Br J Haematol 112:936-944, 2001
77. Schmidt M, Scheidhauer K, Luyken C, et al: Somatostatin receptor imaging in intracranial tumours. Eur J Nucl Med 25:675-686, 1998
78. Haldemann AR, Rösler H, Barth A, et al: Somatostatin receptor scintigraphy in patients with CNS tumors: the role of blood brain barrier permeability. J Nucl Med 36:403-410, 1995
79. Van Eijck CH, Krenning EP, Bootsma A, et al: Somatostatin receptor scintigraphy in primary breast cancer. Lancet 343:640-643, 1994
80. Erspamer V: Discovery, isolation and characterisation of bombesin-like peptides. Ann N Y Acad Sci 547:3-9, 1998
81. Nelson J, Donelly M, Walker B, et al: Bombesin stimulates proliferation of human breast cancer cells in culture. Br J Cancer 63:933-936, 1991
82. Moody TW, Cuttitta F: Growth factor and peptide receptors in small cell lung cancer. Life Sci 52:1161-1173, 1993
83. Moody TW, Leyton J, Garcia-Marin L, et al: Nonpeptide gastrin releasing peptide receptor antagonists inhibit the proliferation of lung cancer cells. Eur J Pharmacol 474:21-29, 2003

84. Miyazaki M, Lamharzi N, Schally AV, et al: Inhibition of growth of MDA-MB-231 human breast cancer xenografts in nude mice by bombesin/gastrin-releasing peptide (GRP) antagonists RC-3940-II and RC-3095. Eur J Cancer 34:710-717, 1998
85. Gugger M, Reubi JC. Gastrin-releasing peptide receptors in non-neoplastic and neoplastic human breast. Am J Pathol 155:2067-2076, 1999
86. Markwalder R, Reubi JC. Gastrin-releasing peptide receptors in the human prostate: relation to neoplastic transformation. J Cancer Res 39:1152-1159, 1999
87. Fathi Z, Way JW, Corjay MH, et al: Bombesin receptor structure and expression in human lung carcinoma cell lines. J Cell Biochem 24:237-246, 1996 (suppl)
88. Preston SR, Woodhouse LF, Jones-Blackett S, et al: High affinity binding sites for gastrin-releasing peptide on human colorectal cancer tissue but not uninvolved mucosa. Br J Cancer 71:1087-1089, 1995
89. Preston SR, Woodhouse LF, Jones-Blackett S, et al: High affinity binding sites for gastrin releasing peptide on human gastric cancer and Menetrier's mucosa. Cancer Res 53:5090-5092, 1993
90. Mahmoud S, Staley J, Taylor J, et al: (Psi13,14) bombesin analogues inhibit growth of small cell lung cancer in vitro and in vivo. Cancer Res 51:1798-1802, 1991
91. Milovanovic SR, Radulovic S, Groot K, et al: Inhibition of growth of PC-82 human prostate cancer cell line xenografts in nude mice by bombesin antagonist RC-3095 or combination of agonist (D-Trp6)-luteinizing hormone-releasing hormone and somatostatin analogue RC-160. Prostate 20:269-280, 1992
92. Orosz A, Schrett J, Nagy J, et al: New short-chain analogues of a substance-P antagonist inhibit proliferation of human small-cell lung-cancer cells in vitro and in vivo. Int J Cancer 60:82-87, 1995
93. Schally AV, Nagy A: Cancer chemotherapy based on targeting of cytotoxic peptide conjugates to their receptors on tumours. Eur J Endocrinol 141:1-14, 1999
94. Kelley MJ, Linnoila RI, Avis IL, et al: Anti-tumour activity of a monoclonal antibody directed against gastrin-releasing peptide in patients with small cell lung cancer. Chest 112:256-261, 1997
95. Davis, TP, Crowell S, Taylor J, et al: Metabolic stability and tumor inhibition of bombesin/GRP receptor antagonist. Peptides 13:401-407, 1992
96. Rogers BE, Rosenfeld ME, Khazaeli MB, et al: Localization of iodine-125-mIP-Des-Met^{14}-bombesin(7-13)NH_2 in ovarian carcinoma induced to express the gastrin releasing

peptide receptor by adenoviral vector-mediated gene transfer. J Nucl Med 38:1221-1229, 1997

97. Breeman W, de Jong M, Bernard BF, et al: Pre-clinical evaluation of (111)In-DTPA-Pro(1), Tyr(4)bombesin, a new radioligand for bombesin-receptor scintigraphy. Int J Cancer 83:657-663, 1999
98. Nock B, Nikolopoulou A, Chiotellis E,et al: [(99m)Tc]Demobesin 1, a novel potent bombesin analogue for GRP receptor-targeted tumour imaging. Eur J Nucl Med Mol Imaging 30:247-58, 2003
99. Van de Wiele C, Dumont F, Vanden Broecke R, et al: Technetium-99m RP527, a GRP analogue for visualisation of GRP receptor-expressing malignancies: a feasibility study. Eur J Nucl Med 27:1694-1699, 2000
100. Reubi JC, Waser B: Unexpected high incidence of cholecystokinin/gastrin receptors in human medullary thyroid carcinomas. Int J Cancer 67:644-647, 1996
101. Reubi JC, Schaer JC, Waser B: Cholecystokinin (CCK)-A and CCK-B/gastrin receptors in human tumors. Cancer Res 57:1377-1386, 1997
102. de Jong M, Bakker WH, Bernard BF, et al: Preclinical and initial clinical evaluation of 111In-labeled nonsulfated CCK8 analog: a peptide for CCK-B receptor-targeted scintigraphy and radionuclide therapy. J Nucl Med 40:2081-7, 1999
103. Reubi JC, Waser B, Schaer JC, et al: Unsulfated DTPA- and DOTA-CCK analogs as specific high-affinity ligands for CCK-B receptor-expressing human and rat tissues in vitro and in vivo. Eur J Nucl Med 25:481-490, 1998
104. Behr TM, Behe MP: Cholecystokinin-B/Gastrin receptor-targeting peptides for staging and therapy of medullary thyroid cancer and other cholecystokinin-B receptor-expressing malignancies. Semin Nucl Med 32:97-109, 2002
105. Kwekkeboom DJ, Bakker WH, Kooij PPM, et al:Cholecystokinin receptor imaging using an octapeptide DTPA-CCK analogue in patients with medullary thyroid carcinoma. Eur J Nucl Med 27:1312-1317, 2000
106. Said SI, Mutt V: Polypeptide with broad biological activity: isolation from small intestine. Science 169:1217-1218, 1970
107. Cohn J: Vasoactive intestinal peptide stimulates protein phosphorylation in a colonic epithelial cell line. Am J Physiol 253:G420-G424, 1987
108. Scholar EM, Paul S: Stimulation of tumor cell growth by vasoactive intestinal peptide. Cancer 67(6):1561-4, 1991

109. Moody TW, Zia F, Brenneman D, et al: A VIP antagonist inhibits the growth of non-small cell lung cancer. Proc Natl Acad Sci USA 90: 4345-4349, 1993

110. Laburthe M, Couvineau A, Marie JC: VPAC receptors for VIP and PACAP. Receptors Channels 8(3-4):137-53, 2002

111. Reubi JC: In vitro evaluation of VIP/PACAP receptors in healthy and diseased human tissues. Clinical implications. Ann N Y Acad Sci 921:1-25, 2000

112. Hessenius C, Bäder M, Meinhold H, et al: Vasoactive intestinal peptide receptor scintigraphy in patients with pancreatic adenocarcinomas or neuroendocrine tumours. Eur J Nucl Med 27(11):1684-1693, 2000

113. Virgolini I, Raderer M, Kurtaran A, et al: ^{123}I-Vasoactive intestinal peptide (VIP) receptor scanning: update of imaging results in patients with adenocarcinomas and endocrine tumors of the gastrointestinal tract. Nucl Med Biol 23: 685-692, 1996

114. Raderer M, Kurtaran A, Leimer M, et al: Value of peptide receptor scintigraphy using (123)I-vasoactive intestinal peptide and (111)In-DTPA-D-Phe1-octreotide in 194 carcinoid patients: Vienna University Experience, 1993 to 1998. J Clin Oncol 18(6):1331-1336, 2000

115. Raderer M, Kurtaran A, Yang Q, et al: Iodine-123-vasoactive intestinal peptide receptor scanning in patients with pancreatic cancer. J Nucl Med 39(9):1570-1575, 1998

116. Raderer M, Kurtaran A, Hejna M, et al: 123I-labelled vasoactive intestinal peptide receptor scintigraphy in patients with colorectal cancer. Br J Cancer 78(1):1-5, 1998

117. Thakur ML, Marcus CS, Saeed S, et al: Imaging tumors in humans with Tc-99m-VIP. Ann N Y Acad Sci 921:37-44, 2000

118. Bem WT, Thomas GE, Mammone JY, et al: Overexpression of σ receptors in nonneural human tumors. Cancer Res 51:6558-6562, 1991

119. Vilner BJ, John CS, Bowen WD: Sigma-1 and sigma-2 receptors are expressed in a wide variety of human and rodent tumor cell lines. Cancer Res 55(2):408-413, 1995

120. Wheeler KT, Wang LM, Wallen CA, et al: Sigma-2 receptors as a biomarker of proliferation in solid tumours. Br J Cancer 82(6):1223-1232, 2000

121. John CS, Bowen WD, Fisher SJ, et al: Synthesis, in vitro pharmacologic characterization, and preclinical evaluation of N-[2-(1'-piperidinyl)ethyl]-3-[125I]iodo-4-methoxybenzamide (P[125I]MBA) for imaging breast cancer. Nucl Med Biol 26(4):377-82, 1999

122. Caveliers V, Everaert H, John CS, et al: Sigma receptor scintigraphy with N-[2-(1'-piperidinyl)ethyl]-3-(123)I-iodo-4-methoxybenzamide of patients with suspected primary breast cancer: first clinical results. J Nucl Med 43(12):1647-1649, 2002

123. John CS, Lim BB, Vilner BJ, et al: Substituted halogenated arylsulfonamides: a new class of sigma receptor binding tumor imaging agents. J Med Chem 41(14):2445-50, 1998

124. Mach RH, Huang Y, Buchheimer N,et al: [[(18)F]N-(4'-fluorobenzyl)-4-(3-bromophenyl) acetamide for imaging the sigma receptor status of tumors: comparison with [(18)F]FDG, and [(125)I]IUDR. Nucl Med Biol 28(4):451-458, 2001

125. He XS, Bowen WD, Lee KS, et al: Synthesis and binding characteristics of potential SPECT imaging agents for sigma-1 and sigma-2 binding sites. J Med Chem 36(5):566-571, 1993

126. John CS, Gulden ME, Vilner BJ, et al: Synthesis, in vitro validation and in vivo pharmacokinetics of [125I]N-[2-(4-iodophenyl)ethyl]-N-methyl-2-(1-piperidinyl) ethylamine: a high-affinity ligand for imaging sigma receptor positive tumors. Nucl Med Biol 23(6):761-766, 1996

127. John CS, Lim BB, Geyer BC, Vilner BJ, et al: 99mTc-labeled sigma-receptor-binding complex: synthesis, characterization, and specific binding to human ductal breast carcinoma (T47D) cells. Bioconjug Chem 8(3):304-309, 1997

128. Chavatte K, Wong E, Fauconnier TK, et al: Rhenium and technetium-99m oxocomplexes of neurotensin (8-13). In: Nicolini M, Mazzi U, eds. Technetium, rhenium and other metals in chemistry and nuclear medicine 5. Padova: SGEditoriali:513-518, 1999

129. Alleman-Tannahill L, Remy N, Blauenstein P, et al: First studies of the cell binding and the metabolism of a Tc-99m labelled neurotensin fragment. Eur J Nucl Med 25:958, 1998 (abstract)

130. Chen JQ, Cheng Z, Hoffman TJ, Jurisson SS, et al: Melanoma-targeting properties of (99m)technetium-labelled cyclic alpha-melanocyte-stimulating hormone peptide analogues. Cancer Res 60:5649-5658, 2000

131. Nelson CA, Moyer BR, Pearson DA, et al: A peptide analog of calcitonin labeled with Tc-99m targets MCF-7 human breast cancer xenografts in nude mice. J Nucl Med 40:103P, 1999

132. Veale D, Ashcroft T, March C, et al: Epidermal growth factor receptors in non-small cell cancer. Br J Cancer 55:513-516, 1987

133. Neal DE, March C, Benett MK, et al: Epidermal growth factor receptors in human bladder cancer: comparison of invasive and superficial tumors. Lancet 1:346-348, 1985

134. Kohler M, Janz I, Wintzer HO, et al: The expression of EGF receptors, EGF-like factors and c-myc in ovarian and cervical carcinomas and their potential clinical significance. Anticancer Res 9:1537–1547, 1989

135. Freeman MR, Washecka R, Chung LW: Aberrant expression of epidermal growth factor receptor and HER-2 (erbB-2) messenger RNAs in human renal cancers. Cancer Res 49: 6221-6225, 1989

136. Korc M, Meltzer P, Trent J: Enhanced expression of epidermal growth factor receptor correlates with alterations of chromosome 7 in human pancreatic cancer. Proc Natl Acad Sci U S A 83(14):5141-5144, 1986

137. Santini J, Formento JL, Francoual M, et al: Characterization, quantification, and potential clinical value of the epidermal growth factor receptor in head and neck squamous cell carcinomas. Head Neck 13:132-139, 1991

138. Hirsch FR, Varella-Garcia M, Bunn PA Jr, et al: Epidermal Growth Factor Receptor in Non-Small-Cell Lung Carcinomas: Correlation Between Gene Copy Number and Protein Expression and Impact on Prognosis. J Clin Oncol 21:3798-3807, 2003

139. Nguyen DC, Parsa B, Close A, et al: Overexpression of cell cycle regulatory proteins correlates with advanced tumor stage in head and neck squamous cell carcinomas. Int J Oncol 22(6):1285-1290, 2003

140. Nicholson RI, McClelland RA, Finlay P, et al: Relationship between EGF-R, c-erB-2 protein expression and Ki 67 immunostaining in breast cancer and hormone sensitivity. Eur J Cancer 29A:1018-1023, 1993

141. Klijn JGM, Berns PMJJ, Schmitz PIM, et al: The clinical significance of epidermal growth factor receptor (EGF-R) in human breast cancer: a review on 5232 patients. Endocr rev 13(1):3-17, 1992

142. Ohsaki Y, Tanno S, Fujita Y, et al: Epidermal growth factor receptor expression correlates with poor prognosis in non-small cell lung cancer patients with p53 overexpression. Oncol Rep 7(3):603-607, 2000

143. Scambia G, Benedettipanici P, Ferrandina G, et al: Epidermal growth factor, estrogen and progesteron-receptor expression in primary ovarian cancer – correlation with clinical outcome and response to chemotherapy. Br J Cancer 72(2):361-366, 1995

144. Mendelsohn J and Baselga J. The EGF receptor family as target for cancer therapy. Oncogene 19:6550-6565, 2000

145. Ciardiello F and Tortora G. A novel approach in the treatment of cancer: targeting the epidermal growth factor receptor. Clin Cancer Res 7:2958-2970, 2001

146. Pateisky N, Schatten C, Vavra N, et al: Lymphoscintigraphy using epidermal growth factor as tumor-seeking agent in uterine cervical cancer. Wien Klin Wochenschr 103(21):654-656, 1991

147. Cuartero-Plaza A, Martinez-Miralles E, Rosell R, et al: Radiolocalization of squamous lung carcinoma with ^{131}I-labeled epidermal growth factor. Clin Cancer Res 2:13-20, 1996

148. Reilly RM, Kairash R, Sandhu J, et al: A comparison of EGF and Mab 528 labeled with ^{111}In for imaging human breast cancer. J Nucl Med 41:903-911, 2000

149. Ramos-Suzarte M, Rodriguez N, Oliva JP, et al: Tc-99m-labeled antihuman epidermal growth factor receptor antibody in patients with tumors of epithelial origin: part III. Clinical trials safety and diagnostic efficacy. J Nucl Med 40(5):768-775,1999

150. Senekowitsch-Schmidtke R, Steiner K, Haunschild J, et al: In vivo evaluation of epidermal growth factor (EGF) receptor density on human tumor xenografts using radiolabeled EGF and anti-(EGF receptor) mAb 425. Cancer Immunol Immunother 42(2):108-114, 1996

151. Dadparvar S, Krishna L, Miyamoto C, et al: Indium-111-labeled anti-EGFR-425 scintigraphy in the detection of malignant gliomas. Cancer 73(3):884-889, 1994 (suppl S)

152. Wen X, Wu QP, Ke S, et al: Conjugation with (111)In-DTPA-poly(ethylene glycol) improves imaging of anti-EGF receptor antibody C225. J Nucl Med 42(10):1530-1537, 2001

153. Slamon DJ, Godolphin W, Jones LA, et al: Studies of the HER-2/neu proto-oncogene in human breast and ovarian cancer. Science 244:707, 1989

154. Shun CT, Wu MS, Lin JT, et al: Relationship of p53 and c-erbB-2 expression to histopathological features, Helicobacter pylori infection and prognosis in gastric cancer. Hepato-Gastroenterology 44: 604-609, 1997

155. Schneider PM, Hung MC, Chiocca SM, et al: Differential expression of the c-erbB-2 gene in human small cell and non-small cell lung cancer. Cancer Res 49: 4968, 1989

156. Tetu B, Fradet Yves Allard P, Veilleux C, et al: Prevalence and clinical significance of HER-2/neu, p53 and Rb expression in primary superficial bladder cancer. J Urology 155: 1784-1788, 1996

157. Latif Z, Watters AD, Bartlett JM, et al: Gene amplification and overexpression of HER2 in renal cell carcinoma. BJU Int 89(1):5-9, 2002

158. Koeppen HK, Wright BD, Burt AD, et al: Overexpression of HER2/neu in solid tumours: an immunohistochemical survey. Histopathology 38(2):96-104, 2001

159. Slamon DJ, Clark GM, Wong SG, et al: Human breast cancer: correlation of relapse and survival with amplification of the HER2/neu oncogene. Science 235:177, 1987

160. Cooke T, Reeves J, Lanigan A, et al: HER2 as a prognostic and predictive marker for breast cancer. Ann Oncol 12:S23-28 (Suppl 1), 2001

161. Brabander J, Danenberg KD, Metzger R, et al: Epidermal growth factor receptor and HER2-neu mRNA expression in non-small cell lung cancer is correlated with survival. Clin Cancer Res 7(7):1850-1855, 2001

162. Nakamura H, Saji H, Ogata A,et al: Correlation between encoded protein overexpression and copy number of the HER2 gene with survival in non-small cell lung cancer. Int J Cancer 103(1):61-66, 2003

163. Piccart M, Lohrisch C, Di Leo A, et al: The predictive value of HER2 in breast cancer. Oncology 61:73-82, 2001 (Suppl 2)

164. Qian X, LeVea CM, Freeman JK, et al: Heterodimerization of epidermal growth factor receptor and wild-type or kinase-deficient Neu: a mechanism of interreceptor kinase activation and transposhorylation. Proc Natl Acad Sci USA 91:1500-1504, 1994

165. McKeage K, Perry CM: Trastuzumab: a review of its use in the treatment of metastatic breast cancer overexpressing HER2. Drugs 62(1):209-243, 2002

166. Behr TM, Behe M, Angerstein C, et al: Does pretherapeutic immunoscintigraphy allow for diagnostic predictions with respect to the toxicity and therapeutic efficacy of cold immunotherapy with trastuzumab (Herceptin®)? J Nucl Med 41(5):287, 2000 (suppl S)

167. Surmacz E, Guvakova MA, Nolan MK, et al: Type I insulin-like growth factor receptor function in breast cancer. Breast Canc Res Treat 47:255-267, 1998

168. Hellawell GO, Turner GDH, Davies DR, et al: Expression of the type I insulin-like growth factor receptor is up-regulated in primary prostate cancer and commonly persists in metastatic disease. Canc Res 62:2942-2950, 2002

169. Lee AV and Yee D: Insulin-like growth factors and breast cancer. Biomed Pharmacother 49:415-421, 1995

170. Maloney EK, McLaughlin JL, Dagdigian NE, et al: An anti-insulin-like growth factor I receptor antibody that is a potent inhibitor of cancer cell proliferation. Cancer Res 63(16):5073-5083, 2003

171. Blum G, Gazit A, Levitzki A: Development of new IGF-1 receptor kinase inhibitors using catechol mimics. J Biol Chem 278(42):40442-40454, 2003

172. Sun BF, Kobayashi H, Le N, et al: Effects of insuline-like growth factor binding proteins on insuline-like growth factor-I biodistribution in tumor-bearing nude mice. J Nucl Med 41(2):318-326, 2000

173. Veikkola T, Alitalo K: VEGFs, receptors and angiogenesis. Cancer Biol 9:211-220, 1999

174. Li S, Peck-Radosavljevic M, Koller E, et al: Characterization of (123)I-vascular endothelial growth factor-binding sites expressed on human tumour cells: possible implication for tumour scintigraphy. Int J Cancer 91(6):789-796, 2001

175. Li S, Peck-Radosavljevic M, Kienast O, et al: Imaging gastrointestinal tumours using vascular endothelial growth factor-165 (VEGF165) receptor scintigraphy. Ann Oncol 14(8):1274-1277, 2003

176. Zinn KR, Kelpke S, Chaudhuri TR, et al: Imaging Tc-99m-labeled FGF-1 targeting in rats. Nucl Med Biol 27(4):407-414, 2000

177. Kobayashi H, Sakahara H, Hosono M, et al: Scintigraphic detection of xenografted tumors producing human basic fibroblast growth factor. Cancer Immunol Immunother 37(5):281-285, 1993

178. Yue W, Santner SJ, Masamura S, Wang JP, Demers LM, Hamilton C, Santen RJ. Determinants of tissue estradiol levels and biologic responsiveness in breast tumors. Breast cancer Res Treat 49:S1-S7, 1998 (suppl 1)

179. Reed MJ, Aherne GW, Ghilchik MW et al. Concentrations of oestrone and 4-hydroxyandrostenedione in malignant and normal breast tissue. Int J Cancer 49: 562-565, 1991

180. Fortunati N, Fissore F, Fazzari A, Berta L, Benedusi-Pagliano E, Frairia R.. Biological relevance of the interaction between sex steroid binding protein and its specific receptor of MCF-7 cells: effect on the estradiol-induced cell proliferation. J Steroid Biochem Mol Biol 45(5):435-444, 1993

181. Daniel P, Gaskell SJ, Bishop H, Campbell C, Robertson RI. Determination of tamoxifen and biologically active metabolites in human breast tumours and plasma. Eur J Cancer Clin Oncol 17(11): 1183-1189, 1981

182. Johnston SRD, Dowsett M. Tamoxifen metabolism and oestrogen receptor function – implications for mechanisms of resistance in breast cancer. In : Kellen JA. Tamoxifen : beyond the antioestrogen. Boston : Quinn-Woodbine, 1996, pp 231-266

183. Johnston SRD, Haynes BP, Sacks NPM, McKinna JA, Griggs LJ, Jarman M, et al. Effect of oestrogen receptor status and time on the intra-tumoural accumulation of tamoxifen and N-desmethyltamoxifen following short-term therapy in human primary breast cancer. Breast Cancer Res Treat 28: 241-250, 1993

184. Jerusalem G, Bours V, Fillet G. Adjuvant treatment of breast cancer: meta-analysis and therapeutic recommendations. Rev Med Liege 55(5): 356-359, 2000

185. Lien EA, Solheim E, Ueland PM. Distribution of tamoxifen and its metabolites in rat and human tissues during steady-state treatment. Cancer Res 51: 4837-4844, 1991

186. Thorpe SM. Estrogen and progesterone receptor determinations in breast cancer. Technology, biology and clinical significance. Acta Oncol 27, 1–19, 1988

187. Chinol M, Bodei L, Cremonesi M et al. Receptor-mediated radiotherapy with ^{90}Y-DOTA-$_{D}$Phe-Tyr^{3}-octreotide: the experience of the European institute oncology group. Sem Nucl Med 2:141-147, 2002

CHAPTER THREE

Oestrogen Mediated Regulation Of Somatostatin Receptor Expression In Human Breast Cancer Cell Lines Assessed With ^{99m}Tc-Depreotide

Bieke Van Den Bossche[1], Eveline D'haeninck[1], Filip De Vos[1], Rudi A. Dierckx[1], Simon Van Belle[3], Marc Bracke[2], Christophe Van de Wiele[1]

[1]Division of Nuclear Medicine, Ghent University Hospital, Ghent, Belgium

[2]Laboratory of Experimental Cancerology, Ghent University Hospital, Ghent, Belgium

[3]Department of Medical Oncology, Ghent University Hospital, Ghent, Belgium

Eur J Nucl Med Mol Imaging 2004; 31(7): 1022-1030

1. Abstract

Investigating three somatostatin receptor (SSTR)-positive(+) breast cancer cell lines, Xu et al. found a time- and dose-dependent up- or down-regulation of SSTR2 mRNA expression by respectively 17β-oestradiol (E_2) or the antioestrogen tamoxifen, respectively, in the two oestrogen receptor-positive (ER+) cell lines but not in the oestrogen receptor-negative (ER–) cell line. This study aimed to confirm the findings of Xu et al. at the protein level by means of western blotting and saturation binding studies using ^{99m}Tc-depreotide (NeoSpect). The ER+/ SSTR+ ZR75-1 and T47D and SSTR+/ER– MDA MB231 breast cancer cell lines were exposed to 1 n*M* E_2 or a combination of 1n*M* E_2 plus 100 n*M* tamoxifen or ICI 182 780 (Faslodex) for 48 h. Exposed and non-exposed controls were incubated with increasing concentrations of ^{99m}Tc-depreotide (0.5 n*M*-15 n*M*) in the absence and the presence of 20 µ*M* of octreotide. Scatchard-Rosenthal plots were derived using commercially available software. SSTR subtypes responsible for E_2-induced changes in ^{99m}Tc-depreotide binding were identified by means of western blotting. Mean K_d values for ^{99m}Tc-depreotide were 13 n*M*, 7 n*M*, 4 n*M* for T47D, ZR75-1 and MDA MB231 cells, respectively. After stimulation with E_2, the ER+ cell line T47D demonstrated a mean increase of 81 % ($P< 0.05$) in ^{99m}Tc-depreotide binding. Adding the partial agonist tamoxifen and full antagonist ICI 182 780 to E_2 blocked the induced increase in T47D cells, either reducing SSTR expression or restoring it to control levels. ZR75-1 cells stimulated with E_2 showed a mean decrease in ^{99m}Tc-depreotide binding of 36% as compared to control cells; this difference, however, proved to be not statistically significant. Similarly, B_{max} values did not change in ZR75-1 cells exposed to E_2 in combination with an ER-antagonist as compared to control cells. Finally, no influence of E_2 on ^{99m}Tc-depreotide binding was noticed on the ER– cell line MDA MB231. Both SSTR2 and SSTR5 were expressed at high levels in T47D cells and ZR75-1 cells. SSTR5 drastically

increased in the absence of E_2 and was restored to a original detection level after E_2 treatment. The presented findings support an oestrogen-dependent regulation of SSTR expression in breast cancer cell lines.

1. Introduction

Somatostatin (SST), or somatotropin release inhibiting factor (SRIF), is a tetradecapeptide originally isolated from the hypothalamus by Brazeau in 1972 and produced by neuro-endocrine, inflammatory and immune cells. It potently inhibits basal and stimulated secretion from a wide variety of endocrine and exocrine cells and functions as a neuromodulator in the central nervous system, with effects on locomotor activity and cognitive functions *(1,2).* Somatostatin also exerts an antiproliferative effect on a wide variety of human malignancies. Although the mechanism of the antiproliferative effect of long-acting SS-analogues has not been well characterized, a prerequisite for SST-induced inhibition of tumour growth is the presence of high affinity SST receptors on neoplastic tissues *(3-6).*

To date, five different subtypes of SST seven transmembrane-spanning domain G (guanine nucleotide binding)-protein-coupled receptors (SSTR1-5, with SSTR2 having two splice variant isoforms, respectively SSTR2A-SSTR2B), encoded by separate genes, have been identified *(3,7-10).* On the basis of their structural and pharmacological characteristics, SSTRs can be classified into two classes. Class SRIF1 receptors, comprising SSTR2A, 2B, 3 and 5, have high affinity for octreotide, a synthetic octapeptide analogue. Class SRIF2 receptors, comprising SSTR1 and 4, have low affinity for octreotide *(11,12).*

Somatostatin receptors have been found in a variety of endocrine and non-endocrine tumours *(5-7).* In primary breast carcinoma, reported incidences of SSTR expression vary from 46% to 98% depending on the methodology used to assess SSTR status *(13-16).* The majority of primary breast carcinoma express SSTR2 and to a lesser extent SSTR1, 3 and SSTR5 *(13, 17-18).* As shown by Reubi and Torhorst in 1989, SSTR-positive (SSTR+) breast tumours are also frequently steroid receptor-positive *(19).* Evidence in favour of an interaction between both receptor systems in breast carcinoma was provided more recently in a paper by Xu et al.*(20).* Investigating three SSTR-positive human breast cancer cell lines, these authors found a time- and dose-dependent up- or down-regulation of SSTR2 mRNA expression by 17β-oestradiol (E_2) or the antioestrogen tamoxifen, respectively, in the oestrogen receptor-positive (ER+) cell lines T47D and ZR75-1 but not in the oestrogen receptor-negative (ER–) cell line MDA MB231. This study aimed to confirm the findings of Xu et al. at the protein level by

means of western blotting and saturation binding studies using ^{99m}Tc-depreotide (NeoSpect), a cyclic decapeptide with high affinity for SSTR2, 3 and 5 *(21-23).*

2. Materials and Methods

Materials

Reagents were purchased as follows: Media were obtained from Invitrogen, Belgium. Sera were obtained from Perbio Science, Belgium. E_2 and 4-OH-tamoxifen were purchased from Sigma-Aldrich, Belgium. The antioestrogen ICI 182 780 (Faslodex) was purchased from Tocris Cookson Ltd (UK). NeoSpect was kindly provided by Nycomed-Amersham, London, UK. Antisera against hSSTR1-5 were kindly provided by Dr. C.E. Stidsen, Novo Nordisk, Denmark.

^{99m}Tc-depreotide radiosynthesis

NeoSpect (kit for the preparation of ^{99m}Tc-depreotide injection) vials were reconstituted with 296 MBq ^{99m}Tc-pertechnetate. Each vial contained 50 µg depreotide, 5 mg sodium glucoheptonate dihydrate, 50 µg stannous chloride dihydrate. All experiments were performed within a 5 h-interval after preparation of the kit. Radiochemical purity of ^{99m}Tc-depreotide was > 97% in all experiments.

Cell cultures and exposure experiment

The ZR75-1 and T47D cell line are ER+ and SSTR+ while the MDA MB231 cell line is ER– and SSTR+.

Cells were grown in either Dulbecco's Modified Eagle Medium (DMEM) (T47D), RPMI 1640 Medium (ZR75-1) or Leibovitz's L15 Medium (MDA MB231), supplemented with 10% FBS, 100 IU/ml penicillin/streptomycin solution and 0.14 µg/ml Fungizone in 10% CO_2 / 90% air (DMEM) or 5% CO_2 / 95% air (RPMI) at 37°C. Before exposure experiments, cells were transferred to phenol red-free medium plus 10% charcoal dextran-treated foetal bovine serum (CS-FBS) for 48 h to remove endogenous oestrogens. Phenol red, a pH indicator present in complete media, exerts a weak estrogenic activity *(24)*.

All three cell lines were exposed to 1 n*M* E_2 or a combination of 1 nM E_2 plus 100 n*M* tamoxifen or ICI 182 780 (Faslodex) for 48 h. E_2 and antioestrogens were added from stocks prepared in 100% ethanol. All cells received an equal volume of ethanol 100%. Non-exposed, oestrogen-depleted, cells served as controls.

Exposed and non-exposed cells were subsequently washed twice with Hanks' Balanced Salt Solution without calcium, magnesium or phenol red (CMF-HBSS) to remove all calcium and incubated in CMF-HBSS at 37°C to obtain separate cells. After 30 min, cells were scraped and counted to prepare a final solution of $5x10^5$ cells/250µl of buffer solution.

^{99m}Tc-depreotide binding assay

Saturation studies were performed under steady-state conditions at 4°C to prevent receptor internalisation, allowing identification of B_{max} and K_d values. Intact cells obtained as described above were incubated with increasing concentrations of ^{99m}Tc-depreotide (0.5 n*M*-15 n*M*) in the absence (total binding) and the presence of 20 µ*M* (non-specific binding) of octreotide. Although depreotide has a markedly higher binding affinity for SSTR3 than octreotide, we used the latter for calculation of non-specific binding in appropriate concentrations because of availability reasons *(10).*

After incubation of cells for 60 min at 4°C, the reaction mixture was diluted 1:2 with assay buffer (CMF-HBSS at 4°C) and rapidly centrifuged (4,000 rpm for 5 minutes at 4°C) to separate bound from free ligand. The resulting pellet was washed twice with buffer and counted in a NaI-gamma counter (Cobra, Packard, USA).

Specific binding was determined as the difference between total and non-specific binding. Scatchard-Rosenthal plots were derived using the commercially available software package GraphPad Prism.

Western blotting

Cells were washed trice with phosphate-buffered saline (PBS) incubated and scraped into lysis buffer (PBS, 1% v/v Triton X-100, 1% v/v NP-40, PMSF 0.35 mg/ml of 2 m*M*, leupeptin 10 µg/ml, aprotinin 10 µg/ml, $NaVO_3$ 1 m*M*, $Na_4P_2O_7$ 2.5 mg/ml and NaF 100x 0.1 m*M*) at 4°C. After centrifugation at 14,000 rpm for 10 min at 4°C, the supernatant was removed and stored at –80°C. Protein concentration was measured using the Lowry assay.

To determine the SSTR subtypes responsible for E_2-induced changes in 99mTc-depreotide binding, we measured the subtype-specific SSTR protein amount with western blot under similar conditions as the binding assays. Specific receptor proteins were detected using subtype-selective antibodies developed by Helboe et al *(25).*

Briefly, 10-20 µg of membrane protein was solubilised in sample buffer (125 m*M* Tris-HCl, 12.3% glycerol, 2.3% SDS, 5% β-mercapto ethanol, 0.0125% bromophenol blue, pH 6.8) by incubation in a Thermomixer at 95°C for 5 min, centrifuged at room temperature for 10 min

at 14,000 rpm and fractionated on a 10% sodium dodecyl sulfate-polyacrylamide gel (SDS-PAGE 10%). Electrophoresed proteins were transferred to a nitrocellulose membrane (Hybond ECL, Amersham PB, UK). The blot was saturated with 5% defatted dry milk in PBS free of calcium and magnesium (PBS^{D-}) containing 0.5% Tween-20 (buffer A) for 1 h at room temperature and reacted with antisera against each of the five somatostatin receptors at dilutions 1:500 or 1:1,000 in buffer A for 1 h at room temperature. Membranes were washed 4x10 min with buffer A, incubated for 45 min at room temperature with horseradish peroxidase-conjugated goat anti-rabbit IgG (Amersham Pharmacia Biotech, UK) at 1:4,000, and consecutively washed 4x10 min with buffer A and 2x10 min with PBS^{D-}+0.5% Tween-20. Immunoreactive proteins were detected with the enhanced chemiluminescent antibody detection system (Amersham PB, UK). Blots were developed on high performance, double-coated, autoradiography film (Amersham PB, UK).

Estimation of relative molecular size was performed using a broad molecular weight marker (45 – 210 kDa).

As a semi-quantitative control of protein load we used antisera against α-tubulin to confirm and normalise the presence of membrane proteins in the samples analysed. All samples included in the study had a high abundance of α-tubuline.

Densitometric analysis of western blot data was performed using software package Image J, available at the website of National Institutes of Health, USA (http://rsb.info.nih.gov/ij/).

In vivo study: patients and gamma camera imaging

This study was approved by the Medical Ethics Committee of the Ghent University Hospital and performed according to Good Clinical Practice. All subjects gave their written informed consent prior to participation in the study. Three patients with a diagnosis of advanced breast cancer in whom first- or second-line hormonal therapy was going to be initiated were included. All patients had histologically proven ER+ tumours. All patients were female and had a mean age of 70 years (range 63-71 years). All patients had metastatic disease detected by various diagnostic procedures (e.g. bone scan, X-rays, CT, MRI). Patients underwent sequential ^{99m}Tc-depreotide scintigraphy, before and 3 weeks after initiating hormonal treatment. Follow-up data were retrieved from routine clinical evaluation by means of physical examination, imaging and blood analysis. Progressive disease was defined as an increase in the number of bone lesions and/or an increase in the number and/or size (>20%) of liver lesions. Disease status was considered stable in the absence of both progressive disease and a serum rise in tumour marker.

Planar whole-body imaging was performed 4 h after intravenous injection of 555-740 MBq (15-20 mCi) ^{99m}Tc-depreotide with a small point source placed between the patient's feet. The distance between the head and the table was kept constant for each patient over sequential scans. Images were acquired using a double- or a triple-headed gamma camera (respectively Axis and Irix, Marconi, Cleveland, Ohio, USA) equipped with low-energy high-resolution parallel-hole collimators. The energy peak was centred at 140 keV with a 15% window. Acquisition was performed simultaneously in the anterior and posterior projections with a scan speed of 15 cm/min. Matrix size was 128x512 pixels.

For quantification of radioactivity uptake after injection of ^{99m}Tc-depreotide, regions of interest (ROI's) were drawn over metastatic lesions and the point source. The shapes and sizes of the ROI's, i.e. the number of pixels, were kept constant for the pre- and posttherapy scan. Correction for non-specific uptake and for activity in tissue in front of and behind the organ of interest was performed by using a region over the lower part of the upper leg. For each ROI, the geometric mean, corrected for physical decay, of total anterior and posterior counts was calculated. Total injected activity was calculated from the syringe activity pre- and post-injection measured in an NaI-gammacounter. Uptake in tumor lesions was expressed as % of the injected dose.

Statistical Analysis

Box and whisker plots were used to define outliers. Comparison of the fits of a one-site binding equation with a two-site binding model was performed using an *F* test. Whether or not B_{max} values derived from Scatchard-Rosenthal plots were normally distributed was assessed using the Kolmogorov-Smirnov test. Differences in B_{max} values between non-exposed and exposed cells were assessed using ANOVA and post hoc Bonferroni correction. The defined level of significance was $P<0.05$.

3. Results

Effect of E_2 on SSTR binding in human breast cancer cells

Results are shown in table 1. Scatchard-Rosenthal plot analysis performed using GraphPad, comparing the fits of a one-site binding equation with a two-site binding model using an *F* test, did not provide evidence for multiple classes of binding sites with different affinity for ^{99m}Tc-depreotide in either of the cell lines studied. Instead, a saturable number of specific binding sites for ^{99m}Tc-depreotide in all three human breast cancer cell lines with mean K_d values of 13 n*M*, 7 n*M*, 4 n*M* for T47D, ZR75-1 and MDA MB231 cells was found.

	Control	E_2	E_2+TAM	E_2+ICI
T47D				
No. of exp.	6	6	6	6
Mean	240	425*	243	271
SD	29	67	37	32
ZR75-1				
No. of exp.	8	9	8	7
Mean	385	192	219	290
SD	77	34	41	64

B_{max} values of control cells and hormonal stimulated cells in fmol/10^6 cells.

*= P<0.05 as defined by ANOVA with post hoc Bonferroni correction

Table 1. Effect of E_2 on SSTR binding in the absence and presence of TAM and ICI 182 780.

After stimulating cells grown in oestrogen-depleted medium with 1n*M* E_2 for 48 h, the ER+ cell line T47D demonstrated a mean increase of 81 % (P< 0.05) in ^{99m}Tc-depreotide binding (Fig 1.A-C). Adding the partial agonist tamoxifen and full antagonist ICI 182 780 to E_2 blocked the induced increase in T47D cells, either reducing SSTR expression or restoring it to control levels. Although ZR75-1 cells stimulated with E_2 showed a mean decrease in ^{99m}Tc-depreotide binding of 36% as compared to control cells, this difference proved not to be statistically significant, likely owing to the fairly high standard deviations of the data sets (Fig 1.D-F). Similarly, B_{max} values did not change in ZR75-1 cells exposed to E_2 in combination with an ER antagonist as compared to control cells. Finally, no influence of E_2 on ^{99m}Tc-depreotide binding was observed in the ER– cell line MDA MB231 (data not shown).

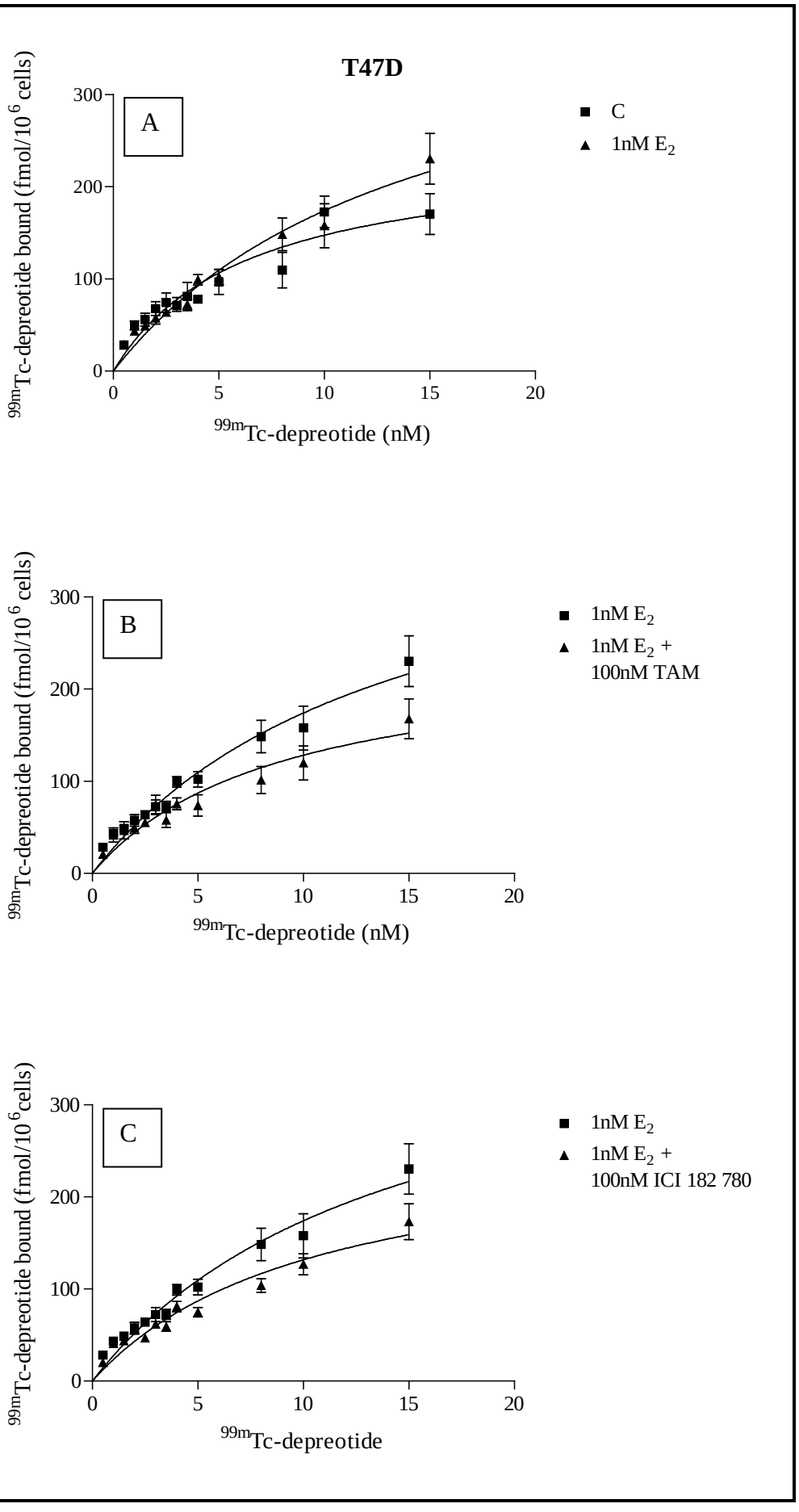
T47D
A
C
1nM E2
99mTc-depreotide bound (fmol/10 6 cells)
99mTc-depreotide (nM)
B
1nM E2
1nM E2 +
100nM TAM
C
1nM E2
1nM E2 +
100nM ICI 182 780
99mTc-depreotide

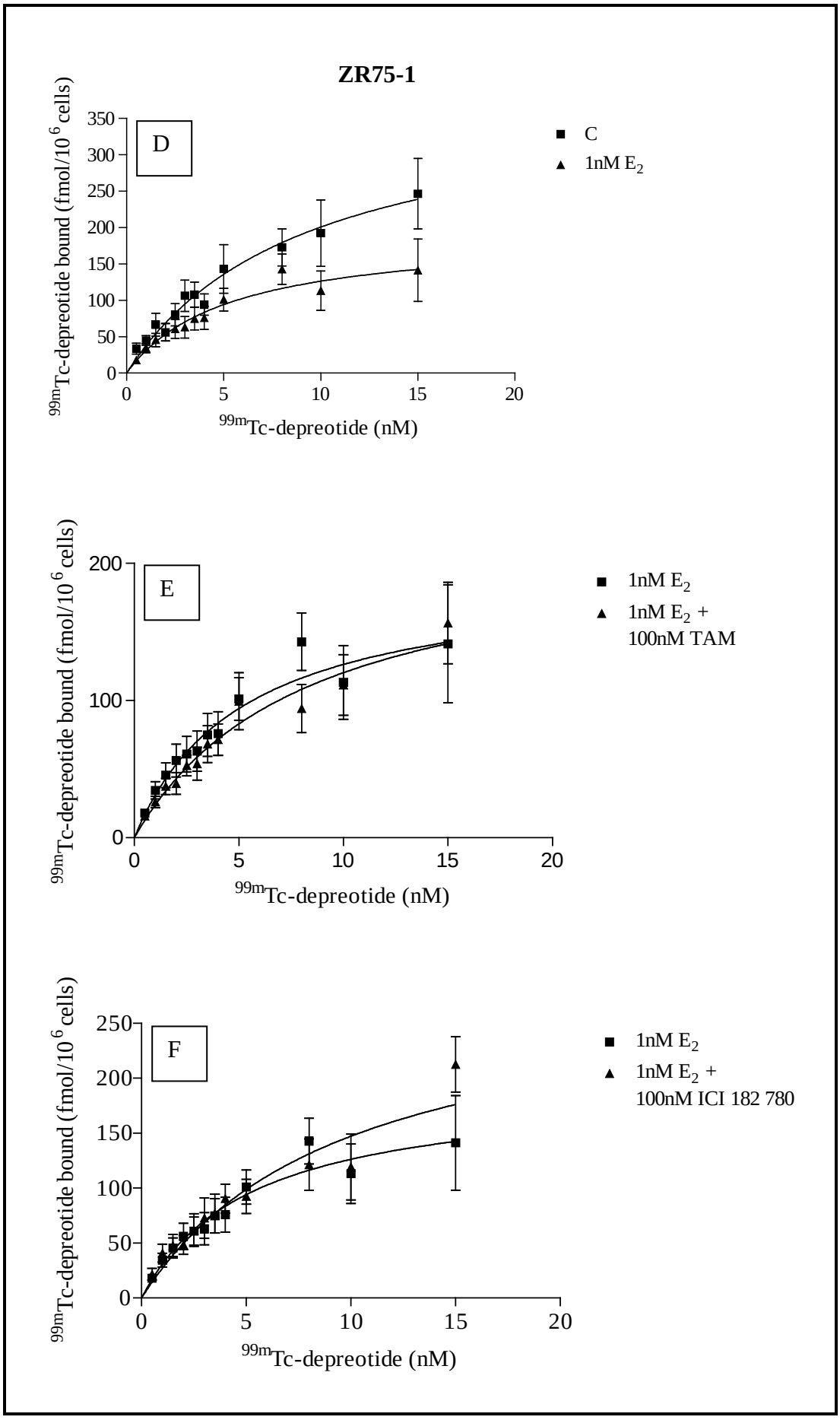
ZR75-1
D
C
1nM E2
99mTc-depreotide bound (fmol/10 6 cells)
99mTc-depreotide (nM)
E
1nM E2
1nM E2 +
100nM TAM
F
1nM E2
1nM E2 +
100nM ICI 182 780

Figure 1. Specific binding of ^{99m}Tc-depreotide to oestrogen receptor-positive (ER+) human breast cancer cell line T47D (**A**-**C**) and ZR75-1 (**D**-**F**). Before exposure experiments, cells grown in complete serum were transferred to phenol red-free media plus CS-FBS for 48 h to remove endogenous oestrogen and then treated (1 n*M* oestradiol) or not (control) with 1 n*M* E_2 for 48 h. Saturation studies were performed in triplicate under steady-state conditions at 4°C. Intact cells were incubated with increasing concentrations of ^{99m}Tc-depreotide (0.5 n*M*-15 n*M*) in the absence (total binding) and the presence (20 µ*M*, non-specific binding) of unlabeled octreotide. The specific binding was calculated by subtracting total binding from non-specific binding. Saturation and nonlinear regression analyses indicated an increase in specific binding sites for ^{99m}Tc-depreotide after oestradiol exposure, displaying a B_{max} of 240 fmol/10^6 cells for control cells and a B_{max} of 425 fmol/10^6 cells for E_2-stimulated cells in T47D cells (**A**). Adding the antioestrogen tamoxifen (*TAM*) restored the B_{max} to 243 fmol/10^6 cells (**B**). Likewise, adding the full antagonist ICI 182 780 (Faslodex) restored the B_{max} to 271 fmol/10^6 cells (**C**). For ZR75-1 cells, B_{max} of 385 fmol/10^6 cells for control cells decreased to 192 fmol/10^6 cells after E_2 stimulation (**D**). Addition of the antioestrogens tamoxifen and ICI 182 780 restored the B_{max} to 219 and 290 fmol/10^6 cells respectively (**E**-**F**).

Effect of E_2 on subtype-specific SSTR protein amount

Results of western blotting assays in unexposed cell lines are shown in Table 2. SSTR2 and SSTR5 were the predominant isoforms in all three cell lines. Both SSTR2 and SSTR5 were expressed at high levels in T47D cells and ZR75-1 cells. In the ZR75-1 cell line, SSTR5 expression was much more pronounced than SSTR2 expression, which was not the case for the T47D cell line (Fig 2).

	SSTR1	SSTR2	SSTR3	SSTR4	SSTR5
T47D	-	++	+	-	+++
ZR75-1	-	++	(+)	-	(+)
MDA MB231	-	++	-	-	-

Table 2. Pattern of SSTR subtype expression in human breast cancer cell lines.

In both cell lines, SSTR2 protein expression was only moderately influenced by E_2 administration, i.e. a modest increase after E_2 treatment and a modest decrease after E_2 removal. In contrast, SSTR5 increased in the absence of E_2 and was restored to the original detection level after E_2 treatment. Observed changes in protein amount were consistently greater in ZR75-1 cells than in T47D cells.

Culturing ER– MDA MB231 cells in phenol red-free medium plus CS-FBS or E_2 did not influence SSTR expression.

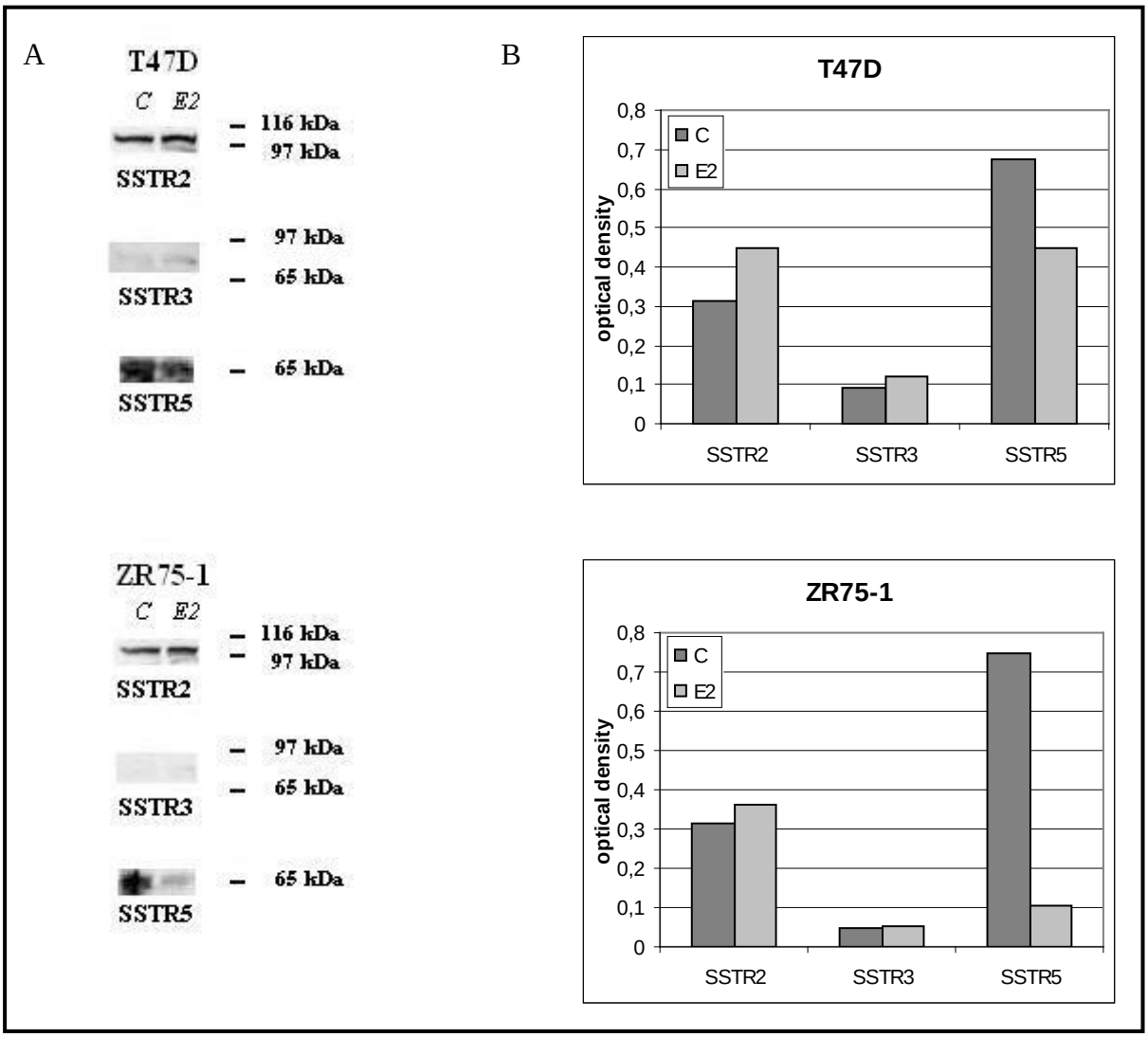

Figure 2. Western blot analysis for evaluation of SSTR receptor subtype-specific expression in ER+ human breast cancer cell lines ZR75-1 and T47D grown in phenol red-free media plus CS-FBS (*C*) and in phenol red-free media plus CS-FBS treated with 1 n*M* oestradiol for 48 h (*E2*).

A Autoradiogram. Molecular weights are comparable to those found by Helboe et al, i.e. SSTR2 ranging from 71 to 95 kDa, SSTR3 ranging from 65 to 85 kDa, SSTR5 ranging from 52 to 66 kDa *(31)*. **B** Densitometric quantification.

In vivo study in patients

In vivo ^{99m}Tc-depreotide scintigraphy visualised metastatic lesions in two of the three breast cancer patients. The results of radioactivity uptake upon quantification are expressed as % injected activity (% IA) and listed in Table 3. Mean clinical follow-up was 20 months (range 18-22 months). In the first patient, bone metastasis was diagnosed 16 years after treatment of the primary tumour. Bone scan revealed extensive lesions in the lumbar and pelvic region,

which were confirmed by conventional imaging (CT and/or MRI). ^{99m}Tc-depreotide scintigraphy both before and 3 weeks after initiation of treatment with tamoxifen (Nolvadex) showed uptake in the known lesions. Uptake in all lesions decreased with a mean value of 56% (range 31-86%) (Fig 3). To date, this patient has had stable disease for more than 22 months.

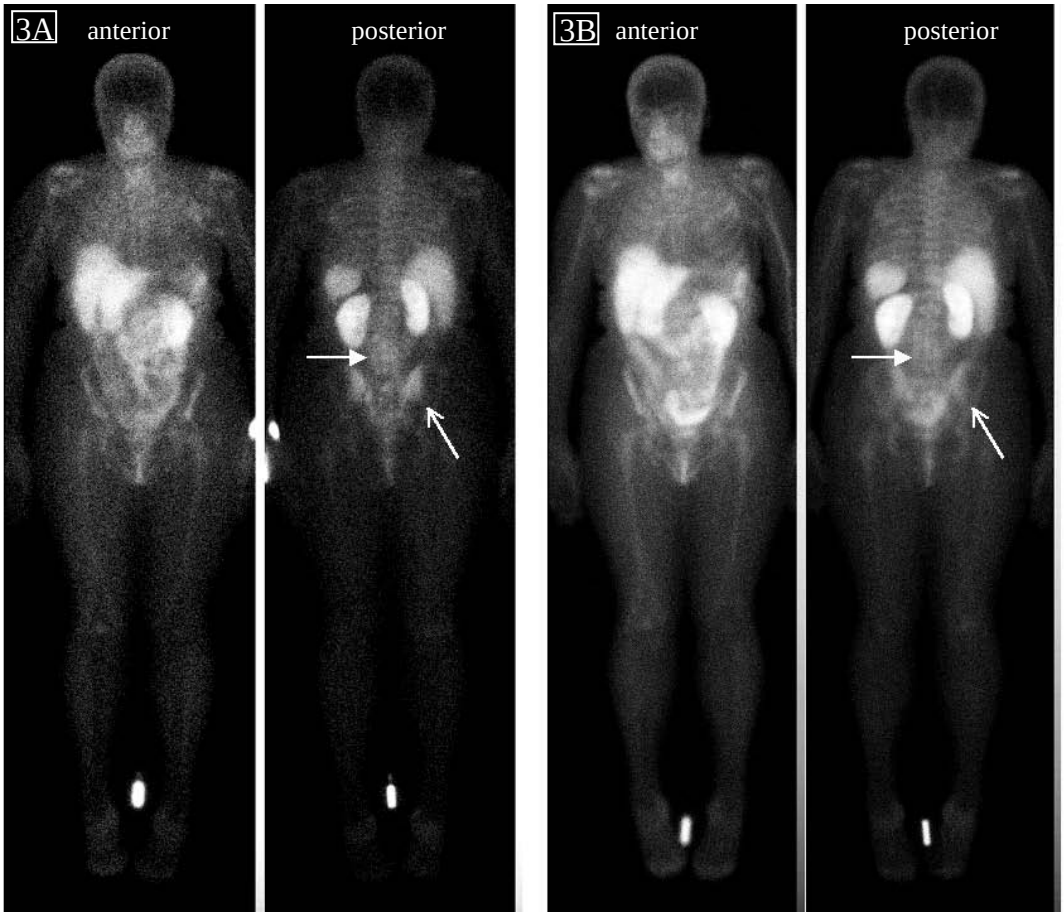

Figure 3. Sequential ^{99m}Tc-depreotide scintigraphy of a breast cancer patient (no. 1) with extensive bone metastasis in lumbar and pelvic region. **A** Pretherapy scan, with visualisation of lumbar lesions (L2-5, *full arrowhead*) and sacro-iliac region on the left (*arrow*) and right. **B** Posttherapy scan 3 weeks after initiation of hormonal treatment with tamoxifen. There is slightly less intense uptake in lumbar lesions (L2-5, *full arrowhead*) and sacro-iliac region on the left (*arrow*) and right as compared with the pretherapy scan.

The second patient had bilateral malignant pleuritis and ^{99m}Tc-depreotide scintigraphy showed high activity in both lungs. Tracer uptake in the lungs slightly increased from the pre- to the posttherapy scan, by 8% and 1% respectively in the left and right lung. This patient presented with progressive disease under hormonal treatment and eventually died.

Patient no.	Age (years)	Lesions	Pretherapy scan (%IA)	Posttherapy scan (%IA)	Change in uptake (%)	Length of follow-up (months)	Clinical status
1	63	L2-L5	0.00037	0.00005	- 86	22	Stable disease
		SIR left	0.03141	0.01222	- 61		
		SIR right	0.01342	0.00855	- 36		
		Sacrum	0.01927	0.00636	- 67		
		Coxo-femoral	0.00217	0.00151	- 31		
2	76	Malignant pleuritis right	2.15509	2.17826	+ 1	21	Progressive disease, deceased
		Malignant pleuritis left	1.97029	2.15063	+ 8		
3	71	Bone lesions	-	-	-	18	Progressive disease
		Malignant pleuritis	-	-	-		

%IA, % injected activity; SIR, sacro-iliac region

Table 3. Clinical data and radioactivity uptake (expressed as % injected activity) during sequential in vivo ^{99m}Tc-depreotide scintigraphy in three breast cancer patients.

Finally, in the third patient, bone lesions were not visualised on ^{99m}Tc-depreotide scintigraphy and hence no quantification was possible. This patient had progressive disease during hormonal treatment, developed liver metastasis and therefore received chemotherapy.

4. Discussion

^{99m}Tc-depreotide is a peptide that contains a bioamino-acid active sequence mimetic of native somatostatin. It has the molecular formula $C_{65}H_{95}N_{16}O_{12}S_2$ and the structure cyclo-(N-Me)Phe-Tyr-(D-Trp)-Lys-Val-Hcy(CH_2CO-(β-Dap)-Lys-Cys-Lys-NH_2), where Hcy is homocysteine and Dap is diaminopropionic acid, the bioactive portion being Tyr-D-Tryp-Lys^{334}-Val *(22,23).* The in vitro binding properties of ^{99m}Tc-depreotide were previously characterized by Virgolini et al. *(21).* Aside from binding with high affinity to many different types of primary tumours, including breast carcinoma , ^{99m}Tc-depreotide was shown to bind to COS7 cells with transfected SSTR subtypes 2, 3 and 5 with median dissociation constant (K_d) of 2.5 n*M*, 1.5 n*M* and 2n*M* respectively (ranging from 0.1 to 10 n*M*). These K_d values are comparable to those found in the three breast cancer cell lines under study (range 4-13 n*M*).

In the series presented, physiological concentrations of E_2 resulted in a statistically significant increase in the number of SSTRs at the level of the cell membrane in T47D cells but not in ZR75-1 and MDA MB231 cells as evidenced by binding assays. Given the minor increase in SSTR2 protein levels as evidenced by western blotting for the T47D cell line, this phenomenon is likely attributable to a predominant recycling of receptors from the inner towards the outer cell membrane. In the ZR75-1 cells, a mean decrease of the number of cell membrane SSTRs after E_2 stimulation was observed, which, however, was not statistically significant. As shown by western blot analysis, this mean decrease may be explained by a drop in the number of SSTR5 receptors. T47D cells also showed a drop in SSTR5 protein content, but it was much less pronounced. In T47D cells, the E_2 effect was reduced or inhibited by the antioestrogens tamoxifen and ICI 182 780; this indicates a requirement for E_2 binding and stimulation of the ER, suggestive of an exclusively E_2-dependent regulation of SSTR2 expression. The reduction seen with tamoxifen as compared to the inhibition seen with ICI 182 780 may be explained by the partial and full antagonist character of the respective molecules.

Oestrogen-dependent regulation of SSTR expression has been reported previously in pituitary cells, prolactinoma cells and MCF-7 human breast cancer cells. Kimura et al. found an increase in SSTR2 mRNA and a strong decrease in SSTR5 mRNA after E_2 treatment in pituitary cells of ovariectomised rats. Examination of the competition curves of ^{125}I-SRIF

binding showed that pituitary membrane receptors from ovariectomised rats and E_2-treated rats displayed similar binding properties characteristic for SSTR2 and SSTR5 *(26).* Djordejevic et al. treated rat pituitary cells with E_2 for 4 days in culture and found a selective overexpression of SSTR2 and 3 and a decrease in SSTR1 and 5 *(27).* In the rat pituitary CH_4C_1 cell line, 24-h E_2 treatment resulted in an increase in SSTR2 and SSTR3 mRNA but also in SSTR1 mRNA *(28).* Furthermore, Visser-Wisselaar et al. added E_2 for 7-14 days to 7315b rat prolactinoma cells in vitro and found induction of the expression of SSTR2 and SSTR3. In their series, administration of the antioestrogen tamoxifen (0.5 µ*M*) decreased ^{125}I-Tyr^3-octreotide binding by 50.5%. Of interest, subcutaneous administration of oestradiol in vivo to 7315b tumour-bearing rats produced SSTR2 mRNA expression only *(29).* So far, an oestrogen-responsive element within a SSTR2 promoter region has not been characterised. On the human SSTR2 gene, an E_2-responsive region has been roughly localised to sequences spanning from kilobase pairs (kb) –5.3 to –3.8 with respect to the transcriptional site in front of the coding region *(30).* Finally, E_2 was shown to down-regulate SSTR5 in the human breast cancer cells MCF-7. In this cell line, the growth-inhibiting effect of Sandostatin (octreotide) was observed to be less pronounced in the presence of oestradiol *(5).*

The results obtained in T47D cells are concordant with results obtained previously by Xu et al. After stimulation of oestrogen-depleted cells with 1 n*M* E_2, these authors found a 12-fold increase in SSTR2 mRNA in T47D cells that was blocked by addition of the antioestrogens tamoxifen or ICI 182 870 *(20).* Although the difference in the magnitude of the mRNA increase as compared with the increase in receptor number on T47D cells might relate to the much higher sensitivity of PCR detection, it should be noted that the authors did not perform quantitative PCR. On the other hand, in ZR75-1 cells the 48-fold increase in SSTR2 mRNA reported by Xu et al. did not coincide with the modest, insignificant increase in SSTR2 protein content found in the series presented. This dissociation between receptor gene transcription and receptor protein translation may be due to an increase in mRNA stability or a decrease in the rate of global protein synthesis. Glucocorticoids are known to modulate gene expression via an intracellular receptor similar to the oestrogen receptor. Experiments in which the half-life of SSTR2 mRNA was measured and nuclear run-on assays suggested that the effects of dexamethasone are mainly due to changes in the transcription rate of the gene and not to changes in mRNA stability *(28).* Of interest, Xu et al. did not detect SSTR5 mRNA in any of the three breast cancer cell lines grown in complete medium and therefore did not further study SSTR5 mRNA regulation by E_2. Possibly, the weak oestrogenic activity of phenol red, a pH indicator present in complete media, suppresses SSTR5 mRNA to very low,

hardly detectable levels *(24)*. Nevertheless, inconsistent expression of somatostatin receptors varying with the intensity of growth during different cell cycle phase or in the course of consecutive passages of a cell line can not be excluded, nor can the authenticity of the cell lines used be guaranteed *(31)*.

As shown by Schaer et al., most human breast carcinomas with octreotide binding sites exhibit SSTR2 mRNA whereas in all cases of octreotide-negative tumours, SSTR2 mRNA is absent *(32)*. The receptors encoded by the SSTR2 mRNA were proven to be those mainly responsible for high ^{111}In-DTPA-octreotide uptake in primary breast cancer *(18)*.

Hypothetically, in analogy with the findings in T47D cells, efficient antioestrogen treatment of metastasised breast cancer patients may result in down-regulation of SSTR at the cell surface level. In an attempt to document this phenomenon, three patients with ER+ breast tumours in whom hormonal therapy was going to be initiated underwent sequential somatostatin receptor scintigraphy. Pretherapy ^{99m}Tc-depreotide scintigraphy depicted SSTR expression of metastatic breast cancer lesions in two of the three patients. SSTR scintigraphy performed 3 weeks later, at a time when intra-tumour steady state levels of tamoxifen are obtained, revealed substantially lower uptake in the lesions of the patient showing a favourable response to hormonal treatment, potentially indicating a down-regulation of SSTR expression and hence an efficient blockade of ER function. The non-responding patient showing uptake of ^{99m}Tc-depreotide in known lesions on the baseline scan exhibited no change in tracer uptake on the post-therapeutic scan. Finally, in the patient not showing ^{99m}Tc-depreotide uptake prior to treatment and not responding to treatment, it may be hypothesised that ER was already non-functional ab initio, as no SSTRs were present.

In conclusion, the findings presented support an oestrogen-dependent regulation of SSTR expression in some breast cancer cell lines. In vivo imaging of this molecular event by means of sequential ^{99m}Tc-depreotide or ^{111}In-DTPA-octreotide scintigraphy appears feasible.

Acknowledgements:

The authors wish to thank Dr C. E. Stidsen (Novo Nordisk, Denmark) for providing the SSTR subtype-specific antibodies and Prof. M. Mareel for encouraging support during binding experiments. Dr B. Van Den Bossche has prepared this manuscript as part of her PhD course in the Nuclear Medicine Unit at the University of Rome "La Sapienza" and wishes to thank Prof. F. Scopinaro and Dr. A. Signore for their support and useful suggestions in preparing the manuscript.

5. References

1. Raynor K, Reisine T. Somatostatin receptors. *Crit Rev Neurobiol* 1992; 16: 273-289.
2. Reichlin S. Somatostatin. *N Eng J Med* 1983;309:1495-1563.
3. Patel YC. Somatostatin and its receptor family. *Front Neuroendocrinol* 1999;20:157-198.
4. Lamberts SWJ, Krenning EP, Reubi JC. The role of somatostatin and its analogs in the diagnosis and treatment of tumors. *Endocr Rev* 1991;12:450-482.
5. Seytono-Han B, Schenkelmans MS, Foekens JA, Klijn JGM. Direct inhibitory effects of somatostatin (analogues) on the growth of human breast cancer cells. *Cancer Res* 1987;47:1566-1570.
6. Scambia G, Panici PB, Baiocchi G, Perrone L, Iacobelli S, Mancusco S. Antiproliferative effects op somatostatin and the somatostatin analogue SMS 201-995 on three human breast cancer cell lines. *J Cancer Res Clin Oncol* 1988;114:306-308.
7. Reisine T, Bell G. Molecular biology of somatostin receptors. *Endocr Rev.* 1995;16:427-442.
8. Panetta R, Patel YC. Expression of mRNA for all five human somatostatin receptors (hSSTR1-5) in pituitary tumors. *Life Sci* 1995;56:333-342.
9. Reubi JC, Kappeler A, Waser B, Laissue JA, Hipkin RW, Schonbrunn A. Immunohistochemical localization of somatostatin receptors SS2A in human tumors. *Am J Pathol* 1998;153:233-245.
10. Bruno JF, Xu Y, Song J, Berelowitz M. Molecular cloning and functional expression of a brain-specific somatostatin receptor. *Proc Natl Acad Sci* 1992;89:11151-11155.
11. Hoyer D, Bell GI, Berlowitz M, et al. Classification and nomenclature of somatostatin receptors. *Trends Pharmacol Sci* 1995;16:86-88.
12. Reubi JC, Krenning E, Lamberts SWJ, Kvols L. In vitro detection of somatostatin receptors in human tumors. *Metabolism* 1992; 41(9 suppl 2):104-110.
13. Vikic-Topic S, Raisch KP, Kvols LK, Vuk-Pavlovic S. Expression of somatostatin receptor subtypes in breast carcinoma, carcinoid tumor, and renal cell carcinoma. *J Clin Endocrinol Metab* 1995;80(10):2974-2979.
14. Bootsma AH, van Eijck C, Schouten KK, et al. Somatostatin receptor-positive primary breast tumors: genetic, patient and tumor characteristics. *Int J Cancer* 1993;54:357-362.

15. Reubi JC, Waser B, Foekens J, et al: Somatostatin receptor incidence and distribution in breast cancer using receptor autoradiography: relationship to EGF receptors. *Int J Cancer* 1990;46:416-420.
16. van Eijck CHJ, Krenning EP, Bootsma A, et al. Somatostatin-receptor scintigraphy in primary breast cancer. *The Lancet* 1994;343:640-643.
17. Reubi JC, Waser B, Schaer JC, Laissue JA. Somatostatin receptor SS1-SS5 expression in normal and neoplastic human tissues using receptor autoradiography with subtype-selective ligands. *Eur J of Nucl Med* 2001;38(7):836-46.
18. Schulz S, Helmholz T, Schmitt J, Franke K, Otto HJ, Weise W. True positive somatostatin receptor scintigraphy in primary breast cancer correlates with expression of sst2A and sst5. *Breast Cancer Res Treat* 2002;72:221-226.
19. Reubi JC and Torhorst J. Relationship between somatostatin, EGF-and steroid-hormone receptors in breast cancer. *Cancer* 1989;64:1254-1260.
20. Xu Y, Song J, Berelowitz M, Bruno JF. Oestrogen regulates somatostatin receptor subtype 2 messenger ribonucleic acid expression in human breast cancer cells. *Endocrinology* 1996;137(12):5634-5640.
21. Virgolini I, Leimer M, Handmaker H, Lastoria S, Bischof C, Muto P, Pangerl T, Gludovacz D, Peck-Radosavljevic M, Lister-James J, Hamilton G, Kaserer K, Valent P, Dean R. Somatostatin receptor subtype specificity and in vivo binding of a novel tumor tracer, ^{99m}Tc-P829. *Cancer Res* 1998; 58: 1850-1859.
22. Lister-James J, Pearson DA, De Rosch MA, et al. Tc-99m P829: characterization of a technetium-99-labeled somatostatin receptor-binding peptide. *Technetium, Rhenium and Other Metals in Chemistry and Nuclear Medicine* 1999;473-478.
23. Vallabhajosalu S, Moyer BR, Lister-James J, et al. Preclinical evaluation of technetium-99m-labeled somatostatin receptor-binding peptides. *J Nucl Med* 1996;37(6):1016-1022.
24. Berthois Y, Katzenellebogen JA, Katzenellebogen BS. Phenol red in tissue culture media is a weak estrogen: implications concerning the study of estrogen-responsive cells in culture. *Proc Natl Acad Sci USA* 1986;83:2496-2500.
25. Helboe L, Møller M, Nørregaard L, Schiødt M, Stidsen CE. Development of selective antibodies against the human somatostatin receptor subtypes SS1-SS5. *Mol Brain Res* 1997;49:82-88.

26. Kimura N, Tomizawa S, Arai KN, Kimura N. Chronic treatment with oestrogen up-regulates expression of SS2 messenger ribonucleic acid (mRNA) but down-regulates expression of SS5 mRNA in rat pituitaries. *Endocrinology* 1998;139:1573-1580.
27. Djordjijevic D, Zhang J, Priam M, et al. Effect of 17beta-estradiol on somatostatin receptor expression and inhibitory effect on growth hormone and prolactine release in rat pituitary cell cultures. *Endocrinology* 1998;139:2272-2277.
28. Xu Y, Berelowitz M, Bruno JF. Dexamethasone regulates somatostatin receptor subtype specific messenger ribonucleic acid expression in rat pituitary GH_4C_1 cells. *Endocrinology* 1995;136:5070-5075.
29. Visser-Wisselaar HA, Van Uffelen CJC, Van Koetsveld PM, et al. 17 estradiol dependent regulation of somatostatin receptor subtype expression in the 7315 b prolactin secreting rat pituitary tumor in vitro and in vivo. *Endocrinology* 1997;138:1180-1189.
30. Xu Y, Berelowitz M, Bruno JF. Characterization of the promoter region of the human somatostatin receptor subtype 2 gene and localization of sequences required for estrogen-responsiveness. *Mol Cell Endocrinol* 1998;139:71-77.
31. Masters JR, Thomson JA, Daly-Burns B, et al. Short tandem repeat profiling provides an international reference standard for human cell lines. *Proc Natl Acad Sci USA* 2001;98:8012-8017.
32. Schaer JC, Waser B, Mengod G, Reubi JC. Somatostatin receptor subtypes SS1, SS2, SS3 and SS5 expression in human pituitary, gastroentero-pancreatic and mammary tumors: comparison of mRNA analysis with receptor autoradiography. *Int J Cancer* 1997;70:530-537.

CHAPTER FOUR

Biodistribution and dosimetry of ^{99m}Tc-depreotide (P829) in patients suffering from breast carcinoma

Bieke Van Den Bossche[1], Eveline D'haeninck[1], Klaus Bacher[3], Hubert Thierens[3], Simon Van Belle[2], Rudi Andre Dierckx[1], Christophe Van de Wiele[1]

[1]Division of Nuclear Medicine, Ghent University Hospital, Ghent, Belgium

[2]Department of Clinical Oncology, Ghent University Hospital, Ghent, Belgium

[3]Department of Biochemical Physics and Radiation Protection, Ghent University, Belgium

Cancer Biother Radpharm 2004; 19(6): 776-783.

---

1. Abstract

This paper reports on the biodistribution and dosimetry of ^{99m}Tc-depreotide in patients. Whole body planar images were acquired 30 minutes, 1, 2, 4, 9 and 24 hours after intravenous injection of 555-740 MBq ^{99m}Tc-depreotide in 5 breast cancer patients. Urine was collected up to 24 hours after injection, allowing for a calculation of renal clearance and interpretation of whole body clearance. Time activity curves were generated for the thyroid, lungs, liver, spleen, kidneys, colon, thoracic vertebrae/sternum, and whole body by fitting the organ-specific geometric mean counts, obtained from regions of interest (ROIs). The Medical Internal Radiation Dose (MIRD) formulation was applied to calculate the absorbed radiation dose for various organs. The whole body images show most of the activity distributed in the liver, spleen and kidneys. Nearly all excretion of activity occurred by the renal system, and hepatobiliary excretion was negligible. Elimination of administered activity occurred predominantly through physical decay. The mean cumulative measured urinary excretion at 24 hours postinjection was 14.0% (standard deviation; 11.8%) of the administered activity. The highest absorbed dose was received by the kidneys, thyroid, and spleen. The average effective dose was estimated to be 1.15E-02 mSv/MBq (standard deviation; 1.41E-03 mSv/MBq). The biodistribution of ^{99m}Tc-depreotide demonstrated low lung and myocardial uptake allowing early imaging of the supradiaphragmatic region and this with a dosimetry favorable for clinical whole body and single photon emission computed tomography (SPECT) imaging.

2. Introduction

In vivo imaging of somatostatin receptor (SSTR) positive tumors is routinely performed using [^{111}In-DTPA-D-Phe^{1}]-octreotide scintigraphy (Octreoscan®) and uptake correlates with

expression of SSTR2A and SSTR5 (1;2). However, technetium labeling offers clinical advantages when compared to indium labeling, including lower cost, better availability and faster tumoral visualization, enabling a 1-day-protocol. The decay characteristics of technetium, more adapted to the photon energy detection ability of gamma cameras, together with the shorter physical half-life permitting a higher dose administration, result in better image quality combined with lower radiation dose. Therefore the technetium-labeled somatostatin analog depreotide (P829) was developed (3). Depreotide is a peptide that contains a bioamino-acid active sequence mimetic of native somatostatin. Its structure is cyclo-(N-Me)Phe-Tyr-(D-Trp)-Lys-Val-Hcy(CH_2CO-(β-Dap)-Lys-Cys-Lys-NH_2), where Hcy is homocysteine and Dap is diaminopropionic acid, the bioactive portion being Tyr-D-Tryp-Lys^{334}-Val (4;5). The *in vitro* binding properties of ^{99m}Tc-depreotide were previously characterized by Virgolini et al (6). Aside from binding with high affinity to many different types of primary tumors, including breast carcinoma, ^{99m}Tc-depreotide was shown to bind to COS7 cells with transfected SSTR subtypes 2, 3 and 5 with median dissociation constant (Kd) of, respectively, 2.5 nM, 1.5 nM and 2 nM (ranging from 0.1-10 nM).

Depreotide (NeoTect®, NeoSpect®) received U.S. Food and Drug Administration (FDA) approval for use in the imaging of suspected malignant tumors in the lung. Blum et al. conducted the first study in patients with suspicious solitary pulmonary nodules (7). The sensitivity and specificity of ^{99m}Tc-depreotide single photon emission computed tomography (SPECT) were, respectively, 93% and 88% with positive and negative predictive values of, respectively, 87% and 93%. A multicenter trial conducted in 19 participating medical centers in the United States and Europe, using the same patient population, found a sensitivity and specificity of respectively 96.6% and 73.1% (8). These values compare favorably with results (e.g., 96% and 74%) obtained by fluorodeoxyglucose-positron emission tomography (FDG-PET) for solitary pulmonary nodule characterization, as reported by Gould et al. in a recent meta-analysis (9). Aside from uptake by solitary pulmonary nodules, ^{99m}Tc-depreotide is also taken up by breast carcinoma, lymphoma and meningeoma (10-12). Available data on cell lines and, to a lesser extent, in patients, suggest a potential role for ^{99m}Tc-depreotide as a marker of response to hormonal therapy in patients suffering from breast carcinoma. As the biodistribution and dosimetry of ^{99m}Tc-depreotide have not been published before, we studied both in patients suffering from breast carcinoma (13).

3. Patients and Methods

Radiopharmaceutical synthesis

NeoSpect was kindly provided by Amersham Health (Little Chalfont, Buckinghamsire, UK). NeoSpect vials were reconstituted with 1480-1850 MBq (40-50 mCi) ^{99m}Tc-pertechnetate diluted with sodium chloride 0.9% w/v solution in a total of 1 mL. Each vial contained 50 µg depreotide, 5 mg sodium glucoheptonate dihydrate, 50 µg stannous chloride dihydrate, pH 7.4. After incubation for 10 minutes in a boiling water bath, the vial was allowed to cool down to body temperature (about 15 minutes) at room temperature. Radiochemical purity of ^{99m}Tc-depreotide, defined by ITLC, was greater than 97%.

Subjects

This study was approved by the Medical Ethics Committee of Ghent University Hospital and performed according to good clinical practice. All subjects gave their written informed consent prior to participation in the study. Five female patients, with a mean age of 58 years (range, 52-62 years), were included in the study. All patients had a history of breast cancer. All had normal kidney and liver functions based upon physical examination, serum chemical analysis and urine analysis. In all of these patients, the injected dose of ^{99m}Tc-depreotide was 555-740 MBq. Total injected activity was calculated based on the syringe activity pre- and postinjection measured in a NaI-gammacounter.

Imaging

Subjects were positioned supine with their arms alongside their body and a point source of 3.7 MBq in a syringe of 5cc placed in a phantom between their feet. Whole body images were performed using a double-headed or a triple-headed gamma camera (respectively, Axis and Irix, Marconi/Picker, Cleveland, OH), equipped with low-energy high-resolution parallel–hole collimators. The energy peak was centered at 140 keV with a 15% window. Whole body planar images were acquired 30 minutes, 1, 2, 4, 9 and 24 hours postinjection. Acquisition was performed simultaneously in anterior and posterior position with a scan speed of 15 cm/min. Matrix size was 256x1024 pixels.

Urine sampling

For all subjects, all voided urine from time of injection until 24 hours following injection was collected. The subjects were requested to collect urine prior to each emission scan and at home *ad libitum*. For each voidance, the urine was collected in a separate container and the

volume and time of voidance recorded. For each voidance time, two 1-mL urine aliquots were sampled and radioactivity was counted in a calibrated NaI (Tl) counter (Cobra III, Packards Instruments Co., Meriden, CT). The amount of radioactivity in the urine at each voidance time was expressed as the percentage of the injected activity (% IA) of ^{99m}Tc-depreotide.

Dosimetry

Image analysis

For quantification of radioactivity uptake after injection of ^{99m}Tc-depreotide, regions of interest (ROIs) over the total body and organs of interest were drawn on the images taken after 4 hours and the shapes and sizes (i.e., number of pixels) were kept constant over all previous and subsequent images. Correction for nonspecific uptake and for activity in tissue in front of and behind the organ of interest was performed by using a region over the lower part of the upper leg. For each ROI (i.e., each organ), the geometric mean, corrected for physical decay, of total anterior and posterior counts was calculated. Quantification of measured activity (from counts to MBq) was performed by means of a point source placed between patients' feet. The total body geometric mean activity (in counts), calculated on the first image (30 min p.i.) was considered the total injected activity (in MBq), as no urine was excreted prior to the first whole body scan. As such, attenuation correction was taken into account when calculating %IA.

Dosimetric calculations

For each individual, time activity curves were generated for the thyroid, lungs, liver, spleen, kidneys, colon, thoracic vertebrae/sternum and whole body. Using SPSS 10.0 (SPSS Inc., Chicago) software, time activity curves were generated for these organs by biexponential and monoexponential fits. Urinary bladder residence times were estimated using the dynamic bladder model of Cloutier et al. and assuming a voiding interval of 4.8 hours (14). Source organ residence times were determined from integration of the time activity curves. Upper large intestine (ULI) and lower large intestine (LLI) residence times were calculated from colon residence times by multiplication with their respective weight factors (0.57 for ULI and 0.43 for LLI). Red marrow residence time was calculated from thoracic vertebrae/sternum residence time taken into account the distribution of red bone marrow in adults (2.3% for sternum and 14.1% for thoracic vertebrae) (15). Residence times were then used to determine target organ radiation doses using the Medical Internal Radiation Dose (MIRD) methodology

for the nonpregnant adult woman applying the MIRDOSE 3.0 (Michael G. Stabin, Vanderbilt University, Nashville) software package (16-18).

4. Results

After injection of 555-740 MBq ^{99m}Tc-depreotide, no adverse or subjective side-effects were noticed in any of the subjects. Anterior whole body images of a female subject showing the biodistribution of radioactivity upon injection of ^{99m}Tc-depreotide at different time points postinjection are presented in Figure 1. The whole body images obtained between 30 min and 24 hours p.i. show most of the activity distributed in the liver, spleen, and kidneys. In addition, uptake in lungs, colon, bone marrow and bucco-pharyringeal mucosa was noticed. Uptake in brain and myocardium was low. Of interest, only in 1 patient was gallbladder activity visualized on the first images acquired. Although of low quality because of low counting statistics, images at 24 hours p.i. showed most of the remaining activity distributed in the kidneys and liver.

Averaged ROI data over all subjects, expressed as % IA, of ^{99m}Tc-depreotide in the total body and in various organs at the different points in time, are presented in Figure 2. At the moment of scintigraphy, 3 patients suffered from bone metastasis, whereas active disease was absent in the other 2 patients. The clearance curves from whole body and individual organs of patients presenting with active disease or of patients in whom active disease could not be substantiated, however, proved similar .

Averaged residence times calculated from individual time activity curves are listed in Table 1. For subject number 2, residence times for the lungs and sternum/thoracic vertebrae were not measured, as she suffered, respectively, from pleural effusion and bone metastasis in that particular region.

Clearance from radioactivity from whole body and individual organs, except for the kidneys and colon, fitted a biexponential curve. The mean calculated effective whole body half-life was 2.3 hours (first exponent) for 14.3% IA and 6.1 hours (second exponent) for 93.6% IA, indicating a predominant elimination of administered activity through physical decay. Of interest, tracer uptake in metastatic bone lesions augmented up to 2-4 hours and remained stable without biological clearance. Nearly all excretion of activity occurred by the renal system; hepatobiliary excretion was negligible. The mean cumulative measured urinary excretion at 24 hours postinjection was 14.0% (standard deviation, 11.8%) of the administered activity (Fig. 3). The residence time was highest for the remainder of the body in all subjects, followed by the kidneys and the liver (Table 1).

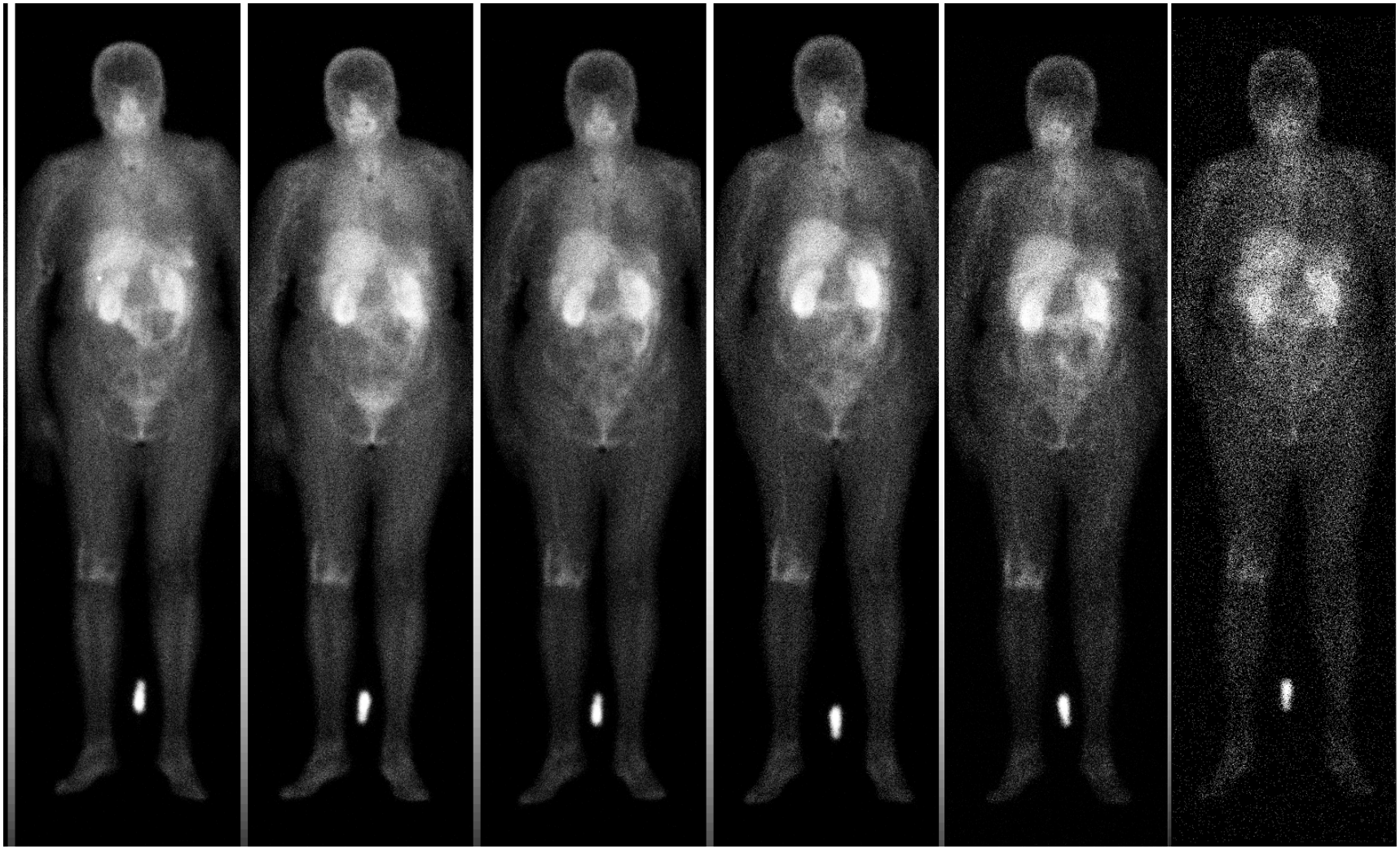

Figure 1. The anterior whole body images obtained at *(from left to right)* 30 minutes, 1, 2, 4, 9 and 24 hours postinjection.

Organ	Subject						
	1	2	3	4	5	Mean	SD
Thyroid	0.0487	0.0251	0.0540	0.0507	0.0495	0.0456	0.0117
Lungs	0.5109	ND*	0.3747	0.3908	0.5519	0.4571	0.0877
Liver	0.7687	0.9529	0.5387	0.4863	0.7335	0.6960	0.1880
Red marrow	0.6190	ND*	0.9774	0.6382	0.9446	0.7827	0.1689
Spleen	0.2247	0.2965	0.1483	0.1285	0.1404	0.1877	0.0716
ULI	0.2527	0.1710	0.2975	0.1952	0.2607	0.2354	0.0514
LLI	0.1907	0.1290	0.2244	0.1472	0.1967	0.1776	0.0388
Kidneys	1.1378	0.6478	0.8735	0.8203	0.6588	0.8276	0.1995
Urinary bladder contents	0.0140	0.1740	0.0281	0.0042	0.0224	0.0485	0.0707
Remainder	4.5413	5.9079	4.7242	5.2076	4.3466	5.0466	0.6737

* For subject number 2, residence time for the lungs and sternum/thoracic vertebrae was not measured, as she suffered from pleural effusion and bone metastasis in the respective region.

ND, not done; SD, standard deviation; ULI, upper large intestine; LLI, lower large intestine.

Table 1. The residence times (in hours) for ^{99m}Tc-depreotide for each source organ.

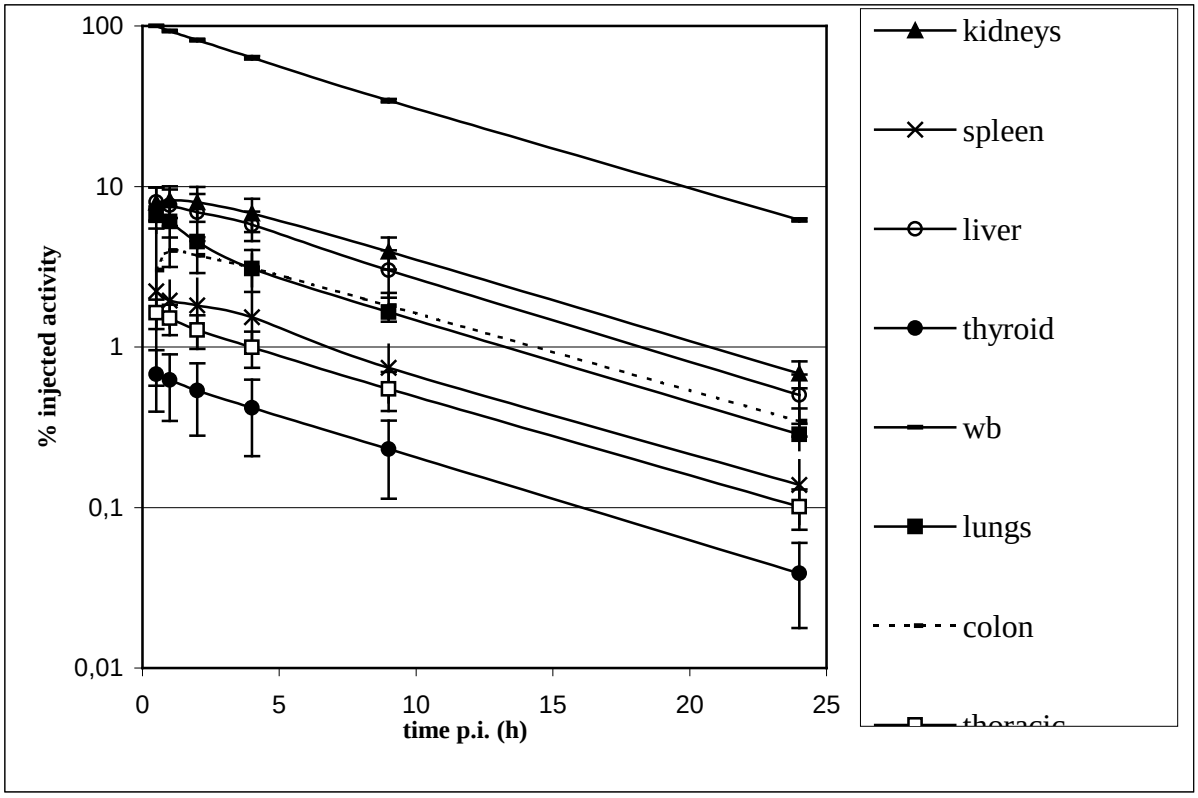

Figure 2. Time-activity curves for the total body (wb) and various organs, calculated from direct measurements of counts in organ-specific regions of interest (ROIs). The data, expressed as % injected activity (IA), are averaged over 5 subjects. The error bars represent 1 standard deviation.

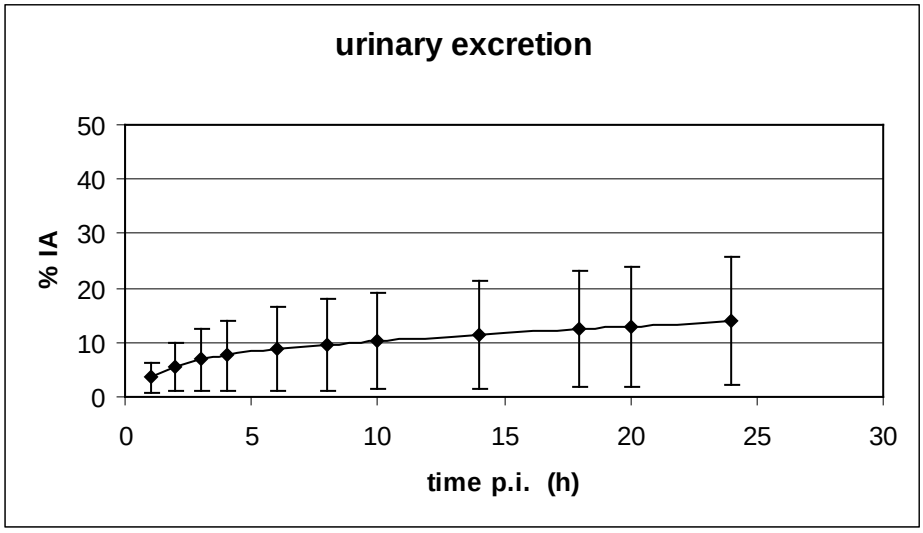

Figure 3. Mean cumulative urinary excretion measured during the first 24 hours postinjection. Physical decay-corrected data are averaged over 5 subjects and expressed in % injected activity (IA). Error bars represent 1 standard deviation.

The mean radiation dose estimates (± standard deviation) were calculated for each subject independently, and then averaged (Table 2). The dose to the thyroid was fairly high, predominantly due to specific tracer uptake. Finally, high uptake resulted in a rather high dose to the lungs.

Target organ	Mean	SD
Adrenals	9.65E-03	7.91E-04
Brain	3.12E-03	2.20E-04
Breasts	3.20E-03	6.19E-05
Gallbladder wall	9.25E-03	8.16E-04
Lower large intestine wall	1.43E-02	3.04E-03
Small intestine	7.67E-03	5.88E-04
Stomach	6.62E-03	3.52E-04
Upper large intestine wall	1.53E-02	3.03E-03
Heart wall	5.89E-03	1.81E-04
Kidneys	5.39E-02	1.14E-02
Liver	1.42E-02	2.77E-03
Lungs	1.01E-02	2.84E-03
Muscle	4.39E-03	7.56E-05
Ovaries	7.75E-03	1.03E-03
Pancreas	9.08E-03	6.81E-04
Red marrow	8.04E-03	2.14E-03
Bone surfaces	9.52E-03	9.27E-04
Skin	2.66E-03	1.11E-04
Spleen	2.62E-02	6.68E-03
Thymus	4.39E-03	8.68E-05
Thyroid	3.34E-02	7.94E-03
Urinary bladder wall	7.07E-03	4.30E-03
Uterus	6.04E-03	3.29E-04
Total body	5.39E-03	1.47E-04
Effective dose*	1.15E-02	1.41E-03

* Units of the effective dose are mSv/MBq. SD, standard deviation.

Table 2. Absorbed dose estimates (mGy/MBq) for ^{99m}Tc-depreotide.

On average, the highest dose was received by the kidneys (mean, 5.39E-02 mGy/MBq; standard deviation, 1.14E-02 mGy/MBq) followed by the thyroid (mean, 3.34E-02 mGy/MBq; standard deviation, 7.94E-03 mGy/MBq) and the spleen (mean, 2.62E-02 mGy/MBq; standard deviation, 6.68E-03 mGy/MBq). The estimated mean effective dose for an adult, calculated using the weighting factors of ICRP publication 60, was 1.15E-02 mSv/MBq (standard deviation, 1.41E-03 mSv/MBq) (19).

5. Discussion

Consistent with its safety profile, no adverse or subjective effects were noticed in any of the subjects. In phase I-III clinical trials including 909 patients, no serious adverse events were reported (20). In 5.4% of all enrolled patients, at least one adverse event occurred. The most commonly reported adverse events were headache (0.9%), diarrhea (0.7%), nausea (0.7%), back pain (0.6%) and dizziness (0.4%). Observed changes in laboratory parameters, e.g., alanine aminotransferase (ALT), white blood cell (WBC) count and eosinophil count, following administration were transient and clinically insignificant.

In our study, most of the activity was observed in the liver, spleen, and kidneys. More specifically, 1 hour following the administration of ^{99m}Tc-depreotide 8.2% of the activity was present in the kidneys and 7.6% in the liver. In contrast, in an animal study using tumor-bearing rats, 30% of the activity was present in the kidneys and less than 5% in the gastro-intestinal tract on the images at 1 hour (4). These data illustrate the species-specific clearance pattern. Although hepatobiliary excretion was negligible, the average activity in the large intestine was 4.0% IA 1 hour postinjection. This uptake is likely due to specific binding to SSTR2 in intestinal mucosa and lymphoid tissue (21). We found low uptake in the lungs representing 6.5% of the total body activity at 1 hour p.i. This is concordant with previous publications describing faint uptake in normal lungs (22).

Mild uptake was noted in ribs, sternum, vertebrae, pelvis and proximal femur. This phenomenon may be explained by specific binding of ^{99m}Tc-depreotide to SSTR2-expressing cells of the human immune system, such as monocytes, T- and B-lymphocytes, present in red bone marrow (21;23;24). Likewise, high uptake in the spleen likely depicts presence of SSTR2 on immune cells, as well as on spleen cells.

Finally, absence of penetration through the blood-brain barrier and, hence, lack of tracer uptake in the normal brain makes it potentially useful for detection of cerebral metastasis.

As opposed to ^{99m}Tc-depreotide, [^{111}In-DTPA-D-Phe]-octreotide exhibits different biodistribution and excretion patterns, resulting in absence of uptake in bone marrow, much

lower uptake in liver and mainly excretion via kidneys with minor hepatic accumulation and minute hepatobiliary excretion (25). Part of these differences may be attributed to the different affinity profiles of both tracers, respectively, a high affinity for SSTR2 and SSTR5 (SSTR2 K_d = 1.5 nM, SSTR3 K_d = 15 nM and SSTR5 K_d = 0.5 nM) of [^{111}In-DTPA-D-Phe]-octreotide, whereas ^{99m}Tc-depreotide exhibits additional high affinity for SSTR3 (SSTR2 Kd = 2.5 nM, SSTR3 Kd = 1.5 nM and SSTR5 Kd = 2 nM) (6). The MIRDOSE 3.0 software provides a calculation of the effective dose as defined in the ICRP 60 (19). Based on the mean effective dose of 1.15E-02 mSv/MBq obtained in this study, patients could easily be investigated with 555-740 MBq ^{99m}Tc-depreotide, allowing both planar and SPECT imaging (data not shown). The corresponding effective dose of 6.4-8.5 mSv is somewhat higher than the reported average effective dose per patient of 4.6 mSv for nuclear medicine procedures worldwide (26). On the other hand, the mean effective dose of 1.15E-02 mSv/MBq is lower than the estimated effective dose of 1.60E-02 mSv/MBq reported on the package leaflet (20). It is unclear how the latter dose (mean dose ?) was derived. More specifically, the number-, gender- of and presence or absence of disease in subjects included is missing on the package leaflet. On the other hand, the doses received by the intestines is higher in our study than the estimated absorbed radiation dose of 0.5E-02 mSv/MBq for both the small and upper large intestine reported on the package leaflet. Theoretically, the higher doses for small and large intestines, as found in our series, might relate to the fact that residence times were effectively derived from ROI analysis over these organs in our series, which may not have been the case in the package leaflet analysis. Lack of data, however, hampers verification of these assumptions.

The aforementioned mean effective dose for ^{99m}Tc-depreotide (6.4-8.5 mSv/555-740 MBq) is substantially lower than that of [^{111}In-DTPA-D-Phe]-octreotide (8-16 mSv/111-222 MBq). Given the 1% probability for severe hereditary disorders in the offspring per Gy received by the ovaries, the associated risk related to injection of 555-740 MBq ^{99m}Tc-depreotide is less than 1/10,000. This is low when compared to the 1.6% prevalence of naturally occurring genetic disorders (ICRP 60). After administration of 555-740 MBq ^{99m}Tc-depreotide, the dose to the uterus amounts to 3-4 mGy. In the event of accidental administration to a pregnant woman, the risk for teratogenic effects (40%/Sv) in the sensitive period (3-15 weeks postconception) is approximately 1/800 - 1/600.

6. Conclusion

In conclusion, the biodistribution of ^{99m}Tc-depreotide demonstrated low lung and myocardial uptake, allowing for early imaging of the supradiaphragmatic region and this with a dosimetry favorable for clinical whole body and SPECT imaging.

7. References

1. Kwekkeboom DJ, Krenning EP. Somatostatin Receptor Imaging. Semin Nucl Med 32(2): 84 (2002).
2. Schulz S, Helmholz T, Schmitt J, et al. True Positive Somatostatin Receptor Scintigraphy in Primary Breast Cancer Correlates With Expression of Sst2A and Sst5. Breast Cancer Res Treat 72(3): 221 (2002).
3. Lister-James J, Moyer BR, Dean T. Small Peptides Radiolabeled With 99mTc. Q J Nucl Med 40(3): 221 (1996).
4. Vallabhajosula S, Moyer BR, Lister-James J, et al. Preclinical Evaluation of Technetium-99m-Labeled Somatostatin Receptor-Binding Peptides. J Nucl Med 37(6): 1016 (1996).
5. Lister-James J, Pearson D, De Rosch MA, et al. Tc-99m P829: Characterization of a Technetium-99-Labeled Somatostatin Receptor-Binding Peptide. Technetium, Rhenium and Other Metals in Chemistry and Nuclear Medicine: 473 (1999).
6. Virgolini I, Leimer M, Handmaker H, et al. Somatostatin Receptor Subtype Specificity and in Vivo Binding of a Novel Tumor Tracer, 99mTc-P829. Cancer Res 58(9): 1850 (1998).
7. Blum JE, Handmaker H, Rinne NA. The Utility of a Somatostatin-Type Receptor Binding Peptide Radiopharmaceutical (P829) in the Evaluation of Solitary Pulmonary Nodules. Chest 115(1): 224 (1999).
8. Blum J, Handmaker H, Lister-James J, Rinne N. A Multicenter Trial With a Somatostatin Analog (99m)Tc Depreotide in the Evaluation of Solitary Pulmonary Nodules. Chest 117(5): 1232 (2000).
9. Gould MK, Maclean CC, Kuschner WG, et al. Accuracy of Positron Emission Tomography for Diagnosis of Pulmonary Nodules and Mass Lesions: a Meta-Analysis. JAMA 285(7): 914 (2001).

10. Montilla-Soler JL, Bridwell RS. Tc-99m Depreotide Scintigraphy of Breast Carcinoma. Clin Nucl Med 27(3): 202 (2002).
11. Montilla-Soler JL, Rexroad JT, Bridwell RS. Tc-99m Depreotide Scintigraphy of Low-Grade Non-Hodgkin's Lymphoma. Clin Nucl Med 28(6): 503 (2003).
12. Hellwig D, Samnick S, Reif J, et al. Comparison of Tc-99m Depreotide and in-111 Octreotide in Recurrent Meningioma. Clin Nucl Med 27(11): 781 (2002).
13. Van Den Bossche B, D'haeninck E, De Vos F, et al. Oestrogen-mediated regulation of somatostatin receptor expression in human breast cancer cell lines assessed with ^{99mTc}-depreotide. Eur J Nucl Med 31(7): 1022 (2004).
14. Cloutier RJ, Smith SA, Watson EE, et al. Dose to the Fetus From Radionuclides in the Bladder. Health Phys 25(2): 147 (1973).
15. ICRP Publication 23: Reference Man: Anatomical, Physiological and Metabolic Characteristics. Oxford, Pergamon Press, 1975.
16. Loevinger R, Budinger T, Watson E. MIRD primer for absorbed dose calculations. New York: Society of Nuclear Medicine; 1988.
17. Cristy M, Eckerman K. Specific absorbed fractions of energy at various ages from international sources. ORNL/TM 8381/VII. Oak Ridge, TN: Oak Ridge National Laboratory; 1987.
18. Stabin MG. MIRDOSE: Personal Computer Software for Internal Dose Assessment in Nuclear Medicine. J Nucl Med 37(3): 538 (1996).
19. ICRP publication 60. Recommendations of the International Commision on Radiological Protection. Oxford, Pergamon Press, 1991.
20. NeoSpect package insert. Amersham plc,Amersham Place, Little Chafont, Buckinghameshire, England HP7 9NA; 2000.
21. Reubi J-C, Waser B, Schaer J-C, Laissue JA. Somatostatin Receptor Sst1-Sst5 Expression in Normal and Neoplastic Human Tissues Using Receptor Autoradiography With Subtype-Selective Ligands. Eur J Nucl Med 28(7): 836 (2001).
22. Shih WJ, Hirschowitz E, Bensadoun E, et al. Biodistribution on Tc-99m Labeled Somatostatin Receptor-Binding Peptide (Depreotide, NeoTec) Planar and SPECT Studies. Ann Nucl Med 16(3): 213 (2002).

23. Bhathena SJ, Louie J, Schechter GP, et al. Identification of Human Mononuclear Leukocytes Bearing Receptors for Somatostatin and Glucagon. Diabetes 30(2): 127 (1981).
24. Scicchitano R, Dazin P, Bienenstock J, et al. Distribution of Somatostatin Receptors on Murine Spleen and Peyer's Patch T and B Lymphocytes. Brain Behav Immun 1(2): 173 (1987).
25. Krenning EP, Kwekkeboom DJ, Bakker WH, et al. Somatostatin Receptor Scintigraphy With [111In-DTPA-D-Phe1]- and [123I-Tyr3]-Octreotide: the Rotterdam Experience With More Than 1000 Patients. Eur J Nucl Med 20(8): 716 (1993).
26. UNSCEAR 2000 report. Vol I. Sources and effects of ionizing radiation. 2000.

CHAPTER FIVE

^{99m}Tc-depreotide-scan compared with ^{99m}Tc-MDP-bone scintigraphy for the detection of bone metastases and prediction of hormonal treatment response in patients with breast cancer

B. Van Den Bossche[1], E. D'haeninck[1], F. De Winter[2], S. Van Belle[3], R.A. Dierckx[1], C. Van de Wiele[1]

[1]Division of Nuclear Medicine, Ghent University Hospital, Ghent, Belgium

[2]Division of Nuclear Medicine, OLV-Hospital, Aalst, Belgium

[3]Department of Clinical Oncology, Ghent University Hospital, Ghent, Belgium

Nucl Med Commun 2004; 25(8):787-792.

---

1. Abstract

The purpose of this study was to determine the potential role of ^{99m}Tc-depreotide scintigraphy for the evaluation of bone metastases compared with ^{99m}Tc-methylendiphosphonate (MDP) bone scintigraphy and for prediction of treatment response in breast cancer patients in whom first- or second-line hormonal therapy was to be initiated. Twelve patients with a diagnosis of advanced breast cancer were included. All patients underwent both a bone scan and a depreotide scan and at least one other conventional imaging procedure, including plain film radiography (*n*=11), CT (*n*=6) or MRI (*n*=5), for confirmation of metastatic disease. The mean time interval between the bone scan and the depreotide scan was 30.6 days. Follow-up data were retrieved from routine clinical evaluation by means of physical examination, imaging and blood analysis. On patient basis we found a sensitivity, specificity and accuracy of, respectively 100%, 50% and 83.3% for bone scan and 62.5%, 100% and 75% for depreotide scan in the diagnosis of bone metastasis. In eight patients with available follow-up data two patients with a positive depreotide scan remained stable and five of six patients with a negative depreotide scan had progressive disease. In this small series of breast cancer patients ^{99m}Tc-depreotide scintigraphy proves less sensitive but more specific as compared to ^{99m}Tc-MDP bone scintigraphy in measuring the extent of bone metastasis. On the other hand ^{99m}Tc-depreotide scintigraphy elucidates, noninvasively, tumour characteristics and may be indicative for prognosis and response to hormonal treatment

2. Introduction

Bone is the most common site of metastatic breast cancer and bone metastases are detected at autopsy in as many as 70% of patients with advanced disease [1]. Since its introduction in

1971, bone scintigraphy has become the most frequently used nuclear medicine procedure worldwide, owing to its high sensitivity for bone pathologies of various origins [2;3]. However, the bone scan suffers from lack of specificity. After injection of ^{99m}Tc-methylendiphosphonate (MDP), this tracer accumulates at hyperaemic sections and free reduced technetium competes with calcium for the binding sites at inorganic bone surfaces, preferably at sites of mineralization where small nuclei of calcium phosphate are being formed. Subsequently it visualizes osteoblastic bone reaction, in this case, to cancer cells. However, tracer accumulation may occur in any skeletal location with an elevated rate of bone turnover and thus may also accompany trauma, infection or arthropathy. Moreover, many breast cancer patients are likely to be simultaneously affected by degenerative or inflammatory bone diseases because of their higher age. The probability that an abnormal bone scan represents metastatic disease is directly related to the location and the number of abnormal foci. As such, the thoracic spine is a highly probable site and the non-axial skeleton is rather infrequently affected, and, for example, a situation showing a few abnormalities in the thoracic and lumbar spine carries a 56% positive incidence of metastases, while a solitary rib lesion only carries a 6% chance of being a bone metastasis [4].

Somatostatin receptor (SSTR) expression of 50-80% in primary breast carcinoma has been reported, as assessed by autoradiography [5-7]. The majority of primary breast carcinomas express SSTR2A and to a lesser extent SSTR1, 3 and SSTR5 [7-9]. Clinical data assign low differentiation grade, slow tumour growth and hence favourable prognosis to patients with SSTR-positive breast tumours [6;10]. *In vivo* visualization of primary and metastatic lesions in patients with breast cancer by means of SSTR scintigraphy has been previously described [11-13]. Depreotide, a somatostatin (SS) analogue, is a cyclic decapeptide with high affinity for SSTR subtypes 2, 3 and 5 [14].

The purpose of this study was to determine the potential role of ^{99m}Tc-depreotide scintigraphy for evaluating bone metastases compared with ^{99m}Tc-MDP bone scintigraphy and for predicting treatment response in breast cancer patients in whom first- or second-line hormonal therapy was to be initiated.

3. Patients, Materials and Methods

Patients

Between January 2002 and October 2003 12 patients with a diagnosis of advanced breast cancer in whom first- or second-line hormonal therapy was to be initiated, were included (Table 1). All patients had histologically proven oestrogen receptor-positive (ER+) tumours.

All patients were female and had a mean age of 63 years (range, 35-77 years). In all patients the diagnosis of advanced breast cancer was based on clinic and divers diagnostic procedures (bone scan, X-ray, computed tomography (CT), magnetic resonance imaging (MRI)). All patients underwent both bone scan and depreotide scan and at least one other conventional imaging procedure, including plain film radiography (*n*=11), CT (*n*=6) or MRI (*n*=5), for confirmation of metastatic disease. Median and mean time interval between bone scan and depreotide scan were, respectively, 17.5 days and 30.6 days (range, 2-189 days). The patient with the interval of 189 days had a negative bone scan 6 months before and 9 months after the depreotide scan and was as such considered eligible for inclusion.

Follow-up data were retrieved from routine clinical evaluation by means of physical examination, imaging and blood analysis. Progressive disease was defined as an increase in number of bone lesions and/or an increase in number and/or size (>20%) of liver lesions. Disease state was considered stable in the absence of both progressive disease and rise of tumour marker. Approval for the study was obtained from the local ethics committee and all patients give written informed consent before scintigraphy.

patient	age (years)	metastatic site	bone scan	depreotide scan		follow-up
				bone lesions	other	
1	60	bone, liver, pleura	+	+	pleura	-
2	57	bone, liver	+	+	-	-
3	35	bone	+	+	-	-
4	59	bone	+	+	-	-
5	63	bone	+	+	-	stable
6	55	bone, liver	+	-	-	stable
7	75	bone	+	-	-	progressive
8	76	bone, pleura	+	-	-	progressive
9	75	liver	+	-	-	progressive after 6m
10	71	bone, liver, pleura	+	-	-	progressive
11	54	liver	-	-	-	progressive after 1y
12	77	T4	-	-	primary lesion	stable

Table 1. Patient information.

Material

Amerscan (medronate) was purchased from Amersham Health (Little Chalfont, Buckinghamsire, UK). Amerscan vials were reconstituted with 11,100 MBq (300mCi) ^{99m}Tc-pertechnetate in 8 mL. Each vial contained 6.25 mg sodium medronate, 0.34 mg stannous fluoride and 2 mg sodium *p*-aminobenzoate.

NeoSpect was kindly provided by Amersham Health (Little Chalfont, Buckinghamsire, UK). NeoSpect vials were reconstituted with 1480-1850 MBq (40-50 mCi) ^{99m}Tc-pertechnetate. Each vial contained 50 µg depreotide, 5 mg sodium glucoheptonate dihydrate, 50 µg stannous chloride dihydrate, pH 7.4. Radiochemical purity of ^{99m}Tc-depreotide was > 90%.

Imaging

Planar whole body imaging was performed 3-6h after intravenous injection of 925 MBq (25 mCi) ^{99m}Tc-medronate and 4h after intravenous injection of 555-740 MBq (15-20 mCi) ^{99m}Tc-depreotide. Images were acquired using a double-headed or a triple-headed gamma camera (respectively, Axis and Irix, Marconi, Cleveland, Ohio, USA) equipped with low-energy high-resolution parallel-hole collimators. The energy peak was centred at 140 keV with a 15% window. Acquisition was performed simultaneously in the anterior and posterior projections with a scan speed of 15 cm·min^{-1}. Matrix size was 128 x 512 pixels.

4. Results

The results of the potential of the two modalities in diagnosing bone metastasis are shown in Table 2. Most of the patients (10/12) had positive bone scans and hence bone metastasis was suspected. The bone scan was true-positive in eight cases and false-positive in two cases. In the latter, both patients were classified as having degenerative lesions based on conventional imaging and clinical follow-up of more than 1 year.

	Bone scan	Depreotide scan
Positive scans	8TP/2FP	5TP/0FP
Pegative scans	2TN/0FN	4TN/3FN
Sensitivity	100% (8/8)	62.5% (5/8)
Specificity	50% (2/4)	100% (4/4)
Accuracy	83.3% (10/12)	75% (9/12)

TP, true-positive; FP, false-positive; TN, true-negative; FN, false-negative.

Table 2. Bone scan and depreotide scan results in the diagnosis of bone metastasis.

Five patients had a true-positive depreotide scan, whereas in three patients with proved metastasis no uptake of depreotide in bony lesions was present. One of these patients had a single lesion on bone scan at the lower thoracic spine that was classified as degenerative by plain film radiography, but proved to be of metastatic origin during follow-up. Possibly, this lesion was masked by liver activity (see below) and was therefore missed on the depreotide scan.

In two patients both the bone scan and depreotide scan were true-negative and bone metastasis was excluded by radiography and follow-up.

Overall in this small series, on patient basis we found a sensitivity, specificity and accuracy of respectively 100%, 50% and 83.3% for bone scan and 62.5%, 100% and 75% for depreotide scan in the diagnosis of bone metastasis.

Lesion	Bone scan	NeoSpect scan	
	TP/FP	TP/FP	TN/FN
Vertebrae	15 /3	7/0	3/8
Rib	11/0	4/0	0/7
Pelvic	14/1	12/0	1/2
Skull	2/0	1/0	0/1
Glenohumeral	1/0	1/0	-
Femur	2/0	1/0	0/1
Acromioclav.	0/1	-	1/0
Total	45/5	26/0	5/19

TP, true-positive; FP, false-positive; TN, true-negative; FN, false-negative.

Table 3. Bone scan positive metastatic lesions in patients (5/12) having a positive depreotide scan and their respective appearance.

Table 3 summarizes in detail all individual bone scan-positive metastatic lesions in patients (5/12) having a positive depreotide scan and compares their respective appearance. Five of 50 lesions judged positive for metastasis on bone scan were defined as degenerative according to CT and/or MRI and were situated in cervical vertebra (*n*=3), near the coxo-femoral (*n*=1) or acromio-clavicular (*n*=1) junction. Only 26 of 45 (57.8%) bone scan true-positive lesions were concordantly detected on depreotide scan. Overall, lesions were consistently less pronounced in the latter due to lower tracer uptake in the lesions and higher background

activity in bone marrow (Fig 1). Physiological uptake of depreotide in liver, spleen, intestines, kidneys and thyroid hampered visualization of lesions in the respective areas on planar images (Fig 2). As such high liver activity masked 11 of the 19 missed lesions, these were situated in the lower thoracic vertebra (5/11) or lower ribs (6/11). Likewise detection of three cervical spine lesions was hampered by thyroid uptake. Other 5/19 were situated in the upper ribs, skull and coxo-femoral region. In addition, increased tracer uptake is noted in the inflamed right knee, possibly due to specific binding to activated T-lymphocytes and aspecific accumulation in synovial fluid [15].

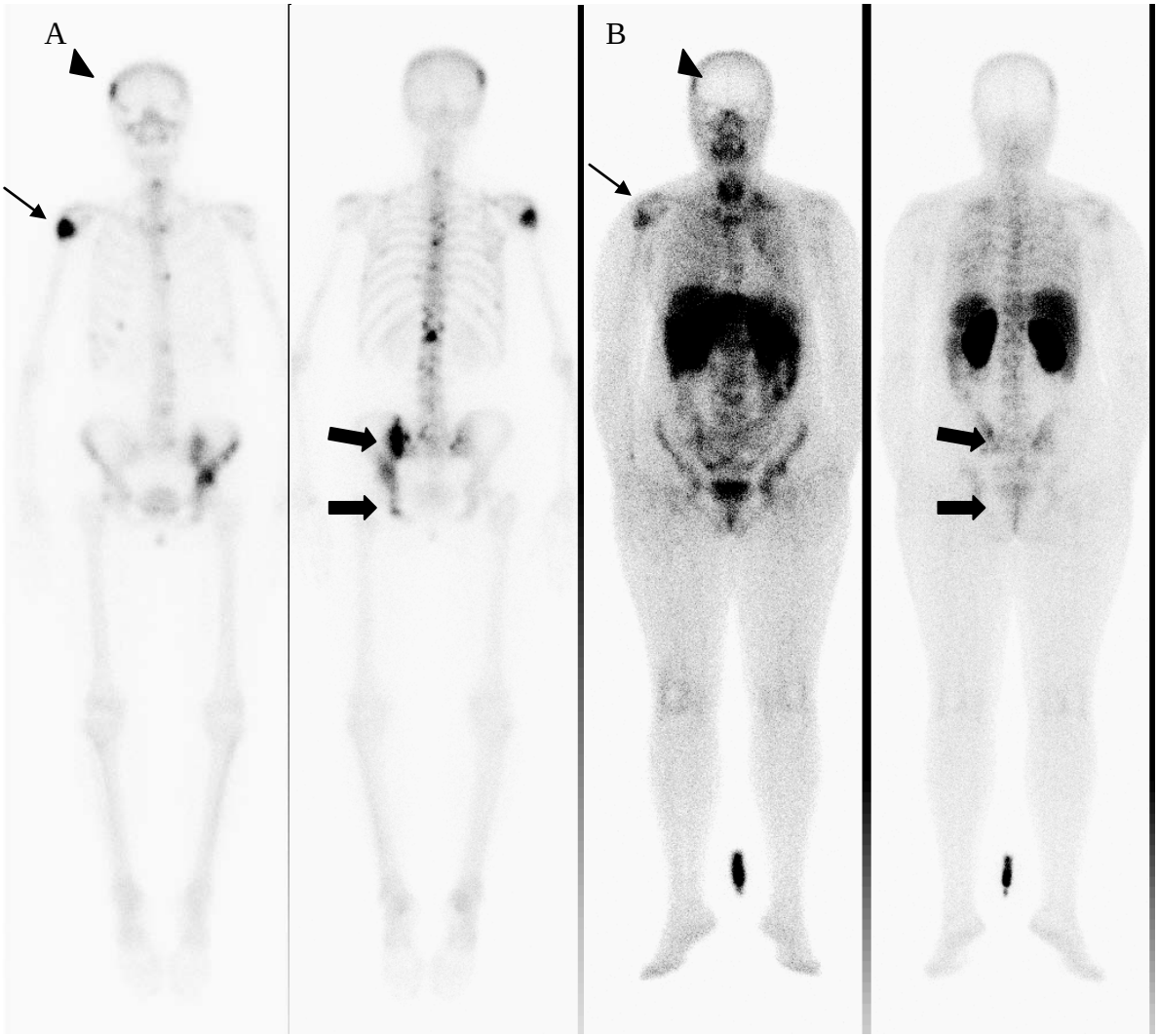

Figure 1. A 57-year-old female with both positive bone and depreotide scans. A. Respectively, anterior and posterior views of ^{99m}Tc-MDP bone scan, showing multiple lesions, amongst others of skull (arrow head), shoulder (thin arrow) and pelvic (thick arrow) region. B. Respectively, anterior and posterior views of ^{99m}Tc-depreotide (NeoSpect) scan, showing lower uptake in the respective pathological lesions, amongst others in skull (arrow head), shoulder (thin arrow) and pelvic (thick arrow) region.

Figure 2. Planar whole body image, respectively anterior (A) and posterior (B) projections, of normal biodistribution of ^{99m}Tc-depreotide (NeoSpect), with physiological uptake in thyroid, liver, spleen, kidneys, bone marrow. The subject is a 62-year-old healthy female with pain in the right knee. Increased tracer uptake is noted in the inflammated right knee due to specific binding to activated T-lymphocytes and aspecific accumulation in synovial fluid.

Clinical follow-up of more than 1 year (range, 14-22 months) was obtained in eight patients who were progressive and therefore started first- or second-line hormonal treatment at the time of depreotide scanning, and in one patient who started with primary palliative hormonal treatment. Three patients responded to hormonal treatment and remained stable for, respectively, 22, 20 and 15 months up to today whereas five had progressive disease: three immediately, one after 6 months and one after 1 year. Of the three responders two had positive depreotide scans while no uptake was noted in the five nonresponders. However two

of the latter had only liver metastasis and hence could not be evaluated on depreotide scan due to high physiological liver uptake.

5. Discussion

In the present study we compared the diagnostic accuracy of ^{99m}Tc-depreotide scintigraphy with ^{99m}Tc-MDP bone scintigraphy for evaluating bone metastasis in a small series of breast cancer patients. Regarding diagnostic accuracy on a patient basis, bone scan proved superior (75% vs 83.3%) due to its higher sensitivity (100% vs 62.5%), whereas specificity was significantly higher on NeoSpect scan (100% vs 50%). In fact depreotide is a SS analogue that binds specifically to SSTR2, 3 and 5 which are overexpressed in 50-80% of breast tumours. In contrast, ^{99m}Tc-MDP accumulates aspecifically in any skeletal location with an elevated rate of bone turnover such as arthropathy, leading in our study to two false-positive diagnoses of bony metastasis.

In previous studies SSTR scintigraphy using ^{111}In-DTPA-octreotide visualized 61-75% of primary breast tumours [11;12]. The sensitivity (62.5%) of ^{99m}Tc-depreotide scintigraphy was in accord with the latter findings and in line with expectations based on SSTR expression patterns assessed by autoradiography.

Fourteen of 19 (73.7%) missed individual lesions in patients with positive depreotide scan were probably due to masking by organs with high physiological tracer uptake (thyroid, liver, spleen, intestines). SPECT imaging, a tomographical technique that provides cross-sectional images of tracer distribution and thus has the ability to remove overlying structures which may obscure abnormal tracer uptake, can overcome similar problems. An additional explanation for the lack of sensitivity of ^{99m}Tc-depreotide in detecting individual lesions lies in the heterogenous distribution of SSTR expression in breast tumours. The latter often display SSTR only in certain tumour regions, although the whole tumour appears to be histopathologically homogenous [16]. This observation supports the idea that some breast tumours are composed of numerous different clones with different biological properties. As a consequence metastatic lesions originating from an SSTR-negative clone may be SSTR-negative even though the primary tumour is SSTR-positive.

In our series, follow-up data are available in eight patients who had progressive disease and therefore started first- or second-line hormonal treatment at the time of depreotide scanning and in one patient who started with primary palliative hormonal treatment. Three patients responded to hormonal treatment and remained stable whereas five had progressive disease: three immediately, one after 6 months and one after 1 year. Both patients with uptake of

depreotide in, respectively, bony lesions and primary tumour had continuously stable disease for, respectively, 20 and 15 months up to today. In six patients without uptake of depreotide five eventually had progressive disease. However, two of the latter had only liver metastasis and hence could not be evaluated on depreotide scan due to high physiological liver uptake. Experimental data suggest that in breast carcinoma the SSTR is an oestrogen response element that is upregulated in the presence of oestradiol [17]. As such, SSTR expression or inversely depreotide positivity may indicate functionality of the oestradiol receptor, a prerequisite for response to hormonal treatment. Accordingly, depreotide scintigraphy may have the potential to select patients that are likely to benefit from hormonal treatment.

In conclusion, in this small series of breast cancer patients ^{99m}Tc-depreotide scintigraphy proves less sensitive but more specific when compared to ^{99m}Tc-MDP bone scintigraphy in measuring extent of bone metastasis. On the other hand ^{99m}Tc-depreotide scintigraphy elucidates, noninvasively, tumour characteristics and may be indicative for response to hormonal treatment.

6. References

1. Coleman RE, Rubens RD. The clinical course of bone metastases from breast cancer. Br J Cancer 1987; **55**: 61-66.
2. Subramanian G, McAffee J. A new complex of 99mTc for skeletal imaging. Radiology 1971; **99**: 192-197.
3. Bares R. Skeletal scintigraphy in breast cancer management. Q J Nucl Med 1998; **42**: 43-48.
4. Ainsly J, Hicks R, Drummond R, Blakey D, Bishop M, McKenzie A. Simulated bone metastases: a case study of two patients with breast cancer. Australiasan Radiology 1999; **43**: 365-368.
5. Reubi JC, Krenning E, Lamberts SW, Kvols L. In vitro detection of somatostatin receptors in human tumors. Metabolism 1992; **41**: 104-110.
6. Bootsma AH, van Eijck C, Schouten KK, Reubi JC, Waser B, Foekens JA, et al. Somatostatin receptor-positive primary breast tumors: genetic, patient and tumor characteristics. Int J Cancer 1993; **54**: 357-362.
7. Schaer JC, Waser B, Mengod G, Reubi JC. Somatostatin receptor subtypes sst1, sst2, sst3 and sst5 expression in human pituitary, gastroentero-pancreatic and mammary tumors: comparison of mRNA analysis with receptor autoradiography. Int J Cancer 1997; **70**: 530-537.

8. Reubi JC, Waser B, Schaer JC, Laissue JA. Somatostatin receptor sst1-sst5 expression in normal and neoplastic human tissues using receptor autoradiography with subtype-selective ligands. Eur J Nucl Med 2001; **28**: 836-846.
9. Vikic-Topic S, Raisch KP, Kvols LK, Vuk-Pavlovic,S. Expression of somatostatin receptor subtypes in breast carcinoma, carcinoid tumor, and renal cell carcinoma. J Clin Endocrinol Metab 1995; **80**: 2974-2979.
10. Foekens JA, Portengen H, van Putten WL, Trapman AM, Reubi JC, Alexieva-Figusch J, et al. Prognostic value of receptors for insulin-like growth factor 1, somatostatin, and epidermal growth factor in human breast cancer. Cancer Res 1989; **49**: 7002-7009.
11. van Eijck CH, Krenning EP, Bootsma A, Oei HY, van Pel R, Lindemans J, et al. Somatostatin-receptor scintigraphy in primary breast cancer. Lancet 1994; **343**: 640-643.
12. Schulz S, Helmholz T, Schmitt J, Franke K, Otto HJ, Weise W. True positive somatostatin receptor scintigraphy in primary breast cancer correlates with expression of sst2A and sst5. Breast Cancer Res Treat 2002; **72**: 221-226.
13. Montilla-Soler JL, Bridwell RS. Tc-99m depreotide scintigraphy of breast carcinoma. Clin Nucl Med 2002; **27**: 202-204.
14. Virgolini I, Leimer M, Handmaker H, Lastoria S, Bischof C, Muto P, et al. Somatostatin receptor subtype specificity and in vivo binding of a novel tumor tracer, 99mTc-P829. Cancer Res 1998; **58**: 1850-1859.
15. Lamberts SW, Krenning EP, Reubi JC. The role of somatostatin and its analogs in the diagnosis and treatment of tumors. Endocr Rev 1991; **12**: 450-482.
16. Reubi JC, Waser B, Foekens JA, Klijn JG, Lamberts SW, Laissue J. Somatostatin receptor incidence and distribution in breast cancer using receptor autoradiography: relationship to EGF receptors. Int J Cancer 1990; **46**: 416-420.
17. Xu Y, Song J, Berelowitz M, Bruno JF. Estrogen regulates somatostatin receptor subtype 2 messenger ribonucleic acid expression in human breast cancer cells. Endocrinology 1996; **137**: 5634-5640.

CHAPTER SIX

Early prediction of endocrine therapy effect in advanced breast cancer patients using 99mTc-depreotide scintigraphy

Bieke Van Den Bossche[1], Simon Van Belle[2], Frederic De Winter[3]†, Alberto Signore[4], Christophe Van de Wiele[1]

[1]Department of Nuclear Medicine, University Hospital Ghent, Ghent, Belgium

[2]Department of Medical Oncology, University Hospital Ghent, Ghent, Belgium

[3]Division of Nuclear Medicine, OLV-Hospital, Aalst, Belgium

[4]Nuclear Medicine Unit, Department of Clinical Sciences, University "La Sapienza", Rome Italy

Submitted J Clin Oncol 12/03/05

---

1. Abstract

In analogy with the oestrogen-dependent regulation of somatostatin receptor (SSTR) expression in endocrine-responsive human breast cancer cell lines, efficient antioestrogen treatment may result in a downregulation of SSTR at the cell surface in breast tumours. In vivo imaging of this molecular event by means of sequential ^{99m}Tc-depreotide scintigraphy could enable selection of breast cancer patients susceptible for endocrine therapy. Twenty patients with a diagnosis of advanced breast cancer in whom first- or second-line hormonal therapy was to be initiated, were included. Patients underwent sequential ^{99m}Tc-depreotide scintigraphy, respectively before and 3 weeks after initiating hormonal treatment. Lesion-to-background ratio's (L/BGs) were calculated on planar and single photon emission computed tomography (SPECT) images and a change of > 25% between pre- and posttherapy scan was considered significant. At 6 months after initiation of treatment eight patients had stable disease and were considered as responding to hormonal treatment, whereas 10 patients had progressive disease and were considered nonresponders. All responders had positive scans and seven of 10 nonresponders had negative scans. Thus all patients with a negative scan did not respond to therapy. Sequential scans were always both positive or both negative. The relative change in ^{99m}Tc-depreotide uptake between sequential scans significantly differed in responders compared to nonresponders (P=.017), uptake decreased in the first group and increased in the latter. Sequential ^{99m}Tc-depreotide scintigraphy could allow for separation of responders and nonresponders immediately or as early as 3 weeks after treatment initiation.

2. Introduction

Hormone-dependent breast tumours are characterized primarily by a functional and intact oestrogen receptor (ER) system. Antioestrogen agents selectively target the ER pathway to abolish its effect on cell growth. Since only about one third of breast cancer patients initially respond to endocrine therapy, there is a need for patient selection. So far, the only predictive factor approved for clinical routine use is the in vitro assessment of hormone receptor status on tissue samples by ligand binding assay (LBA) or immunohistochemistry (IHC). Still, only 50%-60% of patients with ER-positive tumours show response to hormonal therapy, whereas lack of detectable ERs is usually associated with 5%-10% response [1,2,3].

Possible causes of discordance between hormone receptor status and endocrine responsiveness include limits inherent to the available techniques (IHC, LBA) for hormone receptor assessment, such as sampling error and variations in specificity (animal dependent) seen with the preparation of antibodies. Scintigraphy could circumvent these inaccuracies and moreover offers the advantage of noninvasive and repetitive whole body evaluation.

Assessment of hormone receptor status is usually based on tissue samples from the primary tumour, whilst this information is being utilized years or decades later in the metastatic situation, when the biology of the tumour might have changed [4,5,6]. Since breast cancer DNA is reported to undergo structural modification with progression, the predictive value of the hormone receptor status might be limited by its time dependency and decreases about 20% per year, losing significance after approximately 8 years [7,8]. In addition, breast tumours contain multiple cell populations exhibiting a wide range of genetic, biochemical, immunological and biological characteristics [9,10]. Although the whole tumour appears to be histopathologically homogenous, ERs are often displayed only in certain tumour regions [11,12]. Metastatic lesions originating from an ER-negative clone may be ER-negative nevertheless the primary tumour is ER-positive. Scintigraphy has the ability to address the intrinsic heterogeneity of tumoural receptor expression without tissue manipulation and provides an in vivo image of all disease sites at the moment of treatment need. A lot of efforts have been put into synthesis and evaluation of radiopharmaceuticals of which tumoural uptake is believed to relate to ER expression and hence endocrine responsiveness, nevertheless, no clinically useful tracers are available [13,14].

Another explanation for lack of response to endocrine treatment in ER-positive disease is nonfunctioning of the ER. These receptors are recognized and measured by IHC, but in such tumours steroid hormone occupancy of the receptor is not the drive for cellular proliferation and hence antioestrogen therapy is inefficient. Assessment of an end-product of ER

stimulation, such as the progesteron receptor (PgR), could by-pass this problem and has proven to increase predictive accuracy [15,16,17]. Likewise, experimental data suggest that the expression of the somatostatin receptor (SSTR) is mediated by oestrogens [18,19]. In human endocrine-responsive breast cancer cells oestradiol (E_2) stimulation of functional ER results in upregulation of SSTR subtype 2 (SSTR2) at the cell surface (Fig 1). Vice versa, blocking the ER by means of an antioestrogen leads to a decrease of SSTR expression. About 50%-75% of breast tumours are SSTR-positive and express predominantly SSTR2 [20,21,22,23]. SSTR expression is associated with ER-positivity and hormone responsiveness and hence with a better clinical prognosis [24,12]. Hypothetically, in analogy with the in vitro findings, efficient antioestrogen treatment of metastasised breast cancer patients may result in downregulation of SSTR at the cell surface level, which could be visualised in vivo using sequential SSTR scintigraphy (Fig. 1).

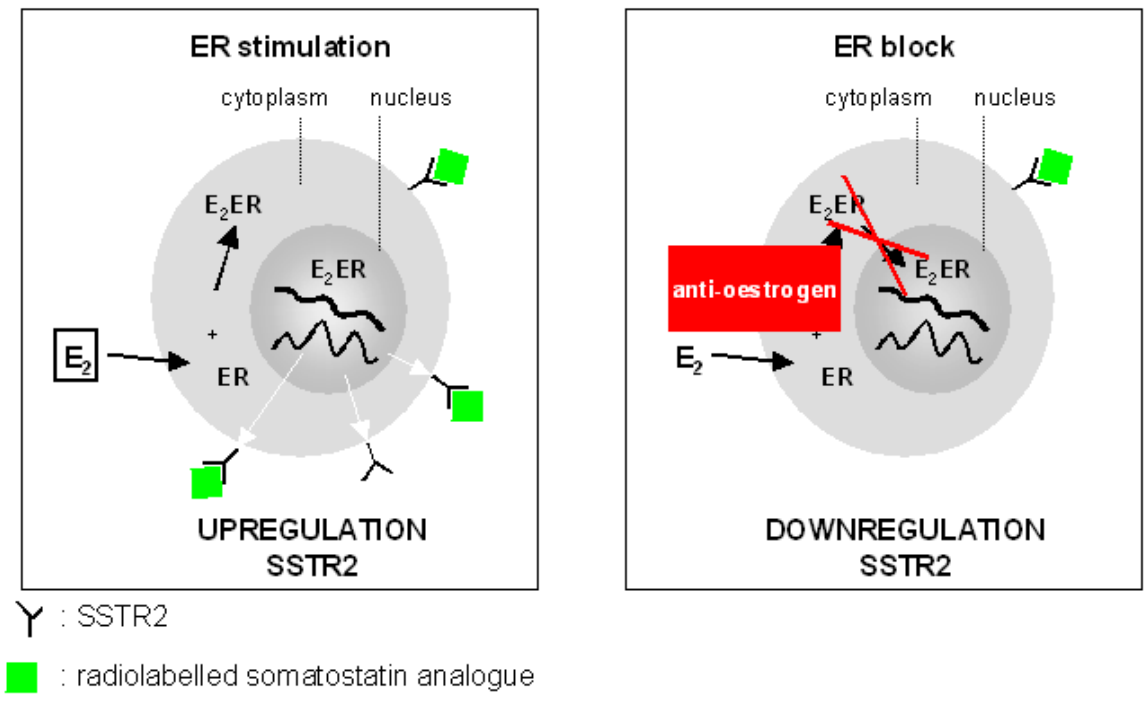

ER: oestrogen receptor, E_2: oestradiol, SSTR2: somatostatin receptor subtype 2

Figure 1. Mechanism of oestradiol-mediated regulation of somatostatin receptor subtype 2 (SSTR2) expression and its in vivo imaging by means of a radiolabelled somatostatin analogue.

Depreotide (P829 - NeoSpect®/NeoTect®) is a ^{99m}Tc-labelled somatostatin analogue. It is a cyclic decapeptide with high affinity for SSTR2, 3 and 5 [25,26,27].

This study was undertaken to evaluate the potential of sequential ^{99m}Tc-depreotide scintigraphy to select patients likely to respond to endocrine therapy.

3. Patients and Methods

Patients

This study was approved by the Medical Ethics Committee of the Ghent University Hospital and performed according to Good Clinical Practice. All subjects gave their written informed consent prior to participation in the study. Twenty patients suffering from advanced breast cancer in whom first- or second-line hormonal therapy was to be initiated, were included. One patient received chemotherapy immediately after starting hormonal treatment and in one patient endocrine therapy was eventually not initiated, both were excluded. As such 18 patients were eligible for the study and patient characteristics are summarized in table 1. All patients were female and had a mean age of 63 years (range 46-76 years). One patient had a first diagnosis of advanced breast cancer and 17 patients suffered progression of previously treated breast cancer, all detected by plural diagnostic procedures (e.g., bone scan, CT, MRI, ultrasound, X-ray). Time to initial diagnosis in the latter patients was 72 ± 68 months. Patients underwent sequential ^{99m}Tc-depreotide scintigraphy, respectively before (pretherapy) and 3 weeks after (posttherapy) initiating hormonal treatment. This timing was chosen since steady-state intratumoural concentrations of tamoxifen are usually achieved following 2 to 3 weeks of daily tamoxifen administration [28]. Plasma concentrations of the aromatase inhibitors anastrozole and letrozole approach steady-state levels at about 7 days respectively 2 to 6 weeks of once daily dosing [29,30]. Two patients had only a pretherapy scan. Follow-up data were retrieved from routine clinical evaluation by means of physical examination, imaging (e.g., bone scan, CT, MRI, ultrasound, X-ray) and blood analysis. Response evaluation was assessed according to RECIST guidelines [31]. Progressive disease was defined as an increase in number of nonmeasurable lesions (e.g., bone lesions) and/or an increase in number and/or size (>20%) of measurable lesions (e.g., liver lesions). Disease status was considered stable in the absence of both progressive disease and a serum rise in tumour marker [32]. Since durable stable disease appears to be a clinically useful criterium of therapeutic remission, patients with stable disease for 6 months or more were considered as responding to hormonal treatment [33,34]. Patients suffering disease progression within 6 months were considered nonresponders.

Radiopharmaceutical Synthesis

NeoSpect® kits were kindly provided by Amersham Health (now part of GE Healthcare, Little Chalfont, Buckinghamsire, UK) and prepared according to the manufacturers' guidelines.

Imaging Studies

Planar whole body and single photon emission computed tomography (SPECT) imaging was performed 4 hours after intravenous injection of 555-740 MBq (15-20 mCi) ^{99m}Tc-depreotide. Total injected activity was calculated based on the syringe activity pre- and postinjection measured in a NaI-gamma counter. Images were acquired using a double-headed or a triple-headed gamma camera (respectively Axis and Irix, Marconi/Picker, Cleveland, Ohio, USA), equipped with low-energy high-resolution parallel–hole collimators. The energy peak was centered at 140keV with a 15% window.

For whole body imaging, subjects were positioned supine with their arms alongside their body and a point source of 3.7 MBq in a syringe of 5 cc placed in a phantom between their feet. Acquisition was performed simultaneously in anterior and posterior position with a scan speed of 15 cm/min. Matrix size was 256x1024 pixels.

For SPECT imaging, patients were positioned supine and at times of imaging of the thoracic region, with the arms raised alongside the head. Images were acquired over 15 minutes by 40 views of 20 seconds per detector with the triple-headed gamma camera and over 23 minutes by 60 views of 20 seconds per detector with the dual-headed gamma camera (120 steps; 3° per step; matrix size: 128x128). Transversal, coronal and sagittal slices were reconstructed iteratively using OSEM (Ordered Subset Expectation Maximization) algorithm with 2 iterations and 6 subsets and postfiltered using a Butterworth filter (cut-off frequency: 1.2 cycles/cm, order 5).

Data analysis

For semiquantification of radioactivity uptake after injection of ^{99m}Tc-depreotide, regions of interest (ROIs) were drawn over lesions and background on planar scans and SPECT images if available. As background, a region over the lower part of the upper leg was chosen on planar scans and a region adjacent to the lesion on SPECT images. The shapes and sizes (i.e. number of pixels) were kept constant for the pre- and posttherapy scan. For each ROI the geometric mean, corrected for physical decay, of total anterior and posterior counts was calculated. Lesion-to-background ratio (L/BG) was calculated for each lesion on planar images and, for SPECT images, activity ratio was calculated in several consecutive slices for each lesion and averaged. In addition, uptake in tumour lesions was expressed as percentage of the injected dose (% ID), calculated on planar images. Since changes in % ID and L/BG were equivalent in the same lesion on sequential scans and assessment of L/BG is simpler and less subject to errors compared to % ID, we further expressed tracer uptake solely as L/BG.

		‡Receptor Expression			Endocrine Treatment			^{99m}*Tc-depreotide uptake*			
No	Age (y)	† date	ER	PgR	Type	Indication	Disease Site(s)	Pretherapy	*Change pre-post	PFI (mo)	Follow-up
1	74	2000	90%	30%	tam → AI	diagnosis M+	bone	negative	NA	0	NR
2	74	1997	0%	0%	tam → AI	progression	bone, pleura	negative	NA	0	NR
3	74	2002	100%	100%	tam	diagnosis M+	liver, bone	negative	NA	3	NR
4	72	2001	++	+	AI	diagnosis M+	bone	negative	NA	0	NR
5	59	2000	30%	50%	AI	stabilisation after CT	bone, liver	negative	NA	0	NR
6	54	1999	90%	90%	AI → FA	progression	bone, liver, soft tissue	negative	NA	0	NR
7	69	1999	98%	99%	tam → AI	progression	bone, pleura	negative	NA	0	NR
8	52	2002	0%	<5%	tam → AI	progression	soft tissue	positive	↑ (+116%)	3	NR
9	60	1997	95%	68%	tam → AI	progression	bone, liver, pleura, lung	positive	↑ (+29%)	0	NR
10	46	2002	70%	50%	AI	diagnosis M+	bone, liver	positive	↑ (+63%)/ = (5%)	0	NR
111	61	1985	(+)	(+)	tam	diagnosis M+	bone	positive	↓ (- 42%)	31	R
2	75	2002	95%	5%	AI	first diagnosis	breast, skin	positive	↓ (- 33%)	°16	R
13	53	2001	80%	0%	tam	stabilisation after CT	liver	positive	= (+1%)	12	R
14	76	2000	90%	40%	tam → AI	progression	bone	positive	= (- 4%)	°22	R
15	57	1996	100%	20%	tam	diagnosis M+	bone	positive	= (+ 5%)	14	R
16	56	1997	100%	10%	AI	progression	bone, pleura	positive	↓ (- 50%)/ = (+ 4%)	°11	R
17	59	2002	100%	100%	tam → AI	progression	bone, breast	positive	↓ (-29%)/ = (- 15%)	°11	R
18	59	1996	80%	10%	tam → AI	diagnosis M+	bone	positive	only preR scan	12	R

‡ Evaluation of hormone receptor status was performed using IHC, except for patient no.11 LBA was applied. Scores immunostaining: percentage of positively stained cells or -: negative; (+): weakly positive; +: intermediately positive; ++: strongly positive. † most recent biopsy. * mean percentage change in all lesions per group. Groups: ↑ (increase in uptake of > 25%), = (increase or decrease in uptake of ≤25%), ↓ (decrease in uptake of >25%).° still responding at concl usion of study. ER, oestrogen receptor; PgR, progesterone receptor; tam, tamoxifen; AI, aromatase inhibitor; FA, full antagonist of ER (fulvestrant); M+, metastasis; CT, chemotherapy; NA, not applicable; PFI, progression-free interval; NR, nonresponder; R, responder.

Table 1 Summary of patient characteristics, imaging data and follow-up.

Change in uptake between pre- and posttherapy scan as percentage of initial uptake on pretherapy scan was recorded. A change of > 25% between pre- and posttherapy scan was considered significant. This cut-off of 25% was chosen based on the uptake measured in a series of organs and soft tissue over sequential scans that never varied more than 25% within the same patient. This is in agreement with biological variations observed in tracer kinetics and the reported reproducibility of nuclear imaging techniques in general [35,36].

Statistical Analysis

Absolute ^{99m}Tc-depreotide uptake on pretherapy scan and relative changes in tracer uptake between pre- and posttherapy scan were compared in responders and nonresponders with use of the Mann-Whitney *U* test.

4. Results

Table 1 and 2 summarize the results of the study. The mean follow-up interval was 20 months (range 8-35 months). Four patients died during this follow-up period. At 6 months after initiation of treatment eight patients had stable disease and were considered as responding to hormonal treatment, whereas 10 patients had progressive disease and were considered nonresponders. Of nine patients receiving first-line hormonal treatment five (56%) responded, of eight patients with acquired endocrine resistance three (38%) responded to second-line antioestrogen therapy. The one patient that initiated third-line endocrine treatment did not respond.

^{99m}Tc-depreotide scintigraphy	***Responder***	***Nonresponder***	Total
Negative	-	7	7
Positive	8*	3	10
ΔUptake (preR versus postR)	↓ (2) = and ↓ (2) = (3)	↑ (1) = and ↑ (2)	
Total	8	10	18

* one patient had only a pretherapy scan; ΔUptake, change in uptake of ^{99m}Tc-depreotide; ( ), number of patients; preR, pretherapy scan; postR, posttherapy scan.

Table 2. Data on tracer uptake and change in tracer uptake on sequential ^{99m}Tc-depreotide scintigraphy in responders and nonresponders.

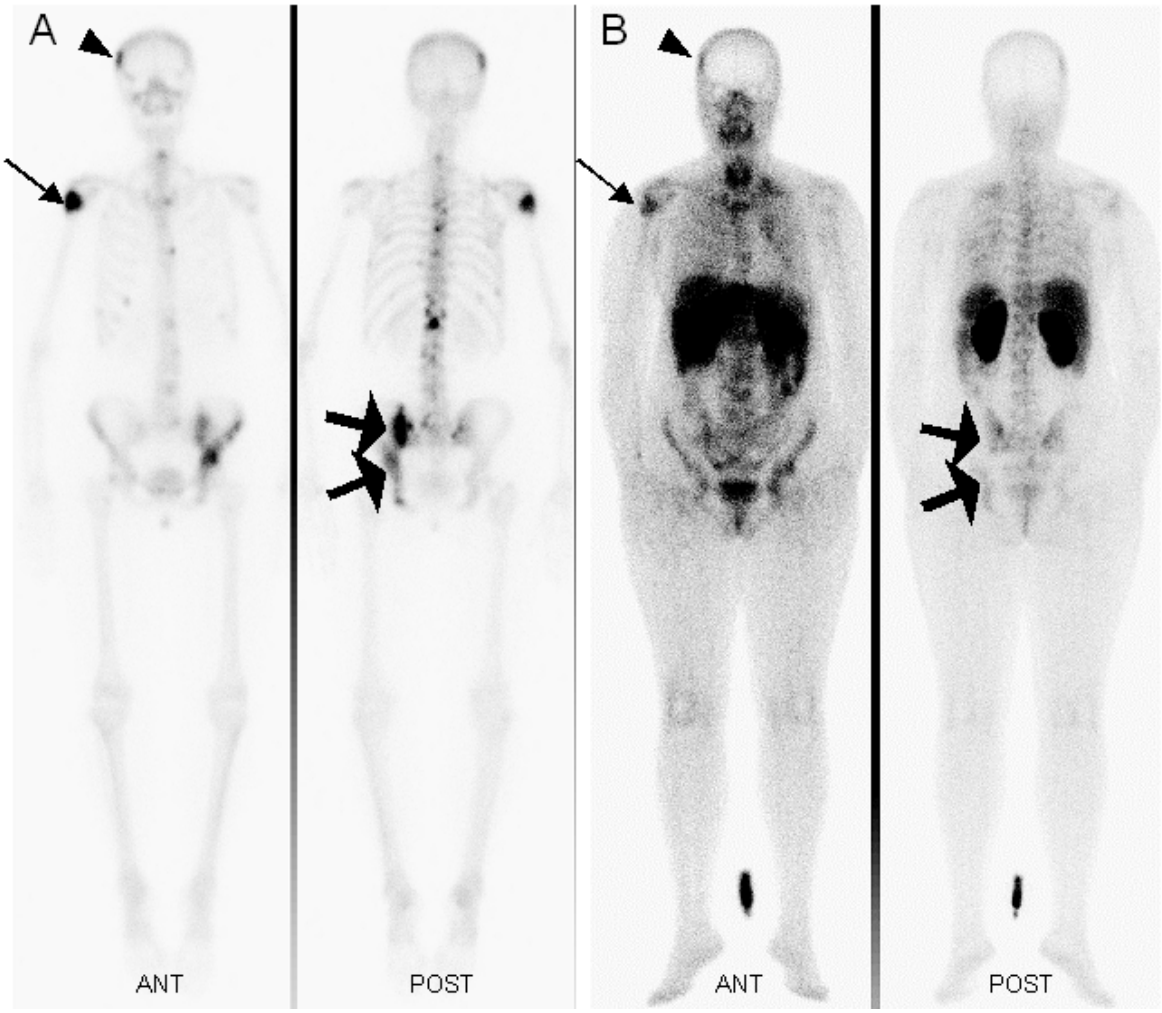

Figure 2. A 57-year-old female (no.15) presented with bone metastasis and achieved sustained disease stabilization upon endocrine treatment. ^{99m}Tc-methylendiphosphonate (MDP) bone scan shows multiple metastatic lesions, amongst others of the skull (arrow head), shoulder (thin arrow) and pelvic (thick arrow) region (A). ^{99m}Tc-depreotide scintigraphy, assessed before initiation of tamoxifen, shows uptake in the respective pathological lesions (B).

^{99m}Tc-depreotide scintigraphy assessed before initiation of antioestrogen treatment was positive in all (or major part of) lesions in 11 (61%) patients (Fig. 2). Contrast of lesions is less compared with ^{99m}Tc- methylendiphosphonate (MDP) bone scan because of relatively high background activity in the bone marrow [37]. Visualization of lesions situated in the low thoracic and high lumbar spine is hampered on planar images because of high physiologic uptake in liver, spleen and kidneys [38]. In some patients, not all lesions could be evaluated since cross-sectional SPECT images were not available for all lesions. In one of the latter patients (no.17), on planar images, tracer uptake was initially only noted in the primary tumour since relatively uniform tracer uptake in the fully invaded spine mimicked the high physiological uptake of ^{99m}Tc-depreotide in normal bone marrow. Upon fusion of MRI with

sagittal SPECT images, bulky lesions coincided with regions of enhanced tracer uptake on SPECT (Fig. 3). All responders had positive pretherapy scans and seven of 10 nonresponders had negative pretherapy scans. Thus all patients with a negative scan did not respond to therapy (Fig. 4). Tracer uptake (expressed as L/BG) on the pretherapy scan was higher for responders compared to nonresponders, with a median [25 – 75 percentile] of 4.43 [3.74 – 5.16] respectively 2.54 [2.37 – 4.36], however this difference was not significant (*P*=.102) (Fig. 5A).

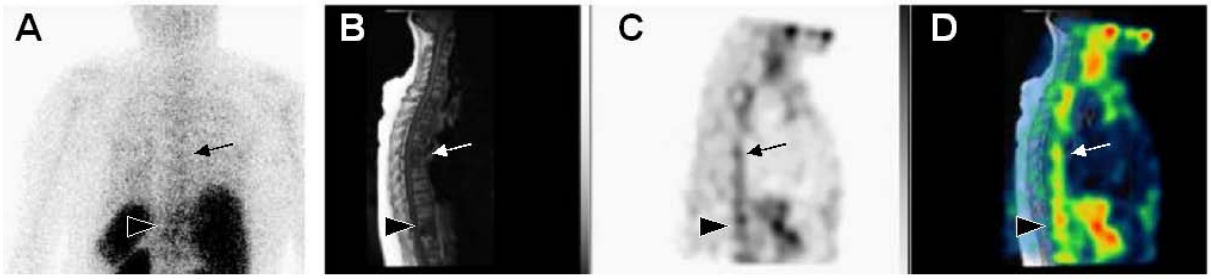

Fig. 3 A 59-year-old patient (no.17) with progression of bone metastasis on tamoxifen switched to second-line endocrine treatment. Posterior view of planar ^{99m}Tc-depreotide scintigraphy shows relatively uniform tracer uptake in the fully invaded spine, mimicking the high physiological uptake of ^{99m}Tc-depreotide in normal bone marrow (A). Sagittal MRI image depicting extensive tumoural invasion of the full spine with total destruction of corpus of thoracic vertebra (T) 11 (arrow head) and bulky lesion and T5-6 (arrow) (B). Upon fusion with sagittal SPECT images, these lesions coincide with regions of enhanced tracer uptake (C-D).

Sequential scans, acquired before and 3 weeks after initiation of antioestrogen treatment, were always both positive or both negative. The relative change in ^{99m}Tc-depreotide uptake between sequential scans significantly differed in responders compared to nonresponders (*P*=.017), uptake decreased in the first group and increased in the latter. The median [25 – 75 percentile] change in L/BG on the posttherapy scan compared to the pretherapy scan was −19.3% [−33% – 1%] for responders and 34% [29% – 116%] for nonresponders (Fig. 5B).

A cut-off of 25% was considered to define a significant increase or decrease in tracer uptake (Fig. 5C). Uptake that changed with less than 25% compared to the uptake on the pretherapy scan was considered as stable. In the group of responders, lesion uptake was stable in three patients, L/BG decreased in two patients and in two patients uptake decreased in some lesions and was stable in others (Fig. 6). In one responding patient only the pretherapy scan was acquired and as such change in uptake could not be assessed. In contrast, of the nonresponders with a positive scan, L/BG increased in one patient and in two patients uptake increased in some lesions and was stable in others.

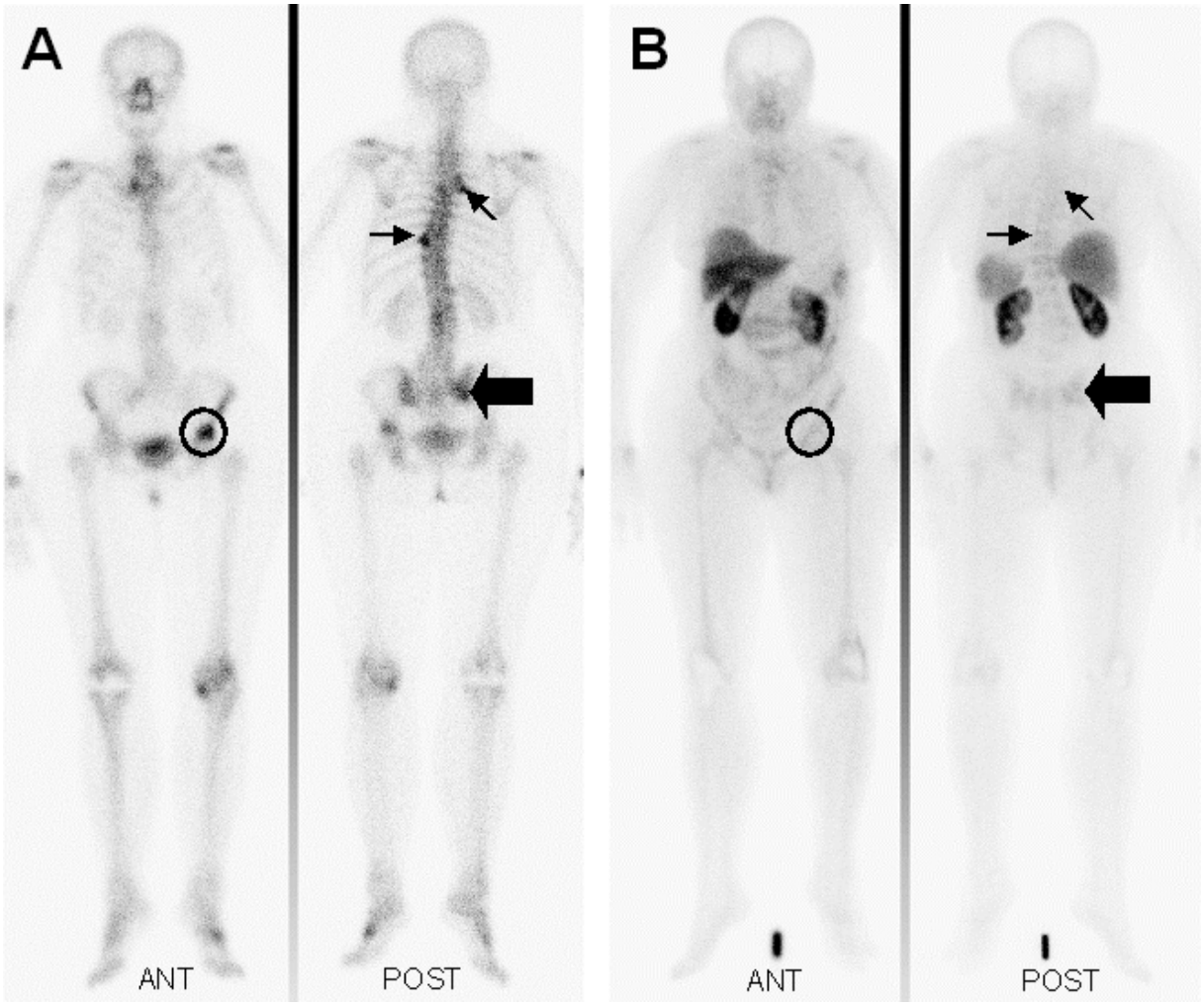

Figure 4. A 74-year-old patient (no.1), under tamoxifen treatment, presented with positive bone scan showing multiple lesions in vertebral spine T3 and ribs, T9 (small arrows), right sacro-iliacal region (thick arrow) and left femur (circle)(A). ^{99m}Tc-depreotide scintigraphy, assessed before switch to second-line hormonal therapy, was negative (B). She was a nonresponder and the number of bone lesions increased.

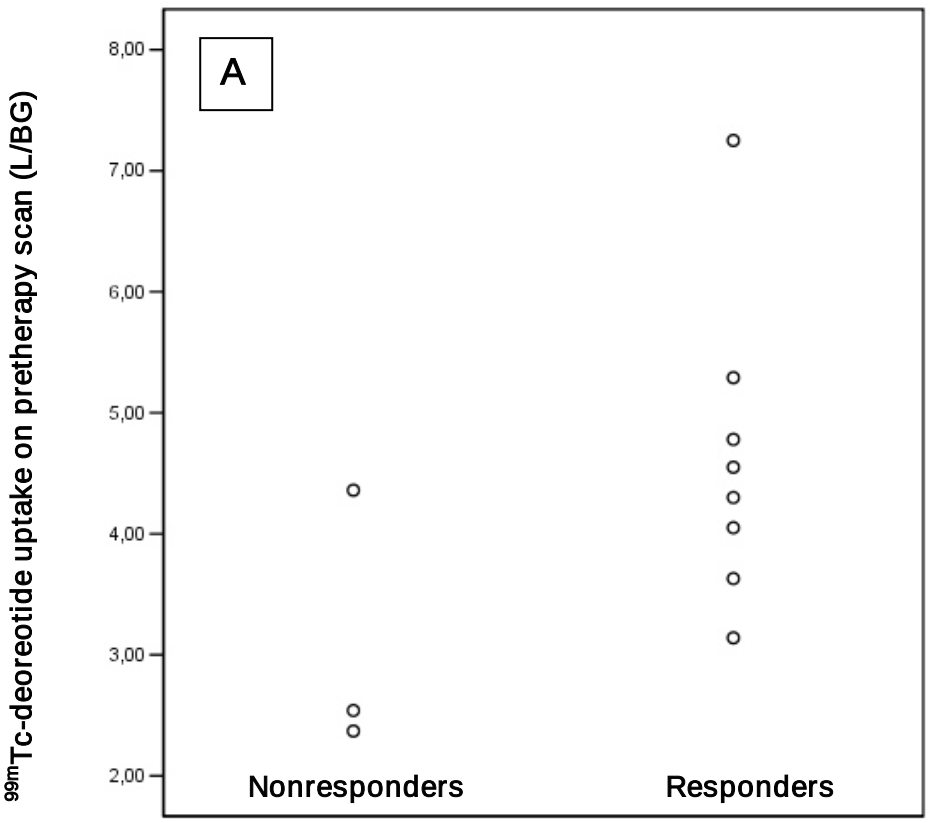
A
^{99m}Tc-deoreotide uptake on pretherapy scan (L/BG)
8,00
7,00
6,00
5,00
4,00
3,00
2,00
Nonresponders
Responders

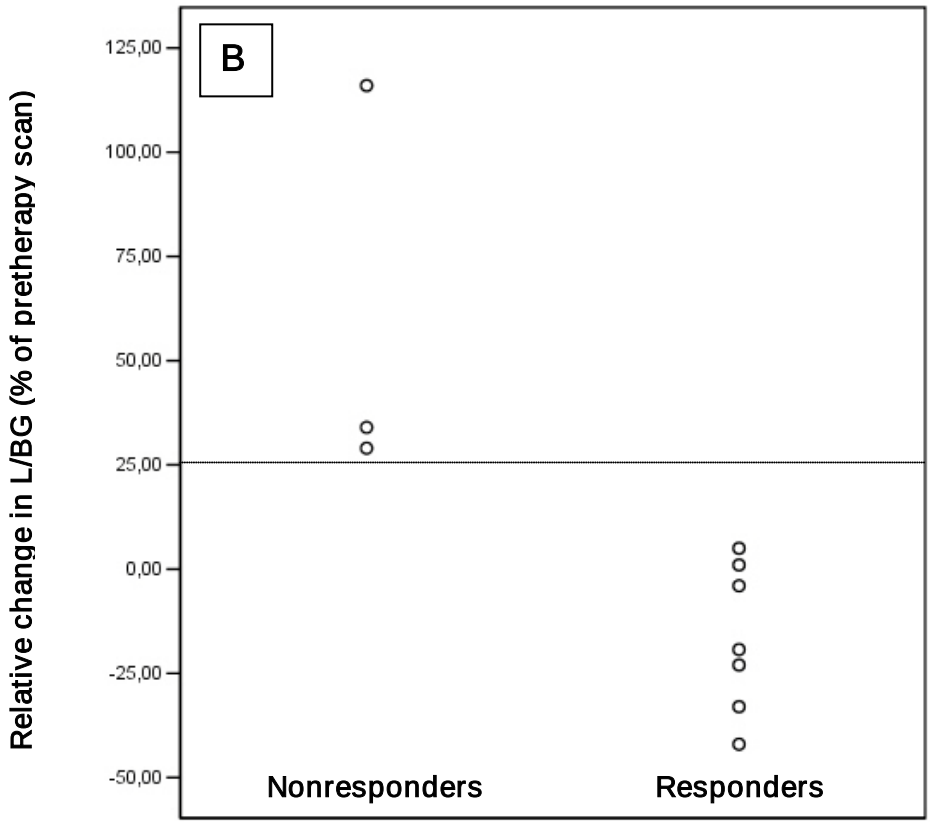
B
Relative change in L/BG (% of pretherapy scan)
125,00
100,00
75,00
50,00
25,00
0,00
-25,00
-50,00
Nonresponders
Responders

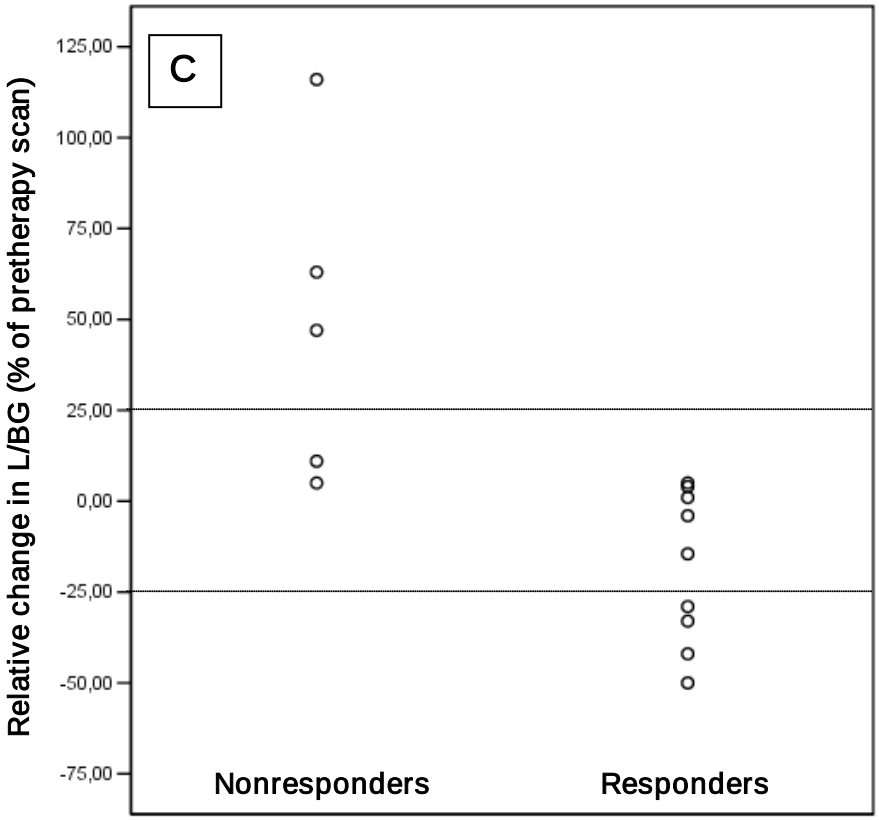

Figure 5. A. Scatter plot of ^{99m}Tc-depreotide uptake (expressed as L/BG) on pretherapy scan, averaged over all lesions, in nonresponders and responders. B. Scatter plot of relative change in tracer uptake (expressed as percentage of uptake on pretherapy scan) on sequential scans, averaged over all lesions, in nonresponders and responders. C. Scatter plot of relative change in tracer uptake (expressed as percentage of tracer uptake on pretherapy scan) on sequential scans, split into 3 groups (increase, stable, decrease) using a cut-off of 25% and averaged, in nonresponders and responders.

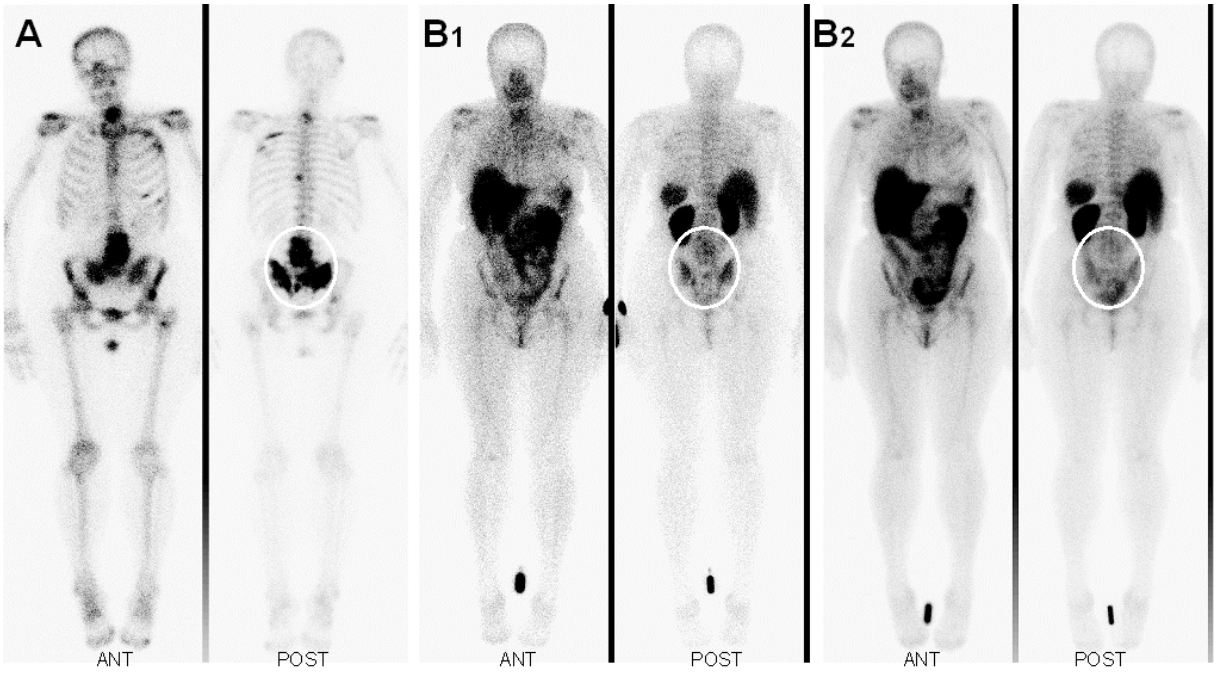

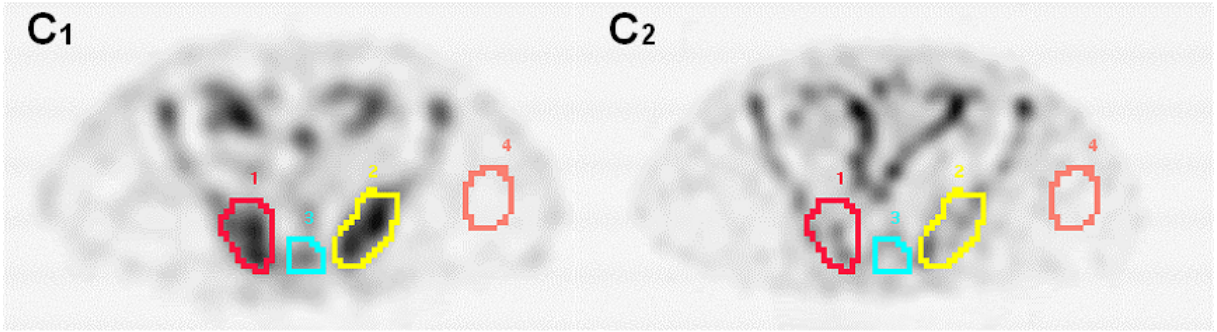

D

	Lesion / BG (ROI 4)		
	ROI 1	ROI 2	ROI 3
Pre-therapy scan (C1)	7.82	7.99	5.57
Post-therapy scan (C2)	3.24	3.57	3.24
Δ uptake (%)	**- 59**	**- 55**	**- 42**

Figure 6. A 61-year-old patient (no.11) presented with multiple lesions on bone scan and had stable disease for 31 months upon tamoxifen treatment (A). Sequential ^{99m}Tc-depreotide scintigraphy visualizes similar extensive bone metastasis as on bone scan, amongst others in lumbar (L2-5) and sacro-iliacal region (B_1: pretherapy scan – B_2: posttherapy scan). Regions-of-interest (ROIs) were drawn over lesions (ROI 1-3) and background (ROI 4) on transversal SPECT images and measured counts were averaged over several slices of total tumour volume (C_1: pretherapy scan – C_2: posttherapy scan). Lesion-to-background ratio's and change in uptake (Δ uptake – expressed as

percentage of uptake first scan) were calculated (D). ^{99m}Tc-depreotide uptake significantly decreased with values of –42% to –55%.

5. Discussion

Endocrine therapy is one of primary treatment options for the majority of patients with metastatic breast cancer. Upon patient selection based on hormone receptor status 50%-75% of patients with ER and/or PgR expressing tumours initially respond. Nearly all responding patients eventually suffer disease progression, but approximately half of patients with acquired resistance obtain clinical benefit from other endocrine therapies. Although response rates progressively decline, they remain in the 20% to 40% range [39]. Our limited patient data are concordant with these reported figures for sequential endocrine responsiveness.

In our study, all patients with hormone-sensitive tumours had positive scans. This could be expected since E_2 stimulation of functional ER enhances SSTR2 gene transcription and hence SSTR2 expression at the cell surface, which is visualized by ^{99m}Tc-depreotide scintigraphy. In this group of responders, tracer uptake on the posttherapy scan tended to be lower compared to the pretherapy scan and, considering a cut-off of 25%, uptake significantly decreased or remained stable. According to our hypothesis, this decrease could be interpreted as a downregulation of SSTR2 at the cell surface level caused by an efficient block of the functional ER that inhibits further transcription of the SSTR2. Unfortunately, for availability reasons, binding of radioligand to breast tumour cells per se could not be confirmed using autoradiography. Therefore, binding of ^{99m}Tc-depreotide to other kinds of cells expressing SSTR2, 3 or 5, such as activated lymphocytes (SSTR2), cannot be excluded [40]. The presence of tumour infiltrating lymphocytes (TILs) has been associated with therapy response and good prognosis, however controversy exists [41,42]. Equivalent uptake on both sequential scans could be interpreted as absence of active stimulation of ER and subsequently absence of SSTR2 transcription. Possibly, intratumoural levels of antioestrogen could have only just or not yet achieved steady state and balance between receptor synthesis and endocytosis/degradation has not yet turned in favour of degradation. However, one patient initiated anastrozole (no.13) which achieves steady state within 7 days [29]. Though this concerns serum levels and not concentrations in the respective tissues of action.

Three patients of the group of responders had acquired resistance to tamoxifen and had positive ^{99m}Tc-depreotide scans before they switched to a second-line aromatase inhibitor. This is in agreement with considerable amount of data indicating that ER in acquired resistant breast cancer commonly remains functional and moreover pivotal to the growth regulation

and gene expression profile of breast tumours on their relapse, despite the presence of tamoxifen [43]. Following their inhibition by tamoxifen during initial responsive phase of the disease, oestrogen-regulated genes can be reexpressed on disease relapse. Clinical experience has shown that hormonal resistance is often reversible, suggesting a cellular adaptation, rather than genetic alterations in many breast cancer patients [44]. Changes in local metabolism and more in particular reduced concentrations of tamoxifen and its metabolites are reported in tamoxifen-resistant tumours [45]. Accordingly, efflux of tamoxifen out of the tumour cell in the presence of a functional ER results in a tamoxifen resistant tumour, expressing oestrogen-regulated genes (e.g., SSTR2), sensitive to aromatase inhibitors. Besides prediction of the likelihood of response to second-line hormonal treatment such as aromatase inhibitors requiring a functional ER, this could allow for prediction of early resistance to tamoxifen treatment.

All negative ^{99m}Tc-depreotide scans belonged to patients with tumours resistant to hormonal therapy. This was in line with expectations since we anticipated a nonfunctional ER, not capable of stimulating transcription and expression of SSTR2. Loss of ER is generally not a feature of acquired endocrine resistance either in vitro or in vivo, hence repeated hormone receptor assessment using routine techniques (LBA, IHC) for determination of endocrine-responsiveness would be inadequate [46].

Three patients (30%) of the group of nonresponders had positive ^{99m}Tc-depreotide scintigraphies. This suggests a ligand-independent stimulation of ER and oestrogen-independent regulation of SSTR2 expression. Constitutively active ER variants might contribute to a tamoxifen resistance breast tumour with similar characteristics, however mutations are extremely rare in vivo and thus refer only to a minority of cases [47]. Even in tumours that are oestrogen-dependent, it is likely that an appropriate growth factor environment is necessary for efficient mitogenesis, with steroid hormone and growth factor signalling pathways "cross talking" to reinforce each others' signalling [48,49,50]. Overexpression of a growth factor (EGF, epidermal growth factor; TGFα, transforming growth factor α; IGF-1, insulin-like growth factor 1) or its receptor (EGFR, HER2/Neu, IGF-1R) may perturb this balance of steroid hormone and growth factor interaction, providing a selective advantage for tumour cell proliferation despite hormone therapy. As such, several kinases, which are themselves activated by membrane growth factor receptors, phosphorylate ER at sites that influence its biological activity. On the posttherapy scan tracer uptake was increased in these patients, suggesting an upregulation of SSTR2 expression as a result of continuous or enhanced stimulation of SSTR2 transcription. However in vitro data in human

breast cancer cells attribute this increase predominantly to an enhanced recycling of the receptor rather than an increased synthesis [19]. Several postreceptor alterations, including changes in coregulators or cAMP and phosphorylation pathways, known to affect transcriptional activity of ER and to enhance the agonistic activity of tamoxifen-like antioestrogens could explain an increase in SSTR2 expression [51]. However, in these three patients endocrine treatment with an aromatase inhibitor was initiated.

Presumably regulation of SSTR expression in breast tumour cells is not exclusively oestrogen-dependent and is influenced by a series of other mediators, as is the case in normal tissue (e.g., pancreas, hypothalamus) [52]. Growth factors and cytokines secreted by tumour cells or adjacent host cells may modify SSTR expression in an autocrine or paracrine manner. A series of radiopharmaceuticals have been developed to specifically investigate this feature [53,54]. Interestingly, the cytokines IL-6 (interleukin 6) and TNF-α (tumor necrosis factor α) that stimulate activity of aromatase, the enzyme that catalyses conversion from androgen to oestrogen in tumour cells, also enhance SSTR expression [55,56]. These cytokines are secreted by tumour associated lymphocytes and other adjacent host cells (e.g., adipocytes) in response to the tumour cells themselves. Upon administration of an aromatase inhibitor, absence of positive feedback could supposedly result in an abundance of the cytokines and augmentation of SSTR at the cell surface. However, regulation of SSTR by IL-6 or TNF-α has not yet been described in human breast cancer cells. Furthermore, SSTR expression is inhibited by growth-inhibitory factor TGF-β (transforming growth factor β) present in breast tumour cells [57]. Several studies have demonstrated increases in plasma and tumour levels of TGF-β in patients following initial exposure to tamoxifen therapy mirroring effective tamoxifen response [58,59,60,61]. In addition, IGF signalling by growth factors IGF-1 and more importantly IGF-2 is likely to play a crucial role in pathogenesis of steroid-hormone-dependent disease and many ER-positive breast carcinomas express high levels of the respective receptor IGF-1R [62,63]. Tamoxifen treatment substantially reduces IGF signalling partly through a decrease in levels of IGF-1 and IGF-2, both also known to stimulate SSTR expression [64,52,65,66]. These mechanisms could play a complementary or alternative role in the decrease in SSTR2 expression and ^{99m}Tc-depreotide binding in the responders in our study. Moreover, a high expression of IGF signalling elements and paradoxically high TGF-β production have been reported in tamoxifen-resistant tumours, which could potentially contribute to the SSTR-positive respectively SSTR-negative phenotype of nonresponders [67,63].

In our series we found a consistent relationship between ^{99m}Tc-depreotide uptake and response to endocrine treatment in metastasized breast cancer patients. Underlying

mechanism is suggested to be an ER-mediated regulation of SSTR2 expression but additional influence by a series of cytokines and/or growth factors present in the tumoural environment is to be expected. Nevertheless, if a larger scale study confirms these findings, this could entail a powerful tool to accurately evaluate endocrine-responsiveness. A protocol with somatostatin receptor scintigraphy before initiation of endocrine treatment and repetition of the scan if positive could be proposed (Fig. 7).

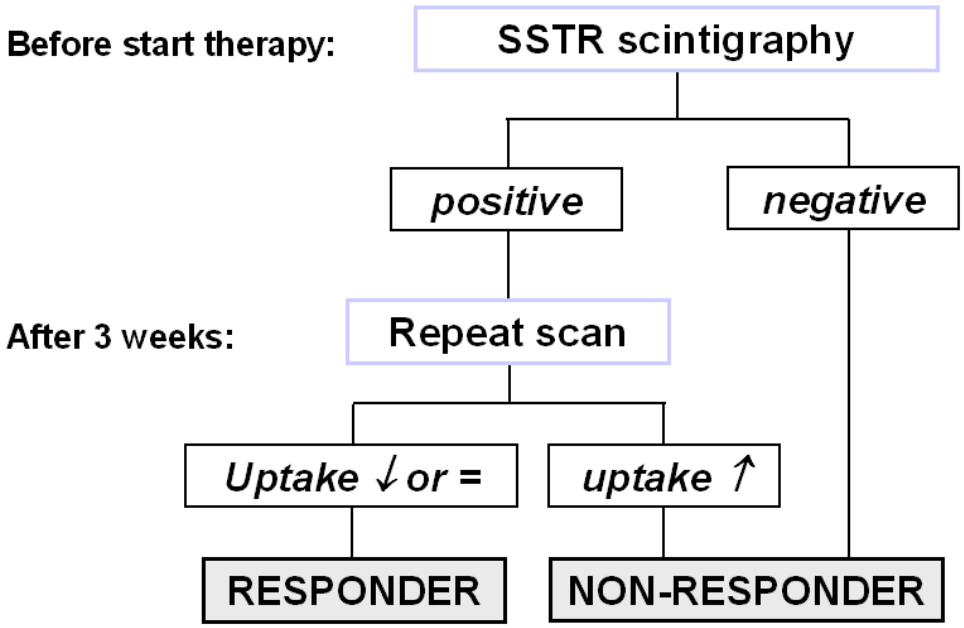

Figure 7. Proposed protocol for selection of advanced breast cancer patients for endocrine treatment using sequential ^{99m}Tc-depreotide scintigraphy.

Realistic goals for treatment of metastatic breast cancer are palliation of symptoms and prolongation of survival with maximizing the quality of life. In general, significant palliation is more likely for a patient who experiences a response to endocrine therapy compared to a similar response induced by chemotherapy, due to a lower toxicity profile. A delay in effective therapy may lead to a decline in performance status and organ function, and as such reduce the likelihood of a subsequent response. Using clinical follow-up and conventional morphological imaging modalities using volumetric changes easily 3 to 6 months are needed for response evaluation. The proposed protocol would allow for separation of responders and nonresponders immediately (negative pretherapy scan) or as early as 3 weeks after treatment initiation (positive pretherapy scan).

Acknowledgements. The authors wish to acknowledge the assistance of V. Renard, S. Rottey, R. Van den Broecke, and G. Codacci for patient referral; F. De Vos and E. D'haeninck for radiopharmaceutical preparation; B. Lambert, I. Goethals and G. Parisella for assessment of ^{99m}Tc-depreotide images; O. De Winter for statistic support.

6. References

1. McGuire WL: Current status of estrogen receptors in human breast cancer. Cancer 36: 638-644, 1975

2. McGuire WL, Horwitz KB, Pearson OH, et al: Current status of estrogen and progesterone receptors in breast cancer. Cancer 39: 2934-2947, 1977

3. Steroid receptors in breast cancer: an NIH Consensus Development Conference, Bethesda, Maryland, June 27-29, 1979. Cancer 46: 2759-2963, 1980

4. Holdaway IM and Bowditch JV: Variation in receptor status between primary and metastatic breast cancer. Cancer 52: 479-485, 1983

5. Kuukasjarvi T, Kononen J, Helin H, et al: Loss of estrogen receptor in recurrent breast cancer is associated with poor response to endocrine therapy. J Clin Oncol 14: 2584-2589, 1996

6. Franco A, Col N, and Chlebowski R: Discordance in estrogen (ER) and progestin receptor (PR) status between primary metastatic breast cancer: a meta-analysis. Proc Am Soc Clin Oncol 23: 2004

7. Spataro V, Price K, Goldhirsch A, et al: Sequential estrogen receptor determinations from primary breast cancer and at relapse: prognostic and therapeutic relevance. The International Breast Cancer Study Group (formerly Ludwig Group). Ann Oncol 3: 733-740, 1992

8. Pichon MF, Broet P, Magdelenat H, et al: Prognostic value of steroid receptors after long-term follow-up of 2257 operable breast cancers. Br J Cancer 73: 1545-1551, 1996

9. Fidler IJ and Hart IR: Biological diversity in metastatic neoplasms: origins and implications. Science 217: 998-1003, 1982

10. Heppner GH: Tumor heterogeneity. Cancer Res 44: 2259-2265, 1984

11. Reubi JC, Waser B, Foekens JA, et al: Somatostatin receptor incidence and distribution in breast cancer using receptor autoradiography: relationship to EGF receptors. Int J Cancer 46: 416-420, 1990

12. Reubi JC and Torhorst J: The relationship between somatostatin, epidermal growth factor, and steroid hormone receptors in breast cancer. Cancer 64: 1254-1260, 1989

13. Van de Wiele C, De Vos F, Slegers G, et al: Radiolabeled estradiol derivatives to predict response to hormonal treatment in breast cancer: a review. Eur J Nucl Med 27: 1421-1433, 2000

14. Van Den Bossche B and Van de Wiele C: Receptor imaging in oncology by means of nuclear medicine: current status. J Clin Oncol 22: 3593-3607, 2004

15. Bloom ND, Tobin EH, Schreibman B, et al: The role of progesterone receptors in the management of advanced breast cancer. Cancer 45: 2992-2997, 1980

16. Bernoux A, de Cremoux P, Laine-Bidron C, et al: Estrogen receptor negative and progesterone receptor positive primary breast cancer: pathological characteristics and clinical outcome. Institut Curie Breast Cancer Study Group. Breast Cancer Res Treat 49: 219-225, 1998

17. Nardelli GB, Lamaina V, and Siliotti F: Estrogen and progesterone receptors status in the prediction of response of breast cancer to endocrine therapy (preliminary report). Eur J Gynaecol Oncol 7: 151-158, 1986

18. Xu Y, Song J, Berelowitz M, et al: Estrogen regulates somatostatin receptor subtype 2 messenger ribonucleic acid expression in human breast cancer cells. Endocrinology 137: 5634-5640, 1996

19. Van Den Bossche B, D'haeninck E, De Vos F, et al: Oestrogen-mediated regulation of somatostatin receptor expression in human breast cancer cell lines assessed with 99mTc-depreotide. Eur J Nucl Med Mol Imaging 31: 1022-1030, 2004

20. Vikic-Topic S, Raisch KP, Kvols LK, et al: Expression of somatostatin receptor subtypes in breast carcinoma, carcinoid tumor, and renal cell carcinoma. J Clin Endocrinol Metab 80: 2974-2979, 1995

21. Schulz S, Helmholz T, Schmitt J, et al: True positive somatostatin receptor scintigraphy in primary breast cancer correlates with expression of sst2A and sst5. Breast Cancer Res Treat 72: 221-226, 2002

22. Reubi JC, Waser B, Schaer JC, et al: Somatostatin receptor sst1-sst5 expression in normal and neoplastic human tissues using receptor autoradiography with subtype-selective ligands. Eur J Nucl Med 28: 836-846, 2001

23. van Eijck CH, Krenning EP, Bootsma A, et al: Somatostatin-receptor scintigraphy in primary breast cancer. Lancet 343: 640-643, 1994

24. Lamberts SW, Krenning EP, and Reubi JC: The role of somatostatin and its analogs in the diagnosis and treatment of tumors. Endocr Rev 12: 450-482, 1991

25. Virgolini I, Leimer M, Handmaker H, et al: Somatostatin receptor subtype specificity and in vivo binding of a novel tumor tracer, 99mTc-P829. Cancer Res 58: 1850-1859, 1998

26. Lister-James J, Pearson D, De Rosch M, et al: Tc-99m P829: characterization of a technetium-99-labeled somatostatin receptor-binding peptide. Technetium, Rhenium and Other Metals in Chemistry and Nuclear Medicine 473-478, 1999

27. Vallabhajosula S, Moyer BR, Lister-James J, et al: Preclinical evaluation of technetium-99m-labeled somatostatin receptor-binding peptides. J Nucl Med 37: 1016-1022, 1996

28. Johnston SR, Haynes BP, Sacks NP, et al: Effect of oestrogen receptor status and time on the intra-tumoural accumulation of tamoxifen and N-desmethyltamoxifen following short-term therapy in human primary breast cancer. Breast Cancer Res Treat 28: 241-250, 1993

29. Data in file. AstraZeneca Pharmaceuticals. 2001

30. Data on file. Novartis Pharmaceuticals Corporation. 2005

31. Therasse P, Arbuck SG, Eisenhauer EA, et al: New guidelines to evaluate the response to treatment in solid tumors. European Organization for Research and Treatment of Cancer, National Cancer Institute of the United States, National Cancer Institute of Canada. J Natl Cancer Inst 92: 205-216, 2000

32. Robertson JF, Jaeger W, Syzmendera JJ, et al: The objective measurement of remission and progression in metastatic breast cancer by use of serum tumour markers. European Group for Serum Tumour Markers in Breast Cancer. Eur J Cancer 35: 47-53, 1999

33. Robertson JF, Willsher PC, Cheung KL, et al: The clinical relevance of static disease (no change) category for 6 months on endocrine therapy in patients with breast cancer. Eur J Cancer 33: 1774-1779, 1997

34. Robertson JF, Howell A, Buzdar A, et al: Static disease on anastrozole provides similar benefit as objective response in patients with advanced breast cancer. Breast Cancer Res Treat 58: 157-162, 1999

35. Weber WA, Schwaiger M, and Avril N: Quantitative assessment of tumor metabolism using FDG-PET imaging. Nucl Med Biol 27: 683-687, 2000

36. Vermeersch H, Ham H, Rottey S, et al: Intraobserver, interobserver, and day-to-day reproducibility of quantitative 99mTc-HYNIC annexin-V imaging in head and neck carcinoma. Cancer Biother Radiopharm 19: 205-210, 2004

37. Van Den Bossche B, D'haeninck E, Bacher K, et al: Biodistribution and dosimetry of (99m)Tc-depreotide (P829) in patients suffering from breast carcinoma. Cancer Biother Radiopharm 19: 776-783, 2004

38. Van Den Bossche B, D'haeninck E, De Winter F, et al: 99mTc depreotide scan compared with 99mTc-MDP bone scintigraphy for the detection of bone metastases and prediction of response to hormonal treatment in patients with breast cancer. Nucl Med Commun 25: 787-792, 2004

39. Cheung KL, Willsher PC, Pinder SE, et al: Predictors of response to second-line endocrine therapy for breast cancer. Breast Cancer Res Treat 45: 219-224, 1997

40. Elliott DE, Li J, Blum AM, et al: SSTR2A is the dominant somatostatin receptor subtype expressed by inflammatory cells, is widely expressed and directly regulates T cell IFN-gamma release. Eur J Immunol 29: 2454-2463, 1999

41. Marrogi AJ, Munshi A, Merogi AJ, et al: Study of tumor infiltrating lymphocytes and transforming growth factor-beta as prognostic factors in breast carcinoma. Int J Cancer 74: 492-501, 1997

42. Georgiannos SN, Renaut A, Goode AW, et al: The immunophenotype and activation status of the lymphocytic infiltrate in human breast cancers, the role of the major histocompatibility complex in cell-mediated immune mechanisms, and their association with prognostic indicators. Surgery 134: 827-834, 2003

43. Johnston SR, Lu B, Dowsett M, et al: Comparison of estrogen receptor DNA binding in untreated and acquired antiestrogen-resistant human breast tumors. Cancer Res 57: 3723-3727, 1997

44. Stoll BA: Rechallenging breast cancer with tamoxifen therapy. Clin Oncol 9: 347-351, 1983

45. Osborne CK, Wiebe VJ, McGuire WL, et al: Tamoxifen and the isomers of 4-hydroxytamoxifen in tamoxifen-resistant tumors from breast cancer patients. J Clin Oncol 10: 304-310, 1992

46. Robertson JF: Oestrogen receptor: a stable phenotype in breast cancer. Br J Cancer 73: 5-12, 1996

47. Fuqua SA and Wolf DM: Molecular aspects of estrogen receptor variants in breast cancer. Breast Cancer Res Treat 35: 233-241, 1995

48. Nicholson RI and Gee JM: Oestrogen and growth factor cross-talk and endocrine insensitivity and acquired resistance in breast cancer. Br J Cancer 82: 501-513, 2000

49. Shou J, Massarweh S, Osborne CK, et al: Mechanisms of tamoxifen resistance: increased estrogen receptor-HER2/neu cross-talk in ER/HER2-positive breast cancer. J Natl Cancer Inst 96: 926-935, 2004

50. Nicholson RI, McClelland RA, Robertson JF, et al: Involvement of steroid hormone and growth factor cross-talk in endocrine response in breast cancer. Endocr Relat Cancer 6: 373-387, 1999

51. Fujimoto N and Katzenellenbogen BS: Alteration in the agonist/antagonist balance of antiestrogens by activation of protein kinase A signaling pathways in breast cancer cells: antiestrogen selectivity and promoter dependence. Mol Endocrinol 8: 296-304, 1994

52. Patel YC: Somatostatin and its receptor family. Front Neuroendocrinol 20: 157-198, 1999

53. Signore A, Capriotti G, Scopinaro F, et al: Radiolabelled lymphokines and growth factors for in vivo imaging of inflammation, infection and cancer. Trends Immunol 24: 395-402, 2003

54. Signore A, Chianelli M, Bei R, et al: Targeting cytokine/chemokine receptors: a challenge for molecular nuclear medicine. Eur J Nucl Med Mol Imaging 30: 801-802, 2003

55. Reed MJ and Purohit A: Breast cancer and the role of cytokines in regulating estrogen synthesis: an emerging hypothesis. Endocr Rev 18: 701-715, 1997

56. Scarborough DE, Lee SL, Dinarello CA, et al: Interleukin-1 beta stimulates somatostatin biosynthesis in primary cultures of fetal rat brain. Endocrinology 124: 549-551, 1989

57. Quintela M, Senaris RM, and Dieguez C: Transforming growth factor-betas inhibit somatostatin messenger ribonucleic acid levels and somatostatin secretion in hypothalamic cells in culture. Endocrinology 138: 4401-4409, 1997

58. Knabbe C, Kopp A, Hilgers W, et al: Regulation and role of TGF beta production in breast cancer. Ann N Y Acad Sci 784: 263-276, 1996

59. Kopp A, Jonat W, Schmahl M, et al: Transforming growth factor beta 2 (TGF-beta 2) levels in plasma of patients with metastatic breast cancer treated with tamoxifen. Cancer Res 55: 4512-4515, 1995

60. Butta A, MacLennan K, Flanders KC, et al: Induction of transforming growth factor beta 1 in human breast cancer in vivo following tamoxifen treatment. Cancer Res 52: 4261-4264, 1992

61. MacCallum J, Keen JC, Bartlett JM, et al: Changes in expression of transforming growth factor beta mRNA isoforms in patients undergoing tamoxifen therapy. Br J Cancer 74: 474-478, 1996

62. Surmacz E: Function of the IGF-I receptor in breast cancer. J Mammary Gland Biol Neoplasia 5: 95-105, 2000

63. Gee JM, Madden T-A, Robertson J, et al: Clinical response and resistance to SERMs 155-189, 2002

64. Guvakova MA and Surmacz E: Tamoxifen interferes with the insulin-like growth factor I receptor (IGF-IR) signaling pathway in breast cancer cells. Cancer Res 57: 2606-2610, 1997

65. Helle SI and Lonning PE: Insulin-like growth factors in breast cancer. Acta Oncol 35 Suppl 5: 19-22, 1996

66. Helle SI, Anker GB, Tally M, et al: Influence of droloxifene on plasma levels of insulin-like growth factor (IGF)-I, Pro-IGF-IIE, insulin-like growth factor binding protein (IGFBP)-1 and IGFBP-3 in breast cancer patients. J Steroid Biochem Mol Biol 57: 167-171, 1996

67. Herman ME and Katzenellenbogen BS: Alterations in transforming growth factor-alpha and -beta production and cell responsiveness during the progression of MCF-7 human breast cancer cells to estrogen-autonomous growth. Cancer Res 54: 5867-5874, 1994

CHAPTER SEVEN

GENERAL DISCUSSION

Hormone-dependent breast tumours are characterized primarily by a functional and intact oestrogen receptor (ER) system. Antioestrogen agents selectively target the ER pathway to abolish its effect on cell growth. Since only about one third of breast cancer patients initially respond to endocrine therapy, there is a need for patient selection. So far, the only predictive factor approved for clinical routine use is the in vitro assessment of hormone receptor status on tissue samples by ligand binding assay (LBA) or immunohistochemistry (IHC). Still, only 50%-60% of patients with ER-positive tumours exhibit response to hormonal therapy, whereas lack of detectable ERs is usually associated with 5%-10% response [1,2,3]. Possible causes of discordance between hormone receptor status and endocrine responsiveness include limits inherent to the available techniques (IHC, LBA) for hormone receptor assessment, such as sampling error and variations in specificity (animal dependent) seen with the preparation of antibodies. Assessment of hormone receptor status is usually based on tissue samples from the primary tumour, whilst this information is being utilized years or decades later in the metastatic situation, when the biology of the tumour might have changed [4,5,6]. In addition, breast tumours contain multiple cell populations exhibiting a wide range of genetic, biochemical, immunological and biological characteristics [7,8]. Metastatic lesions originating from an ER-negative clone may be ER-negative nevertheless the primary tumour is ER-positive. Another explanation for lack of response to endocrine treatment in ER-positive disease is nonfunctioning of the ER. These receptors are recognized and measured by IHC, but in such tumours steroid hormone occupancy of the receptor is not the drive for cellular proliferation and hence antioestrogen therapy is inefficient. Assessment of end-product of ER stimulation, such as PgR receptor, could by-pass this problem and has proven to increase predictive accuracy [9,10,11].

Scintigraphy is the imaging technique of choice since it is noninvasive and offers the advantage of repetitive whole body evaluation. Furthermore, it has the ability to address the intrinsic heterogeneity of tumoural receptor expression without tissue manipulation and provides an in vivo image of all disease sites at the moment of treatment need. In chapter 2 we amplify on receptor imaging by means of nuclear medicine in oncology. In breast cancer in particular, many efforts have been put into synthesis and evaluation of radiopharmaceuticals of which tumoural uptake is believed to relate to ER expression and hence endocrine responsiveness [20,21]. Available data demonstrate a lack of concordance between uptake of radiolabelled oestradiol derivates and ER status [22,23]. This can be explained by the fact that

oestradiol needs are provided by both uptake and local biosynthesis and are highly variable inter- as well as intratumourally [24,25]. Sequential ^{123}I-labelled *cis*-11β-methoxy-17α-iodovinyl-estradiol (^{123}I-z-MIVE) imaging visualised ER-blockage in patients with longer progression-free interval upon antioestrogen treatment [26]. However, this effect was related to a selected patient population, screened for ^{123}I-z-MIVE uptake prior to inclusion. Similarly, imaging of ER-blockade or metabolic flare reaction by means of sequential 16α-^{18}F-fluoroestradiol-17β (^{18}F-FES) positron emission tomography (PET) respectively ^{18}F-fluorodeoxyglucose (^{18}F-FDG) PET was related to response to tamoxifen treatment [27]. Both studies included only patients who received tamoxifen and the latter represent just part of the actual group of breast cancer patients with metastatic disease eligible for endocrine treatment. Tamoxifen derived single photon emission computed tomography (SPECT) tracer suffered from high background activity due to extensive tissue binding related to its lipophilic characteristics and the respective PET tracer showed no correlation with hormone receptor status nor treatment response [28,29]. Several PgR-specific radioligands have been synthesized and validated in animal models, but their potential in patients have yet to be assessed [30,31,32].

Experimental data in human breast cancer cell lines suggest that the somatostatin receptor (SSTR) is another oestrogen-regulated gene [12]. The SSTR is a membrane bound G-protein-coupled receptor that undergoes rapid internalisation upon agonist binding [13]. To date, five distinct subtypes (SSTR1-5, with SSTR2 having two splice variant isoforms, respectively SSTR2A-SSTR2B), encoded by separate genes, have been identified [14,15]. The former data, however, are based on mRNA expression, which may not necessarily reflect functional receptor levels. In fact, recent reports have suggested a lack of parallelism between SSTR mRNA and receptor protein in some human tumours [16,17,18]. In chapter 3 we demonstrated oestrogen-mediated SSTR expression in 2 endocrine responsive ER-positive human breast cancer cell lines (T47D and ZR75-1) but not in endocrine unresponsive ER-negative MDA MB231 cells. Physiological concentrations of E_2 resulted in a statistically significant increase of the number of SSTRs at the level of the cell membrane of T47D cells but not in ZR75-1 and MDA MB231 cells as evidenced by binding assays. Given the minor increase in SSTR2 protein levels as evidenced by western blotting for the T47D cell line, this phenomenon is likely attributable to a predominant recycling of receptors from inner towards the outer cell membrane. In the ZR75-1 cells a mean decrease of the number of cell membrane SSTRs after E_2 stimulation was noticed, which however was not statistically significantly different. As shown by western blot analysis, this mean decrease may be explained by a drop in the number of SSTR5 receptors. T47D cells also evidenced a drop in

SSTR5 protein content but much less pronounced. In T47D cells, the E_2-effect was reduced or inhibited by the antioestrogens tamoxifen and ICI 182 780 (fulvestrant), indicating a requirement for E_2 binding and stimulation of the ER suggestive of an exclusively E_2-dependent regulation of SSTR2 expression. The reduction seen with tamoxifen as compared to the inhibition seen with ICI 182 780 may be explained by the partial- and full antagonist character of the respective molecules. On the human SSTR2 gene, an E_2-responsive region has been roughly localized to sequences spanning from kilobase pairs (kb) –5.3 to –3.8 with respect to the transcriptional site in front of the coding region [19].

For SSTR imaging, we chose to work with depreotide (P829 - NeoSpect®/NeoTect®), a ^{99m}Tc-labelled somatostatin analogue with high affinity for SSTR2, 3 and 5 [33,34,35]. Depreotide received US Food and Drug Administration approval for use in the imaging of suspected malignant tumors in the lung. In vivo imaging of SSTR-positive tumours is routinely performed using [^{111}In-DTPA-D-Phe^1]-octreotide scintigraphy (SMS 201-995 – Octreoscan®) and uptake correlates with expression of SSTR2A and SSTR5. However, technetium labelling offers clinical advantages when compared to indium labelling including lower cost, better availability and faster tumoural visualization enabling a 1-day-protocol. The decay characteristics of technetium, more adapted to the photon energy detection ability of gamma cameras, together with the shorter physical half life permitting a higher dose administration, result in better image quality combined with lower radiation dose. In the biodistribution and dosimetry study of ^{99m}Tc-depreotide in chapter 4, most of the activity was observed in the liver, spleen and kidneys and administered activity was predominantly eliminated through physical decay. In addition, uptake in lungs, colon, bone marrow and bucco-pharyringeal mucosa was noticed. Uptake pattern may be explained by the renal excretion of the tracer and the specific binding of ^{99m}Tc-depreotide to SSTR2-expressing cells of the human immune system, such as monocytes, T- and B-lymphocytes, and to SSTR3-expressing cells of spleen, liver and intestinal mucosa [36,14]. Of interest, tracer uptake in metastatic bone lesions augmented up to 2-4 hours and remained stable without biological clearance. As opposed to ^{99m}Tc-depreotide, [^{111}In-DTPA-D-Phe]-octreotide exhibits different biodistribution and excretion patterns, resulting in absence of uptake in bone marrow, much lower uptake in liver and mainly excretion via kidneys with minor hepatic accumulation and minute hepatobiliary excretion [37]. Part of these differences may be attributed to the different affinity profiles of both tracers, respective a high affinity for SSTR2 and SSTR5 (SSTR2 K_d = 1.5 nM, SSTR3 K_d = 15 nM and SSTR5 K_d =0.5 nM) of [^{111}In-DTPA-D-Phe]-octreotide, whereas ^{99m}Tc-depreotide exhibits additional high affinity for SSTR3 (SSTR2 K_d = 2.5 nM,

SSTR3 K_d = 1.5 nM and SSTR5 K_d = 2nM) [33]. The latter feature may entail an additional benefit since breast tumours express SSTR3 besides SSTR2, albeit to a lesser extent, and SSTR3 expression is also positively regulated by E_2 [38]. The mean effective dose for ^{99m}Tc-depreotide was 6.4-8.5 mSv, which is substantially lower than that for [^{111}In-DTPA-D-Phe]-octreotide (8-16 mSv).

Bone is the most common site of metastatic breast cancer and bone scintigraphy is a sensitive but aspecific technique for evaluation of various bone pathologies. In chapter 5 we compared the diagnostic accuracy of planar ^{99m}Tc-depreotide scintigraphy with planar ^{99m}Tc-methylendiphosphonate (MDP) bone scintigraphy for evaluating bone metastasis in a small series of breast cancer patients. Regarding diagnostic accuracy on a patient basis, bone scan proved superior (75% versus 83.3%) due to its higher sensitivity (100% versus 62.5%), whereas specificity was significantly higher on NeoSpect scan (100% versus 50%). In fact depreotide binds specifically to SSTR2, 3 and 5 that are over expressed in 50-80% of breast tumours. In contrast, ^{99m}Tc-MDP accumulates aspecifically in any skeletal location with an elevated rate of bone turnover such as arthropathy, leading to false-positive diagnoses of bony metastasis. Seventy-four percent of missed individual lesions in patients with positive depreotide scan were probably due to masking by organs with high physiological tracer uptake (thyroid, liver, spleen, intestines). SPECT imaging, a tomographical technique that provides cross-sectional images of tracer distribution and thus has the ability to remove overlying structures which may obscure abnormal tracer uptake, can overcome similar problems. An additional explanation for the lack of sensitivity of ^{99m}Tc-depreotide in detecting individual lesions lies in the heterogeneous distribution of SSTR expression in breast tumours. The latter often display SSTR only in certain tumour regions, although the whole tumour appears to be histopathologically homogenous [39]. This observation supports the idea that some breast tumours are composed of numerous different clones with different biological properties. As a consequence metastatic lesions originating from a SSTR-negative clone may be SSTR-negative nevertheless the primary tumour is SSTR-positive.

Since SSTR2 is the dominant SSTR subtype in breast cancer, we hypothesized, in analogy with the in vitro findings, that efficient treatment of metastasized breast cancer patients by means of antioestrogens or aromatase inhibitors may result in downregulation of SSTR at the cell surface level, which could be visualized in vivo using sequential somatostatin receptor scintigraphy. In chapter 6 we evaluated the potential of sequential ^{99m}Tc-depreotide scintigraphy to select patients likely to respond to endocrine therapy. In our study, all patients with hormone-sensitive tumours had positive scans. This could be expected

since E_2 stimulation of functional ER enhances SSTR2 gene transcription and hence SSTR2 expression at the cell surface, which is visualized by ^{99m}Tc-depreotide scintigraphy. In this group of responders, tracer uptake on the posttherapy scan tended to be lower compared to the pretherapy scan and, considering a cut-off of 25%, uptake significantly decreased or remained stable. According to our hypothesis, this decrease could be interpreted as a downregulation of SSTR2 at the cell surface level caused by an efficient block of the functional ER that inhibits further transcription of the SSTR2. Unfortunately, for availability reasons, binding of radioligand to breast tumour cells per se could not be confirmed using autoradiography. Therefore, binding of ^{99m}Tc-depreotide to other kinds of cells expressing SSTR2, 3 or 5, such as activated lymphocytes (SSTR2), cannot be excluded [(40)]. The presence of tumour infiltrating lymphocytes (TILs) has been associated with therapy response and good prognosis, however controversy exists [(41,42)]. Equivalent uptake on both sequential scans could be interpreted as absence of active stimulation of ER and subsequently absence of SSTR2 transcription. Possibly, intratumoural levels of antioestrogen could have only just or not yet achieved steady state and balance between receptor synthesis and endocytosis/degradation has not yet turned in favour of degradation. Three patients of the group of responders had acquired resistance to tamoxifen and had positive ^{99m}Tc-depreotide scans before they switched to a second-line aromatase inhibitor. This is in agreement with considerable amount of data indicating that ER in acquired resistant breast cancer commonly remains functional and moreover pivotal to the growth regulation and gene expression profile of breast tumours on their relapse, despite the presence of tamoxifen [(43)]. Following their inhibition by tamoxifen during initial responsive phase of the disease, oestrogen-regulated genes can be re-expressed on disease relapse. Clinical experience has shown that hormonal resistance is often reversible, suggesting a cellular adaptation, rather than genetic alterations in many breast cancer patients [(44)]. Changes in local metabolism and more in particular reduced concentrations of tamoxifen and its metabolites are reported in tamoxifen-resistant tumours [(45)]. Accordingly, efflux of tamoxifen out of the tumour cell in the presence of a functional ER results in a tamoxifen resistant tumour, expressing oestrogen-regulated genes (eg, SSTR2), sensitive to aromatase inhibitors. Besides prediction of the likelihood of response to second-line hormonal treatment such as aromatase inhibitors requiring a functional ER, this could allow for prediction of early resistance to tamoxifen treatment. All negative ^{99m}Tc-depreotide scans belonged to patients with tumours resistant to hormonal therapy. This was in line with expectations since we anticipated a nonfunctional ER, not capable of stimulating transcription and expression of SSTR2. Loss of ER is generally not a feature of acquired endocrine

resistance either in vitro or in vivo, hence repeated hormone receptor assessment using routine techniques (LBA, IHC) for determination of endocrine-responsiveness would be inadequate [46]. Three patients (30%) of the group of nonresponders had positive ^{99m}Tc-depreotide scintigraphies. This suggests a ligand-independent stimulation of ER and oestrogen-independent regulation of SSTR2 expression. Constitutively active ER variants might contribute to a tamoxifen resistance breast tumour with similar characteristics, however mutations are extremely rare in vivo and thus refer only to a minority of cases [47]. Even in tumours that are oestrogen-dependent, it is likely that an appropriate growth factor environment is necessary for efficient mitogenesis, with steroid hormone and growth factor signalling pathways "cross talking" to reinforce each others' signalling [48,49,50]. Overexpression of a growth factor (EGF, epidermal growth factor; TGFα, transforming growth factor α; IGF-1, insulin-like growth factor 1) or its receptor (EGFR, HER2/Neu, IGF-1R) may perturb this balance of steroid hormone and growth factor interaction, providing a selective advantage for tumour cell proliferation despite hormone therapy. As such, several kinases, which are themselves activated by membrane growth factor receptors, phosphorylate ER at sites that influence its biological activity. On the posttherapy scan tracer uptake was increased in these patients, suggesting an upregulation of SSTR2 expression as a result of continuous or enhanced stimulation of SSTR2 transcription. However in vitro data in human breast cancer cells attribute this increase predominantly to an enhanced recycling of the receptor rather than an increased synthesis [51]. Several postreceptor alterations, including changes in coregulators or cAMP and phosphorylation pathways, known to affect transcriptional activity of ER and to enhance the agonistic activity of tamoxifen-like antioestrogens could explain an increase in SSTR2 expression [52]. However, in these 3 patients endocrine treatment with an aromatase inhibitor was initiated. Presumably regulation of SSTR expression in breast tumour cells is not exclusively oestrogen-dependent and is influenced by a series of other mediators, as is the case in normal tissue (e.g., pancreas, hypothalamus) [14]. Growth factors and cytokines secreted by tumour cells or adjacent host cells may modify SSTR expression in an autocrine or paracrine manner. A series of radiopharmaceuticals have been developed to specifically investigate these agents [53,54]. Interestingly, the cytokines IL-6 (interleukin 6) and TNF-α (tumor necrosis factor α) that stimulate activity of aromatase, the enzyme that catalyses conversion from androgen to oestrogen in tumour cells, also enhance SSTR expression [55,56]. These cytokines are secreted by tumour associated lymphocytes and other adjacent host cells (e.g., adipocytes) in response to the tumour cells themselves. Upon administration of an aromatase inhibitor, absence of

positive feedback could supposedly result in an abundance of the cytokines and augmentation of SSTR at the cell surface. However, regulation of SSTR by IL-6 or TNF-α has not yet been described in human breast cancer cells. Furthermore, SSTR expression is inhibited by growth-inhibitory factor TGF-β (transforming growth factor β) present in breast tumour cells [57]. Several studies have demonstrated increases in plasma and tumour levels of TGF-β in patients following initial exposure to tamoxifen therapy mirroring effective tamoxifen response [58,59,60,61]. In addition, IGF signalling by growth factors IGF-1 and more importantly IGF-2 is likely to play a crucial role in pathogenesis of steroid hormone-dependent disease and many ER-positive breast carcinomas express high levels of the respective receptor IGF-1R [62,63]. Tamoxifen treatment substantially reduces IGF signalling partly through a decrease in levels of IGF-1 and IGF-2, both also known to stimulate SSTR expression [64,14,65,66]. These mechanisms could play a complementary or alternative role in the decrease in SSTR2 expression and ^{99m}Tc-depreotide binding in the responders in our study. Moreover, a high expression of IGF signalling elements and paradoxically high TGF-β production have been reported in tamoxifen-resistant tumours, which could potentially contribute to the SSTR-positive respectively SSTR-negative phenotype of nonresponders [67,63].

FUTURE PROSPECTS

We found a consistent relationship between ^{99m}Tc-depreotide uptake and response to endocrine treatment in metastasized breast cancer patients. Underlying mechanism is suggested to be an ER-mediated regulation of SSTR2 expression but additional influence by a series of cytokines and/or growth factors present in the tumoural environment is to be expected. Nevertheless, if a larger scale study confirms these findings, this could entail a powerful tool to accurately evaluate endocrine-responsiveness. A protocol with somatostatin receptor scintigraphy before initiation of endocrine treatment and repetition of the scan if positive could be proposed.

Realistic goals for treatment of metastatic breast cancer are palliation of symptoms and prolongation of survival with maximizing the quality of life. In general, significant palliation is more likely for a patient who experiences a response to endocrine therapy compared to a similar response induced by chemotherapy, due to a lower toxicity profile. A delay in effective therapy may lead to a decline in performance status and organ function, and as such reduce the likelihood of a subsequent response. Using clinical follow-up and conventional morphological imaging modalities using volumetric changes easily 3 to 6 months are needed for response evaluation. The proposed protocol would allow for separation of responders and nonresponders immediately (negative pretherapy scan) or as early as 3 weeks after treatment initiation (positive pretherapy scan).

REFERENCES

1. McGuire WL: Current status of estrogen receptors in human breast cancer. Cancer 36: 638-644, 1975

2. McGuire WL, Horwitz KB, Pearson OH, et al: Current status of estrogen and progesterone receptors in breast cancer. Cancer 39: 2934-2947, 1977

3. Steroid receptors in breast cancer: an NIH Consensus Development Conference, Bethesda, Maryland, June 27-29, 1979. Cancer 46: 2759-2963, 15-12-1980

4. Holdaway IM and Bowditch JV: Variation in receptor status between primary and metastatic breast cancer. Cancer 52: 479-485, 1-8-1983

5. Kuukasjarvi T, Kononen J, Helin H, et al: Loss of estrogen receptor in recurrent breast cancer is associated with poor response to endocrine therapy. J Clin Oncol 14: 2584-2589, 1996

6. Franco A, Col N, and Chlebowski R: Discordance in estrogen (ER) and progestin receptor (PR) status between primary metastatic breast cancer: a meta-analysis. Proc Am Soc Clin Oncol 23: 2004

7. Fidler IJ and Hart IR: Biological diversity in metastatic neoplasms: origins and implications. Science 217: 998-1003, 10-9-1982

8. Heppner GH: Tumor heterogeneity. Cancer Res 44: 2259-2265, 1984

9. Bloom ND, Tobin EH, Schreibman B, et al: The role of progesterone receptors in the management of advanced breast cancer. Cancer 45: 2992-2997, 15-6-1980

10. Bernoux A, de Cremoux P, Laine-Bidron C, et al: Estrogen receptor negative and progesterone receptor positive primary breast cancer: pathological characteristics and clinical outcome. Institut Curie Breast Cancer Study Group. Breast Cancer Res Treat 49: 219-225, 1998

11. Nardelli GB, Lamaina V, and Siliotti F: Estrogen and progesterone receptors status in the prediction of response of breast cancer to endocrine therapy (preliminary report). Eur J Gynaecol Oncol 7: 151-158, 1986

12. Xu Y, Song J, Berelowitz M, et al: Estrogen regulates somatostatin receptor subtype 2 messenger ribonucleic acid expression in human breast cancer cells. Endocrinology 137: 5634-5640, 1996

13. Hukovic N, Panetta R, Kumar U, et al: Agonist-dependent regulation of cloned human somatostatin receptor types 1-5 (hSSTR1-5): subtype selective internalization or upregulation. Endocrinology 137: 4046-4049, 1996

14. Patel YC: Somatostatin and its receptor family. Front Neuroendocrinol 20: 157-198, 1999

15. Reisine T and Bell GI: Molecular biology of somatostatin receptors. Endocr Rev 16: 427-442, 1995

16. Fisher WE, Doran TA, Muscarella P, et al: Expression of somatostatin receptor subtype 1-5 genes in human pancreatic cancer. J Natl Cancer Inst 90: 322-324, 18-2-1998

17. Schaer JC, Waser B, Mengod G, et al: Somatostatin receptor subtypes sst1, sst2, sst3 and sst5 expression in human pituitary, gastroentero-pancreatic and mammary tumors: comparison of mRNA analysis with receptor autoradiography. Int J Cancer 70: 530-537, 4-3-1997

18. Reubi JC, Waser B, Liu Q, et al: Subcellular distribution of somatostatin sst2A receptors in human tumors of the nervous and neuroendocrine systems: membranous versus intracellular location. J Clin Endocrinol Metab 85: 3882-3891, 2000

19. Xu Y, Berelowitz M, and Bruno JF: Characterization of the promoter region of the human somatostatin receptor subtype 2 gene and localization of sequences required for estrogen-responsiveness. Mol Cell Endocrinol 139: 71-77, 30-4-1998

20. Van de Wiele C, De Vos F, Slegers G, et al: Radiolabeled estradiol derivatives to predict response to hormonal treatment in breast cancer: a review. Eur J Nucl Med 27: 1421-1433, 2000

21. Van Den Bossche B and Van de Wiele C: Receptor imaging in oncology by means of nuclear medicine: current status. J Clin Oncol 22: 3593-3607, 1-9-2004

22. Van de Wiele C, De Vos F, Slegers G, et al: Radiolabeled estradiol derivatives to predict response to hormonal treatment in breast cancer: a review. Eur J Nucl Med 27: 1421-1433, 2000

23. Van Den Bossche B and Van de Wiele C: Receptor imaging in oncology by means of nuclear medicine: current status. J Clin Oncol 22: 3593-3607, 1-9-2004

24. Reed MJ, Aherne GW, Ghilchik MW, et al: Concentrations of oestrone and 4-hydroxyandrostenedione in malignant and normal breast tissues. Int J Cancer 49: 562-565, 21-10-1991

25. Yue W, Santner SJ, Masamura S, et al: Determinants of tissue estradiol levels and biologic responsiveness in breast tumors. Breast Cancer Res Treat 49 Suppl 1: S1-S7, 1998

26. Bennink RJ, van Tienhoven G, Rijks LJ, et al: In vivo prediction of response to antiestrogen treatment in estrogen receptor-positive breast cancer. J Nucl Med 45: 1-7, 2004

27. Mortimer JE, Dehdashti F, Siegel BA, et al: Metabolic flare: indicator of hormone responsiveness in advanced breast cancer. J Clin Oncol 19: 2797-2803, 1-6-2001

28. Inoue T, Kim EE, Wallace S, et al: Positron emission tomography using [18F]fluorotamoxifen to evaluate therapeutic responses in patients with breast cancer: preliminary study. Cancer Biother Radiopharm 11: 235-245, 1996

29. Van de Wiele C, Cocquyt V, VandenBroecke R, et al: Iodine-labeled tamoxifen uptake in primary human breast carcinoma. J Nucl Med 42: 1818-1820, 2001

30. Katzenellenbogen JA: Designing steroid receptor-based radiotracers to image breast and prostate tumors. J Nucl Med 36: 8S-13S, 1995

31. Rijks LJ, van den Bos JC, van Doremalen PA, et al: New iodinated progestins as potential ligands for progesterone receptor imaging in breast cancer. Part 2: In vivo pharmacological characterization. Nucl Med Biol 25: 791-798, 1998

32. van den Bos JC, Rijks LJ, van Doremalen PA, et al: New iodinated progestins as potential ligands for progesterone receptor imaging in breast cancer. Part 1: Synthesis and in vitro pharmacological characterization. Nucl Med Biol 25: 781-789, 1998

33. Virgolini I, Leimer M, Handmaker H, et al: Somatostatin receptor subtype specificity and in vivo binding of a novel tumor tracer, 99mTc-P829. Cancer Res 58: 1850-1859, 1-5-1998

34. Lister-James J, Pearson D, De Rosch M, et al: Tc-99m P829: characterization of a technetium-99-labeled somatostatin receptor-binding peptide. Technetium, Rhenium and Other Metals in Chemistry and Nuclear Medicine 473-478, 1999

35. Vallabhajosula S, Moyer BR, Lister-James J, et al: Preclinical evaluation of technetium-99m-labeled somatostatin receptor-binding peptides. J Nucl Med 37: 1016-1022, 1996

36. Reubi JC, Waser B, Schaer JC, et al: Somatostatin receptor sst1-sst5 expression in normal and neoplastic human tissues using receptor autoradiography with subtype-selective ligands. Eur J Nucl Med 28: 836-846, 2001

37. Krenning EP, Kwekkeboom DJ, Bakker WH, et al: Somatostatin receptor scintigraphy with [111In-DTPA-D-Phe1]- and [123I-Tyr3]-octreotide: the Rotterdam experience with more than 1000 patients. Eur J Nucl Med 20: 716-731, 1993

38. Visser-Wisselaar HA, Van Uffelen CJ, van Koetsveld PM, et al: 17-beta-estradiol-dependent regulation of somatostatin receptor subtype expression in the 7315b prolactin secreting rat pituitary tumor in vitro and in vivo. Endocrinology 138: 1180-1189, 1997

39. Reubi JC, Waser B, Foekens JA, et al: Somatostatin receptor incidence and distribution in breast cancer using receptor autoradiography: relationship to EGF receptors. Int J Cancer 46: 416-420, 15-9-1990

40. Elliott DE, Li J, Blum AM, et al: SSTR2A is the dominant somatostatin receptor subtype expressed by inflammatory cells, is widely expressed and directly regulates T cell IFN-gamma release. Eur J Immunol 29: 2454-2463, 1999

41. Marrogi AJ, Munshi A, Merogi AJ, et al: Study of tumor infiltrating lymphocytes and transforming growth factor-beta as prognostic factors in breast carcinoma. Int J Cancer 74: 492-501, 21-10-1997

42. Georgiannos SN, Renaut A, Goode AW, et al: The immunophenotype and activation status of the lymphocytic infiltrate in human breast cancers, the role of the major histocompatibility complex in cell-mediated immune mechanisms, and their association with prognostic indicators. Surgery 134: 827-834, 2003

43. Johnston SR, Lu B, Dowsett M, et al: Comparison of estrogen receptor DNA binding in untreated and acquired antiestrogen-resistant human breast tumors. Cancer Res 57: 3723-3727, 1-9-1997

44. Stoll BA: Rechallenging breast cancer with tamoxifen therapy. Clin Oncol 9: 347-351, 1983

45. Osborne CK, Wiebe VJ, McGuire WL, et al: Tamoxifen and the isomers of 4-hydroxytamoxifen in tamoxifen-resistant tumors from breast cancer patients. J Clin Oncol 10: 304-310, 1992

46. Robertson JF: Oestrogen receptor: a stable phenotype in breast cancer. Br J Cancer 73: 5-12, 1996

47. Fuqua SA and Wolf DM: Molecular aspects of estrogen receptor variants in breast cancer. Breast Cancer Res Treat 35: 233-241, 1995

48. Nicholson RI and Gee JM: Oestrogen and growth factor cross-talk and endocrine insensitivity and acquired resistance in breast cancer. Br J Cancer 82: 501-513, 2000

49. Shou J, Massarweh S, Osborne CK, et al: Mechanisms of tamoxifen resistance: increased estrogen receptor-HER2/neu cross-talk in ER/HER2-positive breast cancer. J Natl Cancer Inst 96: 926-935, 16-6-2004

50. Nicholson RI, McClelland RA, Robertson JF, et al: Involvement of steroid hormone and growth factor cross-talk in endocrine response in breast cancer. Endocr Relat Cancer 6: 373-387, 1999

51. Van Den Bossche B, D'haeninck E, De Vos F, et al: Oestrogen-mediated regulation of somatostatin receptor expression in human breast cancer cell lines assessed with 99mTc-depreotide. Eur J Nucl Med Mol Imaging 31: 1022-1030, 2004

52. Fujimoto N and Katzenellenbogen BS: Alteration in the agonist/antagonist balance of antiestrogens by activation of protein kinase A signaling pathways in breast cancer cells: antiestrogen selectivity and promoter dependence. Mol Endocrinol 8: 296-304, 1994

53. Signore A, Capriotti G, Scopinaro F, et al: Radiolabelled lymphokines and growth factors for in vivo imaging of inflammation, infection and cancer. Trends Immunol 24: 395-402, 2003

54. Signore A, Chianelli M, Bei R, et al: Targeting cytokine/chemokine receptors: a challenge for molecular nuclear medicine. Eur J Nucl Med Mol Imaging 30: 801-802, 2003

55. Reed MJ and Purohit A: Breast cancer and the role of cytokines in regulating estrogen synthesis: an emerging hypothesis. Endocr Rev 18: 701-715, 1997

56. Scarborough DE, Lee SL, Dinarello CA, et al: Interleukin-1 beta stimulates somatostatin biosynthesis in primary cultures of fetal rat brain. Endocrinology 124: 549-551, 1989

57. Quintela M, Senaris RM, and Dieguez C: Transforming growth factor-betas inhibit somatostatin messenger ribonucleic acid levels and somatostatin secretion in hypothalamic cells in culture. Endocrinology 138: 4401-4409, 1997

58. Knabbe C, Kopp A, Hilgers W, et al: Regulation and role of TGF beta production in breast cancer. Ann N Y Acad Sci 784: 263-276, 30-4-1996

59. Kopp A, Jonat W, Schmahl M, et al: Transforming growth factor beta 2 (TGF-beta 2) levels in plasma of patients with metastatic breast cancer treated with tamoxifen. Cancer Res 55: 4512-4515, 15-10-1995

60. Butta A, MacLennan K, Flanders KC, et al: Induction of transforming growth factor beta 1 in human breast cancer in vivo following tamoxifen treatment. Cancer Res 52: 4261-4264, 1-8-1992

61. MacCallum J, Keen JC, Bartlett JM, et al: Changes in expression of transforming growth factor beta mRNA isoforms in patients undergoing tamoxifen therapy. Br J Cancer 74: 474-478, 1996

62. Surmacz E: Function of the IGF-I receptor in breast cancer. J Mammary Gland Biol Neoplasia 5: 95-105, 2000

63. Gee JM, Madden T-A, Robertson J, et al: Clinical response and resistance to SERMs 155-189, 2002

64. Guvakova MA and Surmacz E: Tamoxifen interferes with the insulin-like growth factor I receptor (IGF-IR) signaling pathway in breast cancer cells. Cancer Res 57: 2606-2610, 1-7-1997

65. Helle SI and Lonning PE: Insulin-like growth factors in breast cancer. Acta Oncol 35 Suppl 5: 19-22, 1996

66. Helle SI, Anker GB, Tally M, et al: Influence of droloxifene on plasma levels of insulin-like growth factor (IGF)-I, Pro-IGF-IIE, insulin-like growth factor binding protein (IGFBP)-1 and IGFBP-3 in breast cancer patients. J Steroid Biochem Mol Biol 57: 167-171, 1996

67. Herman ME and Katzenellenbogen BS: Alterations in transforming growth factor-alpha and -beta production and cell responsiveness during the progression of MCF-7 human breast cancer cells to estrogen-autonomous growth. Cancer Res 54: 5867-5874, 15-11-1994

CHAPTER EIGHT

SUMMARY

Endocrine therapy achieves good results with minimal toxicity and therefore remains one of primary treatment options for the majority of patients with metastatic breast cancer. Since only about one third of patients initially respond, there is a need for patient selection. So far, the only predictive factor approved for clinical routine use is the in vitro assessment of hormone receptor status on tissue samples by ligand binding assay (LBA) or immunohistochemistry (IHC). Still only 50%-60% of patients with oestrogen receptor (ER)-positive tumours exhibit response to hormonal therapy. A possible explanation for lack of response to endocrine treatment in ER-positive disease is nonfunctioning of the ER. Assessment of an endproduct of ER stimulation, such as progesteron receptor, could by-pass this problem and has proven to increase predictive accuracy. Experimental data in human breast cancer cell lines, based on mRNA expression, suggest that the somatostatin receptor (SSTR) is another oestrogen-regulated gene. This thesis elucidates the role of oestrogen in SSTR expression and explores the potential of the visualization of this molecular event by means of nuclear medicine techniques for selection of breast cancer patients likely to respond to endocrine treatment.

Scintigraphy is the imaging technique of choice since it is noninvasive and offers the advantage of repetitive whole body evaluation. Furthermore, it has the ability to address the intrinsic heterogeneity of tumoural receptor expression without tissue manipulation and provides an in vivo image of all disease sites at the moment of treatment need. In chapter 2 we amplify on receptor imaging by means of nuclear medicine in oncology. In breast cancer in particular, many efforts have been put into synthesis and evaluation of radiopharmaceuticals of which tumoural uptake is believed to relate to ER expression and hence endocrine responsiveness.

In chapter 3 we demonstrated oestrogen-mediated SSTR expression in 2 endocrine-responsive ER-positive human breast cancer cell lines (T47D and ZR75-1) but not in endocrine-unresponsive ER-negative MDA MB231 cells. Physiological concentrations of oestradiol (E_2) resulted in a statistically significant increase of the number of SSTRs at the level of the cell membrane of T47D cells but not in ZR75-1 and MDA MB231 cells as evidenced by binding assays. Given the minor increase in SSTR2 protein levels as evidenced by western blotting for the T47D cell line, this phenomenon is likely attributable to a predominant recycling of receptors from inner towards the outer cell membrane. The E_2-effect was reduced or inhibited by the antioestrogens tamoxifen and ICI 182 780 (fulvestrant),

indicating a requirement for E_2 binding and stimulation of the ER suggestive of an exclusively E_2-dependent regulation of SSTR2 expression. In analogy with the in vitro findings, we hypothesized that efficient antioestrogen treatment of metastasized breast cancer patients may result in downregulation of SSTR at the cell surface level, which could be visualized in vivo using sequential somatostatin receptor scintigraphy.

For SSTR imaging, we chose to work with depreotide (P829 - NeoSpect®/NeoTect®), a ^{99m}Tc-labelled somatostatin analogue with high affinity for SSTR2, 3 and 5. In chapter 4 we studied the biodistribution and dosimetry study of ^{99m}Tc-depreotide in breast cancer patients. Most of the activity was observed in the liver, spleen and kidneys and administered activity was predominantly eliminated through physical decay. In addition, uptake in lungs, colon, bone marrow and bucco-pharingeal mucosa was noticed. The mean effective dose for ^{99m}Tc-depreotide was 6.4-8.5 mSv, which is substantially lower than that for [^{111}In-DTPA-D-Phe]-octreotide (8-16 mSv), the tracer routinely used for imaging of SSTR-positive tumours.

In chapter 5 we compared the diagnostic accuracy of planar ^{99m}Tc-depreotide scintigraphy with planar ^{99m}Tc-methylendiphosphonate (MDP) bone scintigraphy for evaluating bone metastasis in a small series of breast cancer patients. Bone scan proved superior (75% versus 83.3%) due to its higher sensitivity (100% versus 62.5%), whereas specificity was significantly higher on NeoSpect scan (100% versus 50%). In fact, depreotide binds specifically to SSTR2, 3 and 5 that are over expressed in 50-80% of breast tumours. In contrast, ^{99m}Tc-MDP accumulates aspecifically in any skeletal location with an elevated rate of bone turnover such as arthropathy, leading to false-positive diagnoses of bony metastasis.

We evaluated the potential of sequential ^{99m}Tc-depreotide scintigraphy to select patients likely to respond to endocrine therapy in chapter 6. In our study, all patients with hormone-sensitive tumours had positive scans. Tracer uptake on the posttherapy scan, acquired 3 weeks after treatment initiation, tended to be lower compared to the pretherapy scan and, considering a cut-off of 25%, uptake significantly decreased or remained stable. All negative ^{99m}Tc-depreotide scans belonged to patients with tumours resistant to hormonal therapy. Three patients (30%) of the group of nonresponders had positive ^{99m}Tc-depreotide scintigraphies and increase of tracer uptake on the posttherapy scan.

We found a consistent relationship between ^{99m}Tc-depreotide uptake and response to endocrine treatment in metastasized breast cancer patients. Underlying mechanism is suggested to be an ER-mediated regulation of SSTR2 expression but additional influence by a series of cytokines and/or growth factors present in the tumoural environment is to be expected. Nevertheless, if a larger scale study confirms these findings, this could entail a

powerful tool to accurately evaluate endocrine responsiveness. A protocol with somatostatin receptor scintigraphy before initiation of endocrine treatment and repetition of the scan if positive could be proposed. The latter would allow for separation of responders and nonresponders immediately (negative pretherapy scan) or as early as 3 weeks after treatment initiation (positive pretherapy scan).

SAMENVATTING

Hormonale therapie levert goede resultaten met een minimum aan toxiciteit en blijft daarom een van de belangrijkste behandelingsopties voor het merendeel van de patiënten met gemetastaseerd borstkanker. Maar aangezien enkel een derde van hen initieel reageert op deze therapie, moeten patiënten zorgvuldig gescreend worden. Tot op heden is de enige 'voorspellende' factor die goedgekeurd is voor klinisch routineus gebruik de bepaling van de hormoon-receptor status in vitro op stukjes weefsel door middel van bindingsproef of immunohistochemie. Maar ook van de patiënten met oestrogeenreceptor (ER)-positieve tumoren reageert slechts 50% - 60% positief op hormonale therapie. Een mogelijke verklaring voor dit uitblijven van effect is een niet-functionerende ER. De bepaling van een eindproduct van ER-stimulatie, zoals de progesteron receptor, zou dit probleem kunnen omzeilen en heeft reeds bewezen de predicatieve accuraatheid te verhogen. Data bekomen uit experimenten met humane borstkanker cellijnen gebaseerd op mRNA expressie doen vermoeden dat de somatostatine receptor (SSTR) eveneens een gen is waarvan de expressie door oestrogenen geregeld wordt.

In deze thesis wordt de rol van oestrogenen in de expressie van SSTR verder opgehelderd en wordt het vermogen onderzocht dit moleculair gebeuren in beeld te brengen door middel van technieken uit de nucleaire geneeskunde, met de bedoeling borstkanker patiënten te selecteren die hoogstwaarschijnlijk zullen beantwoorden aan endocriene therapie.

We kozen voor scintigrafie als beeldvormende techniek omdat deze niet invasief is en het voordeel biedt het hele lichaam repetitief te kunnen evalueren. Bovendien brengt het de intrinsieke heterogeniteit van de tumorale receptor-expressie in kaart zonder weefsel-manipulatie en verschaft het in vivo beelden van alle ziektehaarden op het ogenblik dat er nood is aan behandeling. In hoofdstuk 2 weidden we uit over receptor beeldvorming in de oncologie door middel van technieken uit de nucleaire geneeskunde. Wat betreft borstkanker in het bijzonder, werden veel inspanningen geleverd voor de synthese en evaluatie van radiopharmaca waarvan men vermoedt dat de opname in de tumor gerelateerd is aan de ER expressie en dus aan hormoongevoeligheid.

In hoofdstuk 3 toonden we aan dat expressie van SSTR door oestrogenen bemiddeld wordt in 2 hormoongevoelige, ER-positieve, humane borstkankercellijnen (T47D en ZR75-1) maar niet in hormoononGevoelige, ER-negatieve, MDA MB231 cellen. Uit bindingsproeven bleek dat fysiologische concentraties van oestradiol (E_2) resulteerden in een statistisch significante stijging van het aantal SSTRs ter hoogte van het celmembraan van T47D cellen

maar niet in ZR75-1 en MDA MB231 cellen. Aangezien Western blot slechts een minimale stijging aantoonde van SSTR2 proteïne in T47D cellen, is dit fenomeen waarschijnlijk voornamelijk te wijten aan het recycleren van receptoren van in de cel naar buiten op het celmembraan. Het E_2-effect werd gereduceerd of verhinderd door de antioestrogenen tamoxifen of ICI 182 780 (fulvestrant), wat erop wijst dat binding van E_2 en stimulatie van ER vereist zijn, en dit doet een exclusieve E_2-afhankelijke regulatie van SSTR expressie vermoeden. Naar analogie met de in vitro bevindingen, hebben we als hypothese gesteld dat een efficiënte hormonale behandeling van patiënten met gemetastaseerd borstkanker aanleiding kan geven tot een daling van SSTRs ter hoogte van het celmembraan. Dit zou dan in vivo in beeld kunnen gebracht worden door sequentiële somatostatine receptor scintigrafie.

Voor de beeldvorming van SSTR verkozen we te werken met depreotide (P829 - NeoSpect®/NeoTect®), een technetium (^{99m}Tc)-gemerkt somatostatine analoog met hoge affiniteit voor SSTR2, 3 en 5. In hoofdstuk 4 bestudeerden we de biodistributie en dosimetrie van ^{99m}Tc-depreotide in borstkanker patiënten. We troffen de meeste radioactiviteit aan in de lever, milt en nieren, en de toegediende radioactiviteit werd hoofdzakelijk geëlimineerd via fysisch verval. Bijkomend werd opname opgemerkt in longen, colon, beenmerg en mucosa van bucco-farynx. De gemiddelde effectieve dosis voor ^{99m}Tc-depreotide was 6.4-8.5mSv, wat substantieel lager is dan voor [^{111}In-DTPA-D-Phe]-octreotide (8-16mSv), de radioligand die routineus gebruikt wordt voor beeldvorming van SSTR-positieve tumoren.

In hoofdstuk 5 vergeleken we de diagnostische accuraatheid van planaire ^{99m}Tc-depreotide scintigrafie met planaire ^{99m}Tc-methyleendifosfonaat (MDP) bot scintigrafie voor de evaluatie van botmetastasen in een kleine reeks van borstkanker patiënten. Botscan bewees beter te zijn (75% versus 83.3%) wegens zijn hogere sensitiviteit (100% versus 62.5%). Daarentegen was de specificiteit van de NeoSpect® scan significant hoger (100% versus 50%). Depreotide bindt namelijk specifiek op SSTR2, 3 en 5 die tot overexpressie komen in 50-80% van de borst tumoren. In tegenstelling daarmee accumuleert ^{99m}Tc-MDP aspecifiek in elke plaats van het skelet met een verhoogde bot-turnover, zoals bij arthropatie, wat aanleiding geeft tot een vals-positieve diagnose van botmetastasen.

We evalueerden het potentieel van sequentiële ^{99m}Tc-depreotide scintigrafie voor de selectie van patiënten die waarschijnlijk zouden beantwoorden aan hormonale therapie in hoofdstuk 6. In onze studie hadden alle patiënten met hormoongevoelige tumoren een positieve scan. Opname van de radioligand op posttherapie scan, opgenomen 3 weken na start van de behandeling, was over het algemeen lager dan op de pretherapie scan en, een cut-off

van 25% in acht nemend, daalde de opname of bleef ze stabiel. Alle negatieve ^{99m}Tc-depreotide scans behoorden bij patiënten met tumoren die resistent waren tegen hormonale therapie. Drie patiënten (30%) van de groep die niet reageerde op de behandeling hadden een positieve ^{99m}Tc-depreotide scintigrafie en stijging van opname van de radioligand op de posttherapie scan.

We vonden een consistent verband tussen opname van ^{99m}Tc-depreotide en het beantwoorden aan hormonale behandeling bij patiënten met gemetastaseerd borstkanker. Het onderliggend mechanisme wordt verondersteld de regulatie van de SSTR expressie via ER te zijn, maar een reeks cytokines en/of groeifactoren aanwezig in de omgeving van de tumor kunnen een bijkomende invloed uitoefenen. Hoe dan ook, indien een studie op grotere schaal deze bevindingen bevestigt, zou deze methode een krachtig middel kunnen bieden om de hormoongevoeligheid van borsttumoren meer accuraat te evalueren. Een protocol bestaand uit het maken van een somatostine receptor scintigrafie vóór de start van een hormonale behandeling en een herhaling van de scan, indien positief, zou kunnen voorgesteld worden. Dit zou toelaten een onderscheid te maken tussen patiënten waarvoor al dan niet een effect van hormonale behandeling kan verwacht worden, en dit zou ofwel onmiddellijk kunnen gebeuren (in geval van negatieve pretherapie scan) ofwel 3 weken na start van de behandeling (in geval van positieve pretherapie scan).

RESUME

La thérapie hormonale assure de bons résultats avec un minimum de toxicité et reste un traitement de choix privilégié pour la plupart des patientes atteintes d'un cancer du sein metastasé. Mais du fait que un tiers seulement des patientes réagit dès l'abord à cette thérapie, il est nécessaire d'effectuer une sélection des patientes avec grand soin. Présentement, le seul indice à valeur prédictive homologué en utilisation clinique de routine est le degré d'affinité hormone-récepteur mesuré in vitro dans un tissu prélevé au moyen d'étude des liaison ligand ou d'immunohistochimie. Mais du nombre de patientes ayant une tumeur exprimant le récepteur d'oestrogènes (RO), 50% à 60 % seulement réagissent positivement à la thérapie hormonale. Une explication possible à l'absence de résultat semble être le non-fonctionnement du RO. La quantification de la substance produite lors de la stimulation RO, comme le récepteur de progesterone, pourrait contourner cette difficulté et a déjà prouvé augmenter la précision prédicative. Des résultats déjà obtenus sur base de l'expression de ARNm dans des lignées cancéreuses humaines (cancer du sein) laissent supposer que le récepteur de somatostatine (SSTR) soit également un gène dont l'expression est régulée par des oestrogènes.

Dans cette thèse le rôle des oestrogènes dans l'expression de SSTR continue à s'éclaircir et on étudie la possibilité de l'illustrer au moyen de techniques appartenant à la médecine nucléaire, avec l'espoir de repérer parmi les patientes atteintes d'un cancer du sein, celles qui réagiront plus que probablement de façon positive à la thérapie endocrine.

Nous avons choisi la scintigraphie comme technique d'imagerie pour la raison suivante: celle-ci n'est pas invasive et a l'avantage de permettre l'évaluation du corps de façon répétitive. Il est de surcroît possible de détecter l'hétérogénéité intrinsèque de l'expression des récepteurs tumoraux sans manipulation d'organes et fournit des images *in vivo* de tous les foyers de contagion lorsqu'un traitement s'avère nécessaire. Le chapitre 2 est consacré à l'imagerie des récepteurs en oncologie au moyen des techniques provenant de la médecine nucléaire. Pour ce qui en est du cancer du sein en particulier, beaucoup d'efforts ont été fournis en ce qui concerne l'expression de la synthèse et l'évaluation de radiopharmaca dont on suppose que l'absorption dans la tumeur est relatée à l'expression RO et donc à la sensibilité hormonale.

Au chapitre 3 nous avons démontré que l'expression de SSTR au moyen d'oestrogènes se retrouve dans deux lignées cellulaires humaines de cancer du sein (T47D et ZR75-1) hormonalement sensibles, RO-positives, et non pas dans les cellules MDA MB231, hormonalement non-sensibles et RO-négatives. Les expériences de combinaisons ont

démontré que les concentrations physiologiques d'oestradiol résultaient en une augmentation statistiquement significative du nombre de SSTR situé sur les membranes cellulaires des cellules T47D, mais non pas sur celles des cellules ZR75-1 et MDA MB231. Etant donné que western blot n'a démontré qu'une très faible augmentation de protéine SSTR2 dans les cellules T47D, ce phénomène sera probablement dû au recyclage de récepteurs de l'intérieur vers l'extérieur de la membrane cellulaire. L'effet E_2 est soit réduit, soit empêché par les antioestrogènes tamoxifen ou ICI 182 780 (fulvestrant), ce qui indique la nécessité d'une liaison E_2 et d'une stimulation RO, ce qui à son tour laisse supposer une expression SSTR entièrement régulée par E_2. Par analogie avec les données *in vitro* nous émettons l'hypothèse qu'un traitement hormonal efficace de patientes atteintes de cancer du sein métastasé peut induire une diminution de SSTR au niveau de la membrane cellulaire. Ceci pourrait être rendu visible *in vivo* par scintigraphie séquentielle du récepteur de somatostatine.

Nous avons choisi de travailler avec dépréotide (P829-NeoSpect®/NeoTect®), un analogue de somatostatine marqué au technétium (^{99m}Tc) à haute affinité au SSTR2, 3 et 5. Au chapitre 4 nous avons étudié la biodistribution et la dosimétrie du ^{99m}Tc-dépréotide auprès de malades atteintes du cancer du sein. Nous avons détecté la plus intense radioactivité dans le foie, dans la rate et dans les reins; la radioactivité est principalement éliminée physiquement. Nous avons de plus remarqué une absorption par les poumons, le colon, la moelle osseuse et la muqueuse du bucco-pharynx. La dose moyenne effective pour le ^{99m}Tc-dépréotide est de 6.4-8.5 mSv, ce qui est substantiellement inférieur à celle de [^{111}In-DTPA-D-Phe]-octréotide (8-16 mSv), un radioligand de routine dans la détection des tumeurs SSTR-positives.

Au chapitre 5 nous avons comparé la précision diagnostique de la scintigraphie ^{99m}Tc-dépréotide planaire et la scintigraphie osseuse ^{99m}Tc-diphosfate de méthylène (MDP) dans l'évaluation des métastases osseuses chez une série de patientes atteintes du cancer du sein. La scintigraphie osseuse a prouvé être meilleur (75% contre 83.3%), grâce à sa plus grande sensibilité (100% contre 62.5%). La spécificité de NeoSpect® scan était toutefois plus élevée (100% contre 50%). Le dépréotide se lie notamment spécifiquement sur SSTR2, 3 et 5 qui sont sur-exprimés sur 50%-80% des cellules cancéreuses. Tout au contraire de ^{99m}Tc-MDP qui est accumulé à tout endroit où le squelette montre un turnover important, comme pour l'artropathie, ce qui donne un diagnostic faussement positif des métastases osseuses.

Nous avons évalué le potentiel de scintigraphie séquentielle ^{99m}Tc-dépréotide pour une sélection de patientes qui répondraient favorablement à la thérapie hormonale au chapitre 6. Tous les scans des patientes reprises dans notre étude et ayant des tumeurs sensibles aux

hormones sont positifs. L'absorption du radioligand en scan postthérapeutique –pris 3 semaines après le début du traitement – fut en ligne générale plus bas que celui pris en pré-thérapie, et, en tenant compte d'un cut-off de 25% resta égale ou inférieure. Tous les scans ^{99m}Tc-dépréotide négatifs appartenaient à des patientes ayant des tumeurs résistant à la thérapie hormonale. Trois patientes (30%) du groupe qui ne réagit pas au traitement montraient une scintigraphie ^{99m}Tc-dépréotide positive et une augmentation de l'absorption du radioligand.

Nous avons trouvé un rapport consistant entre l'absorption du ^{99m}Tc-dépréotide et la réponse au traitement chez des patientes attentes de cancer du sein métastasé. Le mécanisme sous-jacent est sensé être la régulation de l'expression SSTR par RO, mais un nombre de cytokine et/ou facteurs de croissance présents aux alentours de la tumeur peuvent avoir un surcroît d' impact. De toute façon, si une étude à une échelle plus importante entérinait les données, cette méthode représenterait un formidable outil d'évaluation fine de la sensibilité aux hormones des tumeurs du sein. Un protocole consistant en une scintigraphie des récepteurs de somatostine avant traitement (en cas de scan préthérapeutique positif) et une reprise du scan en cas positif pourrait être préconisée. Ceci permettrait de faire la distinction entre les patientes pouvant ou non répondre à la thérapie hormonale, et cela pourrait se faire immédiatement en cas de scan préthérapeutique négatif), soit 3 semaines après début du traitement (en cas de scan préthérapeutique positif).